The Mechanism Of The Electric Spark

The Mechanism Of The Electric Spark

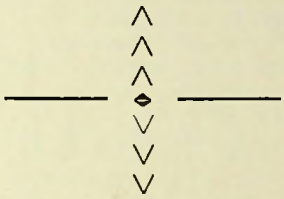

By

LEONARD B. LOEB

Professor of Physics
UNIVERSITY OF CALIFORNIA AT BERKELEY

and

JOHN M. MEEK

Commonwealth Fund Fellow
UNIVERSITY OF CALIFORNIA AT BERKELEY

Research Engineer with Metropolitan Vicars Company
MANCHESTER, ENGLAND

STANFORD UNIVERSITY PRESS
Stanford University, California

LONDON: HUMPHREY MILFORD :: OXFORD UNIVERSITY PRESS

STANFORD UNIVERSITY PRESS
STANFORD UNIVERSITY, CALIFORNIA

LONDON: HUMPHREY MILFORD
OXFORD UNIVERSITY PRESS

THE BAKER AND TAYLOR COMPANY
55 FIFTH AVENUE, NEW YORK

THE MARUZEN COMPANY
TOKYO, OSAKA, KYOTO, SENDAI

PRINTED AND BOUND IN THE UNITED STATES
OF AMERICA BY STANFORD UNIVERSITY PRESS

To

PROFESSOR J. S. TOWNSEND

Whose pioneer researches and theory laid the whole foundation for the study of the mechanism of the electrical spark discharge, this book is appreciatively dedicated

Acknowledgments

In view of the joint authorship of this book a word must be said as to the division of responsibility in this work. Both authors have worked over the manuscript in its final form and are in complete accord with the material presented. To this extent the book is a joint contribution. However, the senior author originally evolved the picture of the streamer mechanism of the corona and spark discharge nearly simultaneously with and quite independently of H. Raether, who proceeded on the basis of observations of a different set of phenomena. The missing applicable, basic quantitative criterion was supplied to the qualitative theory of the senior author by the junior author. To the senior author fell the task of the co-ordination of this criterion with the fundamental processes operative in the gas. Thus the first chapter on the Townsend discharge and the majority of the analyses of the second chapter are the work of the senior author. The extension of the quantitative mechanism to the avalanche retrograde streamer mechanism for longer sparks and the correlation of this with the junior author's criterion is largely the work of the senior author. The original picture of the stepped-leader stroke in lightning discharge as being caused by ion recombination in the pilot streamer channel was the work of the junior author. The reinterpretation of this theory of the stepped leader in terms of the avalanche retrograde streamer mechanism is the work of the senior author. The calculation for the breakdown potentials in various types of gaps and the quantitative application of the theory to various problems is almost exclusively the work of the junior author. Thus chapter iii is to be ascribed to the junior author except for the underlying procedure and discussion in the analysis of the breakdown of the space-charge distorted gap at infinite time, which was outlined and interpreted by the senior author.

In the study of the breakdown of a gap with space-charge distortion, both authors wish to acknowledge their indebtedness to Dr. Wm. R. Haseltine, whose assistance in the application of Varney's space-charge equation was invaluable. They also wish to express their thanks to Dr. Haseltine for his exceedingly able analysis and criticism of other features of the book on which his opinion was sought. The thanks of the authors are also due to Professor Norris E. Bradbury, who reviewed the book for publication, and to Professors Robert N. Varney and Robert E. Holzer, who kindly read the book in manuscript. Finally, both authors wish to acknowledge their gratitude to the Commonwealth Fund for a Fellowship granted to the junior author which made possible the close association of the authors for two years, resulting in the evolution of the present theory and the writing of the book.

LEONARD B. LOEB
JOHN M. MEEK

BERKELEY, CALIFORNIA
June 15, 1940

Preface

ALTHOUGH the electric spark has been known to mankind in its various manifestations from time immemorial, its mechanism has to date been little understood. The initial clarification of the mechanisms involved is due to J. S. Townsend as a result of his brilliant researches in the early nineteen hundreds. On the basis of his theory of ionization by collision by electrons and positive ions, the fundamental mechanisms active and especially the coefficients required in their application were made available to experimental study. The resulting investigations, owing to the facilities existing in those years, were confined to lower potentials limiting both gap lengths and pressures which could be used. The equation which Townsend derived for the ion currents as affected by the first and second coefficients led to a criterion for the development of indefinitely large values of the currents. The achievements of such currents Townsend interpreted as setting the criterion for a spark. As has subsequently been pointed out, this criterion is nearly identical with the condition of stability for a self-sustaining discharge. If that condition is altered in the proper fashion, one has a threshold for the transitions to other discharge conditions. Consequently, though itself erroneously deduced, the Townsend criterion as applied to the low-pressure data at hand was established within the limits of experimental uncertainty.

The initial success of this theory led at once to its being carried over to the occurrence of sparks at higher pressures and longer gap lengths. As time went on, it became increasingly clear that the theory was seriously inadequate. The discovery, about 1927, that the formative time lag of sparking at atmospheric pressure was about $\frac{1}{100}$ that to be expected on Townsend's theory led to various attempts to overcome this difficulty. Meanwhile the great advance in the interpretation of atomic

Contents

Chapter I

THE TOWNSEND THEORY OF THE SPARK

1. Definition of a Spark

In view of what has been said in the Preface concerning the development of spark-discharge study, one may on the basis of the Townsend concepts define a spark as follows:

The spark is an unstable, irreversible, and transient phenomenon sometimes marking the transition from one more or less stable condition of current between electrodes in a gas to another more stable one under imposed conditions. This extends the concept of a spark somewhat beyond the noisy and brilliant phenomenon usually associated with the word. However, it enables one to include a large number of obviously similar occurrences. It does not imply that all transitions of stable current states to other more stable ones, as imposed conditions change, are accomplished by a spark. Thus, for example, a spark may mark the transition from a glow discharge to an arc, although the change can under some conditions be made to occur reversibly without spark by the heating of the cathode. In general, the passage from a dark photoelectrically maintained current in a gap to a glow or an arc will be accomplished by a spark. The same may be said of the transition of a corona discharge to an arc or a glow. It is also permissible to refer, as a spark, to the appearance of a discharge of instantaneous character across a gap which discharges the capacities involved even when external circuit conditions preclude the continuation of the newly achieved stable state. In some of these cases the transition may be relatively noiseless and the only manifestation may be the abrupt change of a current. Where, however, the current increases in some reversible fashion with the applied

potential, one can hardly speak of a spark. On this basis it is probably likely that the onset of a corona discharge is not, properly speaking, a spark. By eliminating, through adequate ionization, chance occurrences which make it seem abrupt, the corona onset can be made to develop quite smoothly and reversibly as potential is altered.

2. The Townsend Sparking Criterion and Its Modifications

It will not be necessary here to derive the famous equation of Townsend for the current i in a gap between electrodes as a function of the photoelectric current i_0 from the cathode, the gap length x and the coefficients α and β. For this information the reader can go to any standard text on discharge through gases.[1]* The equation reads:

$$i = i_0 \frac{(\alpha - \beta)e^{(\alpha-\beta)x}}{\alpha - \beta e^{(\alpha-\beta)x}}$$

In this equation the first Townsend coefficient α represents the number of new electrons created in the gas by an initial electron in its advance of 1 centimeter along the field axis from the cathode.[2] The second Townsend coefficient, β, in Townsend's original theory was the number of new electrons created by a single positive ion in its advance of 1 centimeter along the field axis from the anode.[1]

The quantity α has been extensively studied in various gases. It varies with the ratio of field strength to pressure, X/p, where X is in volts per centimeter and p is in millimeters of Hg. The relation $\alpha/p = f(X/p)$ follows an analytically complicated, somewhat S-shaped curve.[3] The general procedure in the theoretical evaluation of $f(X/p)$ is known;[4] but no one has to date had the patience to undertake the elaborate and tiresome calculations for any one gas. Thus we depend on measured values entirely. Most experimental curves for $f(X/p)$ in different

* For this and subsequent citations, see end of chapter.

gases are correct in order of magnitude only. They are not accurate, owing to the failure to eliminate different impurities present in small traces.[5] For example, 10^{-3} millimeter of Hg at 1 millimeter pressure of N_2 changes α by 17 per cent at high X/p. The data are particularly bad in He, Ne, and A because of the action of metastable states. Inasmuch as we shall use air in our future discussions, the values of Sanders for α/p for Hg-contaminated air will be given in Table III and shown plotted in Figure 25 (p. 110). These are the only values at low enough X/p for use in calculations to follow. In the region of importance to the problems to be considered it is doubtful if the values of α are too high by much more than 5 per cent.

The quantity β has been evaluated, albeit rather inaccurately, from the variation of i with x at various higher values of X/p, by many observers in different gases. Inasmuch as it has now been conclusively shown that with values of X/p existing under sparking conditions positive ions cannot possibly ionize by collision with gas molecules in sufficient amount to give the observed values of β, more must be said.[1, 6] It has further been shown that there are numerous mechanisms other than impact ionization in the gas by positive ions which can liberate the secondary electrons needed in discharge. It also happens that the general type of equation which Townsend deduced for positive-ion ionization is applicable to the mechanisms now known to be active at the cathode.[7] The change in the Townsend equation to conform to active mechanisms is in most cases a minor one involving primarily a reinterpretation of the meaning of the constants. The quantitative differences are largely within limits of experimental accuracy.

There is one difference, however, and that is that the alternative mechanisms make the second Townsend coefficient dependent on cathode material. At high X/p this corresponds to observation.[8] This dependence, however, is not marked in sparks at higher pressures and is entirely absent in some discharges such as the positive point corona discharge. These are

phenomena depending on the properties of the gas entirely. It is for this reason that there has been a disinclination to give up the Townsend mechanism of impact ionizations by positive ions in the gas. The discovery of measurable photoelectric ionization in the gas has now made it possible to explain such cases.[9] The exact way in which photo-ionization in the gas could operate to cause a spark was, however, not clear until the development of the present streamer theory.

Aside from this aspect of the problem, it can be stated that for the low-pressure sparks the experimentally observed values for i as a function of gap length can be equally well represented within the present limits of experimental accuracy by any one of a number of relations depending on different cathode phenomena.[10] Two of these equations are given below, together with Townsend's original equation for comparison.

$$i = i_0 \frac{(\alpha - \beta) e^{(\alpha-\beta)x}}{\alpha - \beta e^{(\alpha-\beta)x}} \tag{1}$$

$$i = i_0 \frac{e^{\alpha x}}{1 - \gamma(e^{\alpha x} - 1)} \tag{2}$$

$$i = i_0 \frac{\alpha e^{\alpha x}}{\alpha - \eta\theta g[e^{(\alpha-\mu)x} - 1]} \tag{3}$$

Equation 2 is one for the liberation of secondary electrons at the cathode by positive-ion bombardment. In this equation γ is the chance that a positive ion will liberate an electron from the cathode on impact. Equation 3 is the equation for liberation of electrons by photoelectric action at the cathode: θ is the number of photons created per centimeter path of advance of an initial electron in the field direction, whose frequency is such that they can liberate an electron from the cathode; g is a geometrical factor, of value about 0.5, which depends on the fraction of photons in the gap that can reach the cathode; η is the fraction of the photons reaching the cathode that succeed in actually liberating electrons from the cathode so that they do

not diffuse back; μ is the absorption coefficient of the photons in the gas. If, as is indicated by observed values, we set β and μ as small compared to α and 1 as small compared to $e^{\alpha x}$, we can write

$$i = i_0 \frac{\alpha e^{\alpha x}}{\alpha - \beta e^{\alpha x}} \tag{1a}$$

$$i = i_0 \frac{e^{\alpha x}}{1 - \gamma e^{\alpha x}} \tag{2a}$$

$$i = i_0 \frac{\alpha e^{\alpha x}}{\alpha - \eta\theta g e^{\alpha x}} \tag{3a}$$

In these equations it is seen that $\alpha/\beta \equiv 1/\gamma \equiv \alpha/\eta\theta g$. It is further seen that when at $x = \delta$,

$$\alpha/\beta = e^{\alpha\delta}, \quad 1/\gamma = e^{\alpha\delta}, \quad \text{and } \alpha/\eta\theta g = e^{\alpha\delta} \tag{4}$$

the denominator in each of the equations (1), (2), and (3) becomes 0. Under these conditions the current i becomes indefinitely large irrespective of the externally imposed photocurrent from the outside. This condition Townsend initially set as the criterion for a spark, and the gap length δ at which sparking occurs was supposed to be set by these equations.[11] For the sake of simplicity in what follows we will leave the exact mechanism active in causing the second Townsend coefficient unspecified, except to note that it cannot be due to ionization of the gas by positive ions. In conformity with this decision we will follow modern practice and designate the second coefficient by the symbol γ instead of β/α or $\eta\theta g/\alpha$. Thus the Townsend criterion for a spark will be set as $1/\gamma = e^{\alpha\delta}$ and stated as such in what follows. This will not be seriously wrong, for it will appear that in most low-pressure cases γ is largely due to impact of positive ions at the cathode.

We must now digress to point out that in reality the use of Townsend's equation for i as a function of δ in spark discharge is not justified.[12] In the first place, if we are to be precise, it makes the sparking potential a function of i_0 in a sense which

is not in accord with experiment. When one carefully tries to analyze the role of i_0 in producing a spark under these conditions one at once arrives at mathematical or physical indeterminacies. The reason for this is that equations of the form 1 to 3 are derived for steady state processes that are completely reversible. They cannot thus be applied to a spark.

It fortunately happens that the condition of Equation 4, $1/\gamma = e^{\alpha\delta}$ is capable of an entirely different interpretation.[13] Now γ is the chance that a positive ion will liberate a new electron from the cathode, and the number of positive ions produced by an initial electron is equal to $e^{\alpha\delta}$. Thus the condition, $\gamma e^{\alpha\delta} = 1$, means that the supply of secondary electrons from the cathode is just enough to maintain the *avalanches* of $e^{\alpha\delta}$ electrons produced by one electron in going δ. That is, for each initial electron which crosses this gap, γ is such that the positive ions created by it generate a new electron at the cathode. This means that the existing discharge conditions in the gap are *self-sustaining*. Such a criterion has actually been applied with some success to the solution of the steady-state glow discharge.[13]

If now $\gamma e^{\alpha\delta} < 1$, then the current initiated by one electron will cease unless electrons are artificially created at the cathode by external agents. That is, below $\gamma e^{\alpha\delta} = 1$, Townsend's Equation 1*a*, 2*a*, or 3*a* for i applies. When $\gamma e^{\alpha\delta} > 1$, then it is clear that more positive ions will be created than are needed to maintain a discharge. If these excess ions can be dissipated by lateral diffusion to the walls or by other processes nothing will happen. If they accumulate faster than such losses can accommodate, positive space charges will build up in the gap. If the space-charge accumulations can produce field arrangements which will lead to a larger current for the same potential by a new form of discharge, then the old self-sustaining discharge will irreversibly and suddenly revert to the new form of discharge via a spark. That rearrangements of space-charge distribution even with ionization only by electrons can lead to such a condition has been mathematically demonstrated. Now the quan-

tity γ is a probability. Thus it can happen that sometimes by fortuitous circumstances, when $\gamma e^{\alpha\delta} = 1$, or possibly less, a spark might occur. Vice versa, above $\gamma e^{\alpha\delta} = 1$ an unfortunate chance sequence of ionizing events would break off such a discharge (see Sec. 5, p. 20).

On the average, however, *the condition for a stable self-sustaining discharge is given by* $\gamma e^{\alpha\delta} = 1$. In consequence, this relation sets the *threshold* for the transition called a spark. With this new interpretation of the equation wrongly derived from Equations 1*a*, 2*a*, and 3*a*, we will then consider the success of the Townsend criterion, $\gamma e^{\alpha\delta} = 1$, in predicting sparking phenomena.

3. The Test of Townsend's Theory at Low $p\delta$

Experiment has shown that for various surfaces γ is some function $\phi(X/p)$ of X/p, albeit at times a complicated one. Likewise $\alpha = pf(X/p)$ is also some function of X/p. Hence the Townsend criterion as interpreted above sets

$$\frac{1}{\phi(X/p)} = e^{pf(X/p)\delta} \tag{5}$$

as the criterion for a spark. Thus we have

$$\log 1/\phi(X/p) = p\delta f(X/p)$$

which can also be written

$$\log \frac{1}{\phi\left(\frac{X\delta}{p\delta}\right)} = p\delta f\left(\frac{X\delta}{p\delta}\right) \tag{6}$$

For a uniform gap in the absence of space-charge distortions such as is used in all these studies, $X\delta = V_s$ the sparking potential. If the gap is distorted, so that X is a function of distance x in the gap $V_s = \int_0^\delta X dx$, we are justified in writing in place of $X\delta/p\delta$ for the uniform field gap

$$\frac{V_s}{p\delta} = \frac{\int_0^\delta X dx}{p\delta} = \frac{\overline{X}\delta}{p\delta} \tag{7}$$

Under these conditions the sparking threshold is given by

$$\log \frac{1}{\phi\left(\frac{V_s}{p\delta}\right)} = p\delta f\left(\frac{V_s}{p\delta}\right) \tag{8}$$

It is seen that the solution of this equation makes $V_s = F(p\delta)$. This is known as Paschen's law and was discovered experimentally in 1889.

The law has been justified theoretically[14] on more general dimensional grounds and has been established within experimental accuracy over the low-pressure range. It also appears to hold at higher values of $p\delta$ within experimental accuracy, which is not high. A careful study of the origin and nature of the law indicates that it will hold for any sparking mechanism in which the threshold depends on the *total number of ions* or electrons formed in the gap. Its physical significance, then, is merely that the materialization of a spark is conditioned on the presence of enough molecules in the gap length to insure the production of adequate electrons or ions to achieve the threshold value.

In the event that the mechanism of the spark depends on the *concentration* of ions rather than on the total number produced, it appears that Paschen's law will not be obeyed. This was first discovered by Varney[15] in a study of space-charged induced sparks in a uniform gap with high ultraviolet induced-current densities at the cathode. As will later be seen it is also found to be true in the newly proposed theory of sparking. The extent of the departure from Paschen's law is in both cases small where it has been calculated. It lies within the limits of error of existing experimental data.

From the condition $\gamma e^{\alpha\delta} = 1$, one can evaluate the sparking potential for any gap of a given length δ at any given pressure p. Exact solutions must be carried out by successive approximations from curves for $\alpha = pf(X/p)$ and $\gamma = \phi(X/p)$. This task is less formidable than it seems, as the values of γ are not very critical, owing to their slow variation with X/p and the

rapid variation of α/p in all but the higher regions of X/p. Thus, an approximate value of γ being chosen, the value of α needed is found. This gives a more accurate value of X/p and thus allows one to pick a fairly good value of γ. Again solving for α then yields a sufficiently good value of X_s and hence of V_s. Owing to the relative unimportance of small changes in γ one can calculate V_s over whole regions of values of $p\delta$ where an approximation to an analytical form for α/p as a $f(X/p)$ is at hand.[16]

Even the early rather crude values of the Townsend coefficients sufficed to indicate that, in the regions where these were measured, values of V_s in satisfactory agreement with observations were obtained. The later refinements of the observations of these coefficients confirm this agreement.[17] This is shown in the curve of Figure 1 for H_2 from data of Hale and Ehrenkrantz. Exact agreement cannot be expected owing to the changes of the values of γ for surfaces with time, the presence of uncontrollable traces of gaseous impurities affecting γ, effects of previous sparking on the value of γ, and the uncertainties in the measurements of V_s. Finally, no practically achieved cathode has a uniform value of γ over its surface. Sparks will take place at the lowest values of γ present, while measurements of γ for the cathode as a whole give average values. Thus in the region where γ can be measured, agreement with the sparking criterion is satisfactory but never perfect.

Attempts have been made to carry these computations up to higher values of $p\delta$. Now assuming the equation valid, it is possible to estimate values of a γ from one or two sparking potentials at high $p\delta$.[18] Using these and an analytical form of α/p from experiment, it is then possible to calculate the full sparking potential-$p\delta$ curves in satisfactory agreement with observation. All that this procedure does is to show that an equation of the approximate form used employing empirical constants evaluated from experiment suffices to reproduce observed values. Such calculations, which can in some cases be

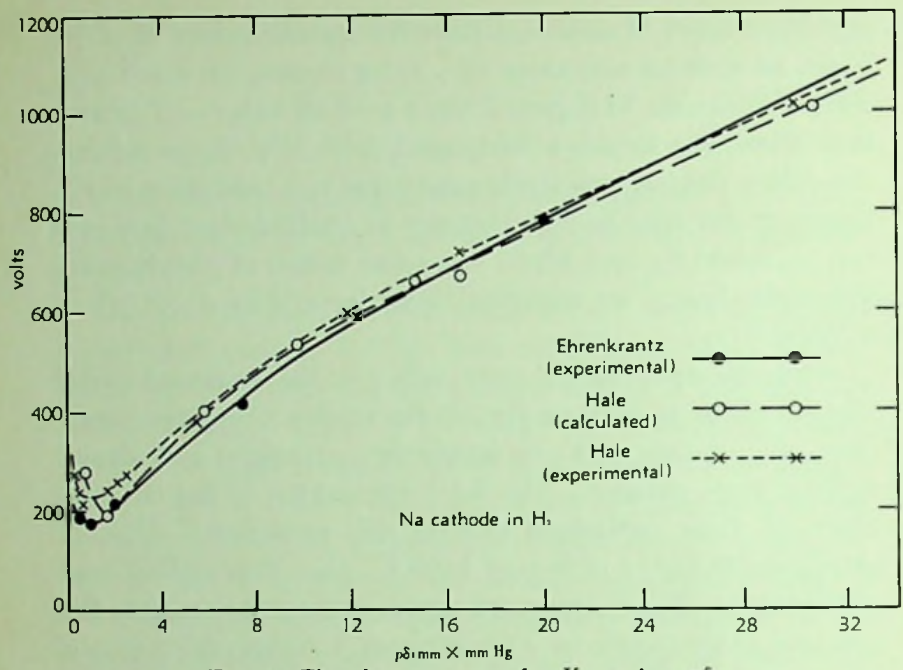

FIG. 1.—Ehrenkrantz curves for V_s against $p\delta$

carried over even to non-uniform fields, are, however, no test of the theory and especially of its assumed underlying mechanism. For, as seems to be the uncanny characteristic of this field of study, the condition $\gamma e^{\alpha\delta} = 1$ has a form analogous to the dominating terms in the sparking mechanism based on streamer formation. Thus by fitting an arbitrary constant γ, which we know today cannot have any relation to the quantity γ as defined on page 4 to the observed sparking potential, we obtain a set of values of γ which, used in the equation under various conditions, will always give back nearly the correct value of the sparking potential.

The reason for the fact that the correct theory and one which does not apply equally well yield the same curves lies entirely in the dominance of the $e^{\alpha\delta}$ term and the fact that α varies nearly exponentially with X/p. Hence false terms in the rest of the equation due to almost any theory are compensated for by minor changes in X_s or V_s. This will later be seen to be true.

Thus extrapolation of the Townsend threshold condition for a spark beyond regions of X/p and $p\delta$ where the second coefficient can directly be observed is meaningless and, worse than that, illusory. For it happens that in most sparks at $p\delta > 200$ in air *there is no action at the cathode* and γ has no physical meaning.

In what precedes it has been shown that Townsend's theory predicts the proper values of V_s and other laws observed to hold at *low* $p\delta$. There is thus little doubt of its validity in this region. In one direction of study, however, the theory has not been analyzed. This is as to the way in which the space charge accumulates and the time taken for the discharge to materialize on this basis.

4. Time Lags in Sparking and Further Tests of Townsend's Theory

So far we have merely indicated that, if $\gamma e^{\alpha\delta} > 1$, then space charges of positive ions may accumulate that will eventually lead to a more stable current arrangement, at low $p\delta$, usually a glow discharge. We have, however, not said anything about how this can occur. One thing at the outset is clear. For the consequences of $\gamma e^{\alpha\delta} > 1$ to manifest themselves the positive ions produced largely near the anode by the initial electron in its passage must have time to cross to the cathode. If $\gamma e^{\alpha\delta} \gg 1$ the space-charge distortion will arise relatively rapidly after very few passages of electrons and successive waves of positive ions. If $\gamma e^{\alpha\delta} \doteq 1$, the number of such passages may have to be very high to give an adequate space-charge distortion. Now the time of crossing of the positive ions is of the order of 100 times that of the electrons. For ordinary gaps the time of crossing of positive ions does not fall very much below 10^{-5} second. Thus the time for a discharge to build up must on Townsend's theory exceed about 10^{-5} second for the usual gaps used. The time required for the spark to develop once it has begun is termed the *formative time lag* in contrast to the statistical time lags

experimentally first observed.[28]* This *formative time lag* in excess of 10^{-5} second must also be longer the more nearly $\gamma e^{\alpha\delta} = 1$.

Now the time lags of sparks were not studied before 1925, as inadequate facilities were at hand for their study. However, by 1927–1928 many different[19] types of measurement revealed that for sparks about atmospheric pressure the formative time lags were nearer 10^{-7} second than 10^{-5} second. The study of time lags for the low-pressure spark in the breaking of a glow discharge was not undertaken until 1936. The only work on this question so far was published by Schade in 1937.[20] This study has revealed that in fact the formative time lags at low $p\delta$ extend from about 10^{-5} second upward and confirm the Townsend theory. Inasmuch as this investigation reveals a great deal more about the mechanism of spark breakdown at low pressures, it is of importance that it be discussed at this point.

Schade confines his investigations to the growth of the current i, as given in an extension of Equation 2, with time. He assumes uniform fields in the gap and ignores changes of γ and especially α due to space charges. As in general he works near the threshold of sparking, $\gamma e^{\alpha\delta} = 1$, he considers that the major portion of the formative time lag occurs in building up the current i to a value i_e, at which space charges causing rearrangement can occur. The results obtained appear to bear out the validity of this assumption.

In his development of the theory Schade does not define the value which his current must reach before space charges can cause the appearance of the spark. He says, however, that it does not appear until currents of the order of 10^{-5} ampere or

* *Statistical time lags* are those caused by the chance occurrences necessary to initiate a spark, such as the appearance of an initiating electron in the gap, or the sequence of chance events which make the development of a spark channel possible. The *formative time lag* is the actual time between the occurrence of that initiatory happening leading to a spark and the completion of the sparking process. Schade's work confined itself largely to a study of formative lags.

more are reached. In practical application Schade sets i_a as equal to the glow discharge current *after* the spark has occurred. His predicted values of the lag from theory using this criterion are in rough agreement with observation. This can mean only that, once i reaches such values that space charges change the value of α, the subsequent increase in i and the materialization of the spark occurs in times short compared to the building up the current to that value. There are no exact data as to how the space charge builds up. Theoretical equations have been developed for atmospheric pressures by Schumann, Rogowski, Franck[21] and von Hippel, Kapzov, and also by Varney. The effect is cumulative and in a sense autocatalytic in its action. As shown by Varney, it is much dependent on the rate at which α/p increases with X/p, being more rapid the higher the rate of increase of α/p with X/p. The time element has been considered by Franck and von Hippel,[22] assuming the positive ions virtually immobile.

Returning to the theoretical considerations of Schade, we see that he confines his investigation entirely to the growth of the current i in time. To achieve this analysis one must first define certain terms. These are

$i_0 =$ inducing photoelectric current at the cathode produced by external ultraviolet illumination of the cathode.

$i(t) =$ the total electron current from the cathode at a time (t).

$i_a(t) =$ the electron current at the anode at a time t.

$i_+(t) =$ the $+$ ion current at the cathode at a time t.

$i_{a+}(t) =$ the $+$ ion current at the anode at a time t.

$t_i =$ the time for $+$ ions to go from anode to cathode.

With these definitions the following relations obviously exist:

$$\left.\begin{aligned} i(t) &= i_0 + \gamma i_+(t) && (a)\\ i_+(t) &= i_{a+}(t - t_i) && (b)\\ i_{a+}(t) &= i_a(t) - i(t) && (c)\\ i_a(t) &= i(t)e^{\alpha\delta} && (d) \end{aligned}\right\} \quad (9)$$

These at once yield

$$i(t) = i_0 + \gamma i_{a+}(t - t_i) = i_0 + \gamma[i_a(t - t_i) - i(t - t_i)]$$
$$= i_0 + \gamma i(t - t_i)(e^{a\delta} - 1)$$
$$i(t) = i_0 + \gamma(e^{a\delta} - 1)\left[i(t) - \frac{di(t)}{dt} t_i \right] \tag{10}$$

Let us call $\mu = \gamma(e^{a\delta} - 1)$ and $\epsilon = \mu - 1$. Then μ is the value of the quantity $\gamma e^{a\delta}$ which determines the sparking threshold. As in this study we shall use a range of values of $e^{a\delta}$, it is safer to use the exact quantity $\gamma(e^{a\delta} - 1)$ instead of $\gamma e^{a\delta}$. The threshold condition for the spark is seen to be $\mu = 1$, or $\epsilon = 0$. Inserting μ into the equations above one has

$$\mu t_i \frac{di(t)}{dt} = (\mu - 1) i(t) + i_0 \tag{11}$$

Solution of this equation yields

$$t = \frac{\mu t_i}{\mu - 1} \log \frac{1 + (\mu - 1)\, i(t)/i_0}{\mu} \tag{12}$$

Now $\mu = 1 + \epsilon$ and when ϵ is small we can neglect it. Thus we have,

$$t = \frac{t_i}{\epsilon} \log \left(1 + \epsilon \frac{i_e}{i_0} \right) \tag{13}$$

to a fair degree of approximation. For the sake of discussion we at this point replace $i(t)$ by i_e, the value of i at which space-charge distortions begin and lead to a spark. Then t is the time for the current to grow from i_0 to that of a spark i_e. Here α and γ are assumed constant with time. It is seen that t depends on t_i, on the existing value of $\gamma(e^{a\delta} - 1) - 1$ or ϵ, and the ratio of i_e/i_0.

Using different values of ϵ corresponding to various values of X/p and a value of t_i chosen for a 1 centimeter gap in Ne gas as 5×10^{-6} second the curves shown in Figure 2 were computed. The curves plotted give the ratio of $i(t)/i_0$ as a

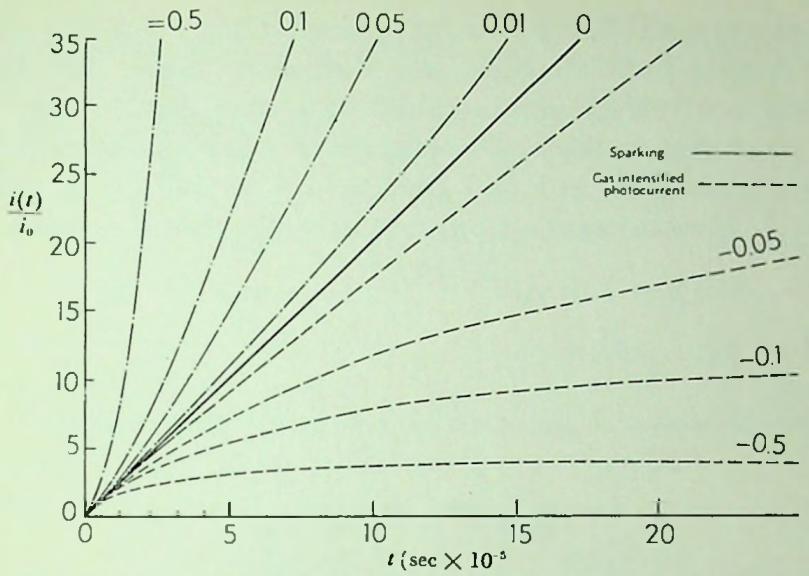

FIG. 2.—$i(t)/i_0 = f(t)$

function of t for various values of ϵ. For $\epsilon = 0$ the current rises linearly with time. Thus if $i_a = \infty$ as on the original Townsend criterion, the appearance of a spark should take infinite time. Since actually at i equal to a finite i_a a spark occurs by space charge, the time for the development of the spark will be finite, though perhaps long. For $\epsilon < 0$ the current initially rises proportionally to time. It then rises less rapidly and approaches the limiting value i in Equation 2, as $t = \infty$. This applies to the stable reversible regime covered by Townsend's original theory below sparking. For $\epsilon > 0$ the current rises with time at an accelerated rate indefinitely and, reaching i_e, goes to a spark via space-charge distortion. The rapid rise of $i(t)/i_0$ with t after a certain initial time explains why the criterion for a spark $i = i_a$ is so insensitive to i_a for larger values of the ratio. The time taken in order for the rise of i with t to become sharp, however, depends markedly on the magnitude of ϵ.

In order to test the equation experimentally it is best to transform it so that t can be expressed in terms of the *overvoltage* $V - V_s$ applied to a gap. Here V_s is the potential giv-

ing an ϵ to equal 0, and V is the applied voltage. For this solution certain approximations are desirable. Hence we shall restrict our calculations to values of ϵ such that $1 > \epsilon > 0$. Let us assume in this region just above sparking, but near it, that γ is constant. At $V = V_s$, $\epsilon = 0$, $\mu = 1$, and $\alpha = \alpha_0$ while $\gamma = \gamma_0$. If we increase α from α_0 to $\alpha_0 + \Delta\alpha$, then ϵ increases to

$$\epsilon = \mu - 1 = \gamma_0(e^{(\alpha_0+\Delta\alpha)\delta} - 1) - \gamma_0(e^{\alpha_0\delta} - 1)$$

$$= \gamma_0 e^{\alpha_0\delta}(e^{\Delta\alpha\delta})$$

Now $\gamma e^{\alpha_0\delta} \sim \mu_0 = 1$ and if $\epsilon < 1$, $\epsilon \doteq \Delta\alpha\delta$. Hence we have

$$t = \frac{t_i}{\Delta\alpha\delta} \log\left(1 + \Delta\alpha\delta \frac{i_c}{i_0}\right) \tag{14}$$

In a limited region in the regime of X/p where we are interested $\alpha/p = Ae^{-B/(X/p)}$. This relation was originally deduced by Townsend on an erroneous assumption.[23] It has since in a limited region been theoretically justified by von Engel and Steenbeck.[24] Actually it is a purely empirical equation which can be fitted in the narrow range at large X/p used by a judicious choice of the constants. For the sake of analysis we will then set $\alpha = Ape^{-B\delta p/V} = ae^{-b/V}$. Hence $\alpha_0 = ae^{-b/V_s}$ and $\alpha_0 + \Delta\alpha = ae^{-b/V}$. Hence $\Delta\alpha = ae^{-b/V}(1 - e^{-(V-V_s)b/VV_s})$. For small values of $V - V_s$ the quantity in the parenthesis above is

$$[(V - V_s)/V_s^2]b,$$

and we can write

$$\epsilon = \Delta\alpha\delta = \frac{(V - V_s)ab\delta}{V_s^2} e^{-b/V}$$

$$= \frac{ABp^2\delta^2(V - V_s)}{V_s^2} e^{-Bp\delta/V_s}$$

Thus we have

$$t = \frac{t_i V_s^2}{ABp^2\delta^2} \frac{1}{V - V_s} e^{Bp\delta/V} \log\left\{1 + \frac{ABp^2(V - V_s)}{V_s^2} e^{-Bp\delta/V} \frac{i_c}{i_0}\right\} \tag{15}$$

For small values of i_0 the quantity $\epsilon \frac{i_c}{i_0} \gg 1$. Hence the value of the logarithmic term will be nearly constant if $V - V_s$ is not too large. Thus to a rough approximation

$$t = \frac{a}{V - V_s} e^{-b/V} \tag{16}$$

This equation is independent of i_0. It makes $t \doteq \infty$ as $V - V_s \doteq 0$. Since the equation is not rigorous, this conclusion is not justified. To determine the effect of i_0 on sparking time at V_s one can take the limit of the rigorous equation

$$t = \frac{t_i}{\epsilon} \log \left(1 + \epsilon \frac{i_c}{i_0}\right) \text{ as } \epsilon \doteq 0,$$

which yields

$$t_{V_s} = \frac{t_i i_c}{i_0}$$

This implies a finite time to achieve a spark which is the smaller the larger i_0. If i_c/i_0 is set as $(10^{-5}/10^{-15}) = 10^{+10}$, then, since $t_i \sim 10^{-6}$, $t_{V_s} \sim 10^4$ seconds, which is a long time.

Measurements were conducted to determine t as a function of $V - V_s$ in H_2 and He, using natural ionization present in the gap due to the Paetow[25] phenomenon or metastable states.* Here i_0 is of no consequence. In Figure 3 the curve for t as a function of $\frac{1}{V - V_s}$ is shown for small values of $V - V_s$. It is

* Paetow found that minute insulating dust particles on both electrodes become highly charged after the first spark or discharge passes owing to accumulations of ions or more effectively photo-ionization by high-energy photons. The fields across such charged specks $\backsim 10^{-4}$ to 10^{-5} cm in diameter amount to $\backsim 10^5 - 10^6$ volts/cm. They can furnish triggering electrons in profusion by localized discharges, photo-ionization of the gas, or field emission in the process of neutralizing themselves. Cf. p. 65 and Loeb, *Fundamental Processes of Electrical Discharge in Gases*, pp. 498–500.

seen that where $V - V_s$ is small the curve is nicely linear. The observed values of t at $V - V_s \sim 0.1$ where $V_s \sim 300$ volts was of the order of 1 second. In Figure 4 the value of t is plotted as a function of V for Ne. The full curve represents the equation $t = \frac{a}{V - V_s} e^{-b/V}$ plotted from values of a and b as determined from two observed points. The agreement is satisfactory and here includes the logarithmic term.

A test of the equation in absolute magnitude is somewhat difficult, owing to the uncertainty in the value of i_c/i_0. Choosing i_e as the glow discharge current, and taking A and B as observed for Ne, one can from the expression for a from Equation 15 and with Equation 16 write

$$t_i = \frac{a}{1.81 \log (1 + \epsilon i_e/i_0)}.$$

Inserting the value of a, one can evaluate t_i as $5 \pm 1.5 \times 10^{-6}$ second. The value computed for the same gap from the mobility of positive ions in pure Ne is $t_i = 6.8 \times 10^{-6}$ second, which is a fortuitously good agreement.

The most significant test of the theory was the measurement of the variation of t as a function of i_0 for various values of V in Ne. To this end a photoelectric surface giving values of i_0 from 10^{-9} to 10^{-6} ampere on illumination was used. Here t plotted against log i_0 in Equation 13 should be a linear function which goes to 0 as $i_0 = i_c$. The absolute values of i_0 are uncertain by a factor of 2. It is seen that in the curves of Figure 5 the equation is justified when V is well above V_s. At $V = 189$ volts where $\frac{V - V_s}{V_s} = 0.02$, $\epsilon i_c/i_0$ becomes so nearly unity that the approximations made are no longer valid and the equation is inaccurate.

The curves indicate clearly that no space charges are active in the early stages of building up the spark and that the formative time lag is largely due to the time for the currents to grow

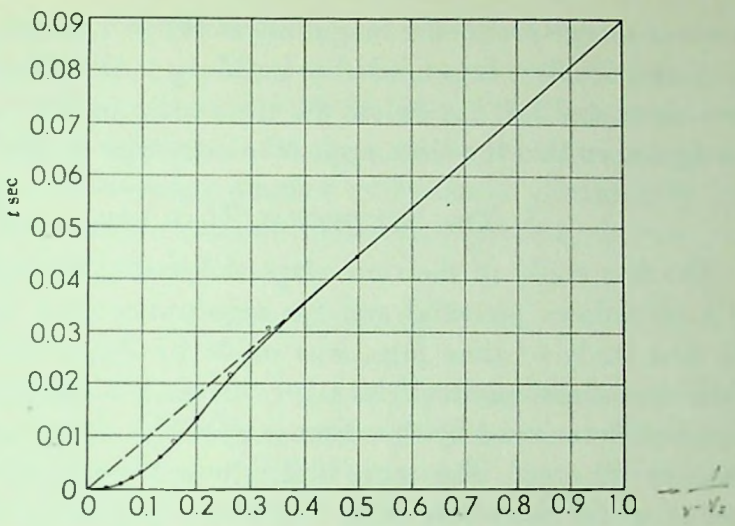

FIG. 3.—$t - \frac{1}{V - V_s}$

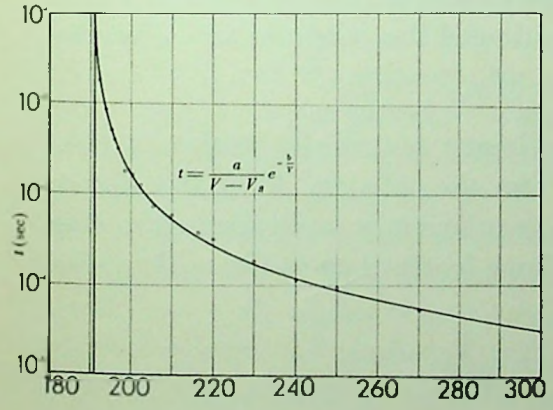

FIG. 4.—$t - f(V)$

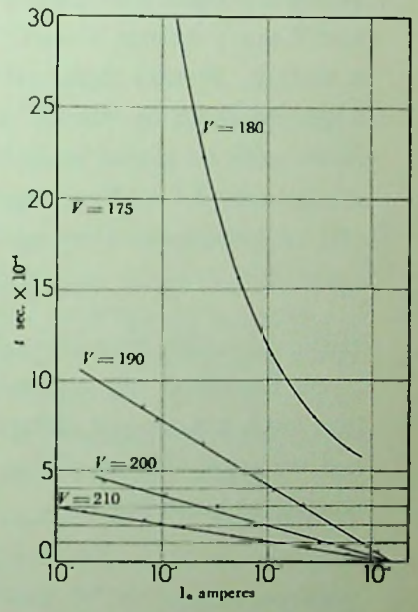

FIG. 5.—$t - f(i)$ in amperes

to space-charge-producing magnitudes. When i_0 becomes large, the formative time lags needed to build up to the value of i_c are very short and fall far below the time scale of 10^{-4} second of the figure, so that the lines appear to converge at 10^{-6} ampere.

5. The Statistical Time Lag

The first study of the time elapsed between the application of a breakdown potential and the appearance of a spark, i.e., the first study of time lags, was made by Zuber and Laue.[28] Their investigations dealt largely with the so-called *statistical time lags* occasioned by the absence of adequate initiating electrons in the gap. The more difficult techniques involved in studies of the *formative lags*, i.e., in the growth of the spark after initiation, were not developed until later. The pioneer work of Zuber and Laue, which established the statistical lags, sufficed for a long time, especially since the formative lags were believed to be capable of throwing more light on the mechanism of the discharge. As early as 1926 Braunbek[43] developed a theory of the statistical time lag on the basis of Zuber and Laue's initial studies and the simple Townsend sparking equation. It was deduced in a more simple and slightly more accurate form by Hertz[44] in 1937. In what follows the conclusions will be given in brief. Laue and Zuber showed that the probability of a discharge *starting* in a time interval dt at the end of t seconds after application of the potential was given by

$$w(t)\,dt = \mathcal{W} n_0 e^{-\mathcal{W} n_0 t}\,dt.$$

Here n_0 is the number of primary potentially initiating electrons liberated per second from the cathode. $\mathcal{W}$ is the chance that such a primary electron is sufficiently multiplied as to give a discharge. The equation above leads us to evaluate the mean statistical time lag as

$$t_s = \frac{1}{\mathcal{W} n_0}$$

To simplify calculations we assume that n_0 electrons start from

the cathode and that each makes $n = e^{a\delta} - 1$ electrons in crossing. Actually some make more and some less, but as $n = e^{a\delta} - 1$ is between 50 and 500 the statistical fluctuations are unimportant compared to the fluctuations in secondary processes. Now the average number of electrons liberated by the *ions* produced at the cathode (secondary process) by one *primary* electron of the n_0 is

$$(e^{a\delta} - 1)\gamma = M.$$

The threshold for the self-sustaining discharge is of course that $(e^{a\delta} - 1)\gamma = M = 1$. Now γ represents the *chance* that a positive ion liberates an electron. Hence while M *on the average* has the value $(e^{a\delta} - 1)\gamma$, it will not be this in individual cases. Thus M may be 0 one time, 1 another, and 2 another, and so on giving $M = 1$ on the average. When $M = 0$ the succession of events which occur when $M = 1$ ceases; i.e., the discharge is not maintained. This same condition with $M = 0$ can occur for the avalanche of the second or third ionizing cycle, corresponding to the second or third succeeding avalanche initiated by an electron, and the subsequent $(e^{a\delta} - 1)\gamma$ electrons liberated at the cathode. That is, starting with one of the n_0 electrons an avalanche $e^{a\delta} - 1$ is started. If M is 0 there will be no spark. If M is 1 then the process will repeat itself, but the second M may be 0, or 1, or 2, so that the process may cease or even multiply, and so forth. When n_0 or subsequent values of M exceed unity, on the average, the chance of extinction is less. Thus even above the threshold when the average M is unity we can expect a finite chance of the spark or breakdown not materializing. Let us designate by W the chance that above the threshold, even with a long succession of avalanches, the process will *not* break off. This is what we wish to know. We can then set $W = 1 - Q$, where Q is the chance that after a number of successive trips the discharge will break off. If then we perform an experiment in which a number of separate ionizing sequences are allowed to be initiated in turn from the cathode

a fraction $Q = 1 - W$ will be observed to break off without a spark. We can segregate the observed results into $n + 1$ groups, where $n = e^{a\delta} - 1$, according to what happened in the transit of the first avalanche in crossing the gap. The group designated as 0 is the one in which the positive ions of the first avalanche do not liberate an electron from cathode. The group designated as 1 is the one in which the avalanche ions liberate 1 electron. The group designated as M is one in which M electrons are liberated. Call u_M the chance that one experiment yields the group M. It is now possible to calculate for any one group the chance that a further continuation of the process will lead to a breaking off of the discharge chain. For $M = 0$ this chance is 1. For $M = 1$ the chance is Q by definition of Q. Since the chances of subsequent events following an avalanche are independent of any previous events we can write that for the Mth class the chance of breaking off is Q^M. The net value of Q is then the sum of all the values in each independent group of experimental results. That is

$$Q = \sum_{M=0}^{n} u_M Q^M.$$

But u_M is determined by n and γ. Then u_M is the chance that out of n ions reaching the cathode M ions liberate an electron, and $n - M$ liberate no electron. The chance of liberation of an electron by 1 positive ion is γ, the chance of not liberating an electron is $1 - \gamma$. The chance that out of n ions M liberate an electron and $n - M$ liberate none is given by well-known laws of probability as:

$$u_M = \binom{n}{M} \gamma^M (1-\gamma)^{n-M} = (1-\gamma)^n \binom{n}{M} \left(\frac{\gamma}{1-\gamma}\right)^M$$

This combined with the expression for Q above yields at once

$$Q = (1-\gamma)^n \sum_{M=0}^{n} \binom{n}{M} \left(\frac{\gamma}{1-\gamma}\right)^M Q^M =$$

$$(1-\gamma)^n \left(1 + Q\frac{\gamma}{1-\gamma}\right)^n$$

Since $Q = 1 - W$, we get on rearrangement that

$$1 - W = (1 - \gamma W)^n.$$

Inasmuch as γ is very small, $\log (1 - \gamma W)$ can be expanded in a series and replaced by the first order term $-\gamma W$, then

$$\frac{\log (1 - W)}{W} = n\gamma = (e^{\alpha\delta} - 1)\gamma = M.$$

The plot of this function is one which begins at 0 with $M = 1$ and rises at first steeply as M increases to fairly close to unity at $M \sim 4$. To be specific, when $M = 1.4$ the value of $W = 0.5$; that is, only half of the electrons succeed in causing a spark; when $M = 2$ only 80 per cent of the avalanches give sparks. It is clear that if we have the value of n_0 and W as calculated from $M = (e^{\alpha\delta} - 1)\gamma$ under any discharge conditions we can at once calculate $t_s = 1/n_0 W$. Hertz applies the theory to an A discharge studied by Schade. Here the values of α in A for various values of the potential for the 8 mm gap at 10.6 mm pressure are taken from the curves of Penning and Kruithoff. Using the single value of $\gamma = 0.02$ afforded by this study, Hertz then calculates M and W at various values of the applied potential. Assuming $n_0 = 10$, the value of t_s can be determined from the value of the threshold of 350 volts, at which $M = 1$, up to higher potentials. Starting at $t_s = \infty$ at 350 volts, the calculated curve for t_s drops rapidly to 0.25 second at 360 volts and at 400 volts approaches its limiting value of $t_s = 0.1$ second when $W = 1$ and every electron gives a spark. Such a curve is reasonable. The theory is rather simplified when regarded in the light of the proper interpretation of the sparking criterion. It strictly applies only to the Townsend mechanism in a simplified version. It does *not apply where space-charge accumulation by successive avalanches plays any role.* For in that case later ionizing events are not independent of the succeeding ones. The theory also is not applicable to cases where the ionizing agent furnishes a burst of electrons from the

cathode in a time interval short compared to the average value of the electron liberation. In that case, e.g., for α particle or γ-ray ionization $W = 1$ and t_s does not depend on the number of ions, i.e., on $1/n_0$, but rather on the number of α particle bursts per second.

With these remarks one may leave the question of statistical time lags as being clarified in principle in the case of the Townsend discharge.

6. The Character of the Spark Channel, Time Lags, and Townsend's Theory

There remains one aspect of the question of sparks at low $p\delta$ which must be discussed in connection with Townsend's theory. It was clearly indicated above that the time of growth of the spark giving a glow discharge depends on the photocurrent i_0. This dependence connotes that the whole area effectively illuminated and giving i_0 breaks into the glow discharge. That means the spark involves a broad and diffuse area. Since the initiating current i_0 is on at the time that the potential is applied, there should for the usual values of i_0 be but a *very short* statistical time lag and the only time lag of consequence should be the formative lag. This formative lag it was seen for low i_0 is determined primarily by the time to build up a space charge forming current i_e. In Schade's experiments in Ne adequate currents i_0 were always present, owing either to metastable atoms or to a strongly illuminated surface. In the case of H_2, and especially before the first discharge had initiated the Paetow[25] effect giving an i_0, there were statistical time lags of considerable length present. These were due to an effective i_0 so low that there were actually inadequate initiating electrons, i.e., a low value of n_0 in $t_s = \frac{1}{n_0 W}$. In the time-lag measurements of Schade with low i_0 the equations tested in Figures 3 and 4 were the approximations independent of i_0. Here also statistical time lags were avoided.

There are, however, observed cases of sparking at low $p\delta$—though not as low as those used here and not necessarily leading to a glow discharge—which follow Townsend's equation but where *the formative lag is independent of* i_0. Such sparks are accompanied by statistical time lags which vanish only on adequate illumination.[20] They vanish the more readily the more ϵ exceeds 0 or the greater the overvoltage as indicated on page 23. At $\epsilon = 0$ they require very high values of i_0 in order to vanish for W is very small. In those cases t depends only on ϵ and on the diffusion of ions and electrons during the time of building up the discharge. These sparks are characterized by narrow channels and much more intense light emission along the channel.

Such sparks arise as follows. At a value of ϵ greater than 0 a single fortunate photoelectron starts an avalanche of $e^{\alpha\delta}$ electrons across the gap. The positive ions from the anode region t_i second later have crossed the gap along the path of the avalanche with some slight lateral diffusion. Thereupon the $\gamma e^{\alpha\delta}$ electrons from the cathode start new avalanches from the same general region of the cathode that originated the first avalanche. These again send back $(\gamma e^{\alpha\delta})e^{\alpha\delta}$ ions in a second interval t_i. Thus the current increases along a single filamentary channel whose radius is largely determined[27] by $\sqrt{2Dt}$. In this relation D is the electronic diffusion coefficient and $t = \Sigma t_i$ for the avalanches that have preceded. It is possible that the positive charges act somewhat to reduce the value of D and to confine the channel. When this localized current i_e has reached a value such that it has a density of positive ions sufficient to cause an increase of α near the cathode, especially where α/p increases rapidly with X/p, then the localized current rapidly increases to a value where a filamentary spark materializes. The value of i_e, or current density j_e, for the development of space charges is the lower the higher $p\delta$ and the lower the value of X/p. Thus, while space charges only begin to be active at 10^{-5} ampere in Schade's case, they are active at smaller currents at higher

$p\delta$ and lower X/p. If ϵ is large then Σt_i is short, the spark channel is narrow and chance statistical fluctuations in the value of ϵ are not likely to prevent the initiated avalanche from going to a spark, i.e., W is large. Thus any initiating electron will suffice to cause a spark. The average statistical time lag will then depend only on the average time between initiating avalanches given by i_0, or better by $1/n_0$; i.e., it will vary inversely as i_0, an observed experimental[28] fact. If, however, $\epsilon = 0$, then many of the avalanches started by i_0 will fail to achieve a spark, owing to statistical fluctuations in the value of ϵ (small W). Hence, despite a high i_0, there may be considerable statistical lags. In this case, and especially at lower pressures where D is large, the paths will be diffuse. In such sparks the following conditions will apply.

a) Statistical lags will depend on i_0 and will be proportional to $1/Wi_0$, where W depends on overvoltage and increases from unity as overvoltage decreases.

b) The length of the lags at constant i_0 will decrease as ϵ is increased above 0.

c) The *formative time lags will be independent of* i_0 but will depend on ϵ, p, and δ.

Such sparks have been observed in the intermediate region of pressures between the regime studied by Schade and the region of high $p\delta$ where the new streamer theory applies. They have not been studied extensively as yet.

One may finally inquire as to whether the value of i_0 can alter V_s as well as the statistical and formative time lags. It can at once be seen from Schade's theory and from what has been said above that in the absence of space-charge distortion i_0 *cannot change the value of* V_s. If, however, under any theory the values of i_0, or better the photoelectric current densities j_0, are great enough at the values of X/p and $p\delta$ existing to cause a space-charge distortion in the gap, the values of j_0 or i_0 will definitely reduce V_s. The cases where this can occur are covered by the equations set up by Varney[15] for space-charge produc-

tion by photocurrents in Townsend gaps. In the region of higher $p\delta$ and lower X/p where α/p changes rapidly with X/p, the effects can be considerable. Thus Meek[42] has shown that for the streamer mechanism a lowering of V_s by tens of per cent can follow from adequate j_0. Rogowski[29] has developed a somewhat different and perhaps doubtful theory on the basis of Townsend's mechanism which indicates that the same thing can occur with the mechanism under consideration. Both these calculations are borne out by the studies of H. J. White[30] and of Rogowski and Wallraff,[30] who used intense values of j_0 at atmospheric pressure. For short periods of illumination of the gaps at high j_0 they observed reductions of V_s by as much as 10 per cent. The effect is most pronounced at high $p\delta$ and lower values of X/p where distortions can readily take place.

From what has now been said it is clear that at appropriately low values of $p\delta$ the Townsend equation as modified by a proper interpretation of the second Townsend coefficient appears adequate to explain the sparking phenomena observed. The same situation does not apply when $p\delta$ reaches higher values. In air the failure appears above a $p\delta$ of about 200 mm $\times$ cm. It is now of interest to present the nature of the failure of the Townsend theory at high $p\delta$.

7. Difficulties Encountered by the Classical Theory at Larger Values of $p\delta$

Although the Townsend theory in its initial form had some success for sparks at low values of $p\delta$, it presented considerable difficulties when it came to visualizing sparks at higher values of $p\delta$. The difficulties, however, did not become insuperable until after 1927, when the measured formative time lags of sparking were found to be of the order of 10^{-2} of those to be expected on Townsend's theory. The interpretation of the condition $\gamma e^{\alpha\delta} \geqq 1$ as a sparking threshold in a measure improved the situation. On the other hand, the realization that positive ions could not ionize by impact in gases made the application of

Townsend's mechanism more difficult. Many attempts were made in the years following 1928 to salvage the theory so as to fit the facts. None of them, however, proved satisfactory. While in principle even as late as 1936 the present senior author[31] still adhered to the modified Townsend theory, it had became increasingly clear to him that the mechanism was not adequate at high $p\delta$. The inadequacy can best be illustrated by listing a series of phenomena which the Townsend theory must under these circumstances account for:

a) The formative time lags of sparks at atmospheric pressure are observed to be of the order of 10^{-7} second or less for a one-centimeter gap with small overvoltages.[19] These time intervals are of the order of one one-hundredth the time intervals t_i required for the passage of positive ions from anode to cathode. In fact they are of such lengths as entirely to preclude the movement of positive ions in the gaps. Thus the proper spark-discharge mechanism must materialize through electron movement alone. Various attempts were made by Franck and von Hippel,[22] by the present senior author,[32] and others to develop mechanisms by which this could occur. These proposals, while suggestive, each had inherent in them difficulties which made such pictures unlikely in many discharges, especially if taken together with other difficulties to be mentioned below.

b) At atmospheric pressure the sparking potential has been found to be largely if not entirely independent of cathode material.[33] Townsend's theory, while somewhat insensitive to the value of γ at higher pressures, requires a definite dependence on the value of γ of the order of some 2 to 15 per cent.[34] The values of $p\delta$ where cathode dependence experimentally appears to become unimportant lie about $p\delta > 200$. This difficulty occurs only where the second Townsend mechanism is confined to the cathode. Where, as by photo-ionization in the gas or by ionization by positive ions in the gas, β depends on the gas alone, this condition causes no difficulty. Ionization by positive ions in the gas is, however, definitely ruled out,[1] and photo-ionization

in the gas requires a mechanism other than Townsend's mechanism.

c) There are gaseous discharges such as the positive-point corona and lightning discharge where there is no cathode action involved at all. A proper spark-discharge mechanism must thus also include an explanation of these discharges.

d) It has been observed that in the study of the currents between parallel plates as a function of plate distance x at lower values of X/p there occurred sparks at values of x where the log $i/i_0 - x$ curves showed absolutely no curvature[35] indicating a γ. At first this fact was ascribed to fluctuations in the potential source. Today these fluctuations can be eliminated. Still sparks occur, owing apparently to an electron ionization alone with no detectable value of γ. These also occur at such low current densities that they cannot be due to space-charge distortions of the type envisaged by Varney. The only conclusion to be drawn is that there is a sparking mechanism at higher $p\delta$ that is independent of a cathode-conditioned γ.

e) Observations of sparks by visual, photographic,[36] cloud-track,[37] and Kerr-cell-shutter methods[38] indicate that sparks occur along very narrow filamentary channels even in their very early stages. Such channels, *especially the branched and irregular ones observed with longer gaps,* are hard to reconcile with the original Townsend theory. The straight filamentary channels can, however, be made compatible with the modification of Townsend's mechanism, which is independent of i_0. This mechanism has statistical time lags dependent on i_0 and was discussed on page 25. The mechanism there discussed, however, requires long formative lags.

f) It has been shown on page 24 that there are two mechanisms of the Townsend type which can lead to sparking. One of these at lower p has no measurable statistical time lag but a formative lag dependent on i_0, and is a diffuse discharge. The other at higher values of $p\delta$ is one with statistical time lags depending on i_0 and with a formative time lag dependent on over-

voltage, but independent of i_0. The spark channel there is narrow. Neither of these has the value of the sparking potential V_s dependent on i_0 until the current densities j_0 cause a space-charge distortion in the gap as the potential is raised. The current densities j_0 involved in such an effect are very high and cannot be produced short of illumination by a condensed spark discharge. The observations on sparks at $p\delta > 200$ indicate that if the Townsend mechanism is applicable at all the mechanism must be the second alternative mechanism depending on localized processes initiated by one electron.

g) The Kerr cell[38] and cloud-track photographs[37] of the early phases of spark discharge reveal the initial phases of spark breakdown as consisting of *midgap* and *anode streamers* in overvolted gaps or *anode streamers* in other gaps. The development of intense ionization outward from the cathode, or at least a channel extending well across the gap from the cathode, as would be expected on the Townsend mechanism classified under (*e*) has *not* been observed above $p\delta \sim 200$.

8. The Indications as to the Conditions to Be Met by a Correct Theory at High $p\delta$

We must thus conclude that Townsend's mechanisms do not occur in the air much above a $p\delta > 200$. What the active mechanism is remained obscure until revealed by the phenomena observed in positive-point corona under some conditions. However, one can, from the criteria above, indicate certain conditions which a successful mechanism must conform to. These are:

a) The mechanism must depend essentially on electron movements, the ions remaining relatively fixed during the short time intervals involved in spark breakdown.

b) The spark must be initiated by a single electron along a narrow path.

c) The spark must depend on *secondary processes in the gas* and cannot involve the cathode.

d) The mechanism is favored by large $p\delta$ and lower X/p

and may involve space-charge processes. The processes needed, however, have not been considered before.

e) The intense phases of ionization in breakdown must proceed from the anode or the midgap region toward the cathode.

The discovery of the positive streamer in positive point-to-plane corona and the explanation of its mechanism by Loeb, Trichel, and Kip[39] in 1936 to 1939 clearly indicated the character of the mechanism sought for. Loeb then carried the concept of this streamer process over to the mechanism of spark breakdown in a qualitative fashion. Nearly simultaneously H. Raether,[40] from his cloud-track pictures, arrived at the concept of a positive-streamer process as being the essential feature of the missing mechanism. It was not until Meek[41] proposed a criterion which placed the streamer theory on a quantitative basis that a real advance could be made. Since then this mechanism has been found to correlate practically all observed spark-discharge occurrences, at a $p\delta$ in air greater than 200 in terms of modifications of a single mechanism, with unbelievable success. It is the purpose at this point to depart from classical and historical procedure and to develop the streamer theory and its consequences in a straightforward logical fashion.

REFERENCES TO CHAPTER I

[1] L. B. Loeb, *Fundamental Processes of Electrical Discharge in Gases* (Wiley and Sons, New York, 1939), pp. 372, 377, 379, and 409; also R. N. Varney, L. B. Loeb, and W. R. Haseltine, *Phil. Mag.*, **29**, 379 (1940).

[2] L. B. Loeb, *Fundamental Processes of Electrical Discharge in Gases*, p. 341.

[3] L. B. Loeb, *ibid.*, pp. 342, 346, 354, 361.

[4] L. B. Loeb, *ibid.*, pp. 219, 364.

[5] L. B. Loeb, *ibid.*, pp. 342 ff., 351, 354 ff.

[6] L. B. Loeb, *ibid.*, p. 374.

[7] L. B. Loeb, *ibid.*, pp. 377 ff.

[8] L. B. Loeb, *ibid.*, pp. 415 ff., 418, 419.

[9] A. M. Cravath, *Phys. Rev.*, **47**, 254 (A) (1935); C. Dechene, *Jour. de Phys. et Radium*, **7**, 533 (1936); E. Greiner, *Zeits. f. Physik*, **81**, 543 (1933); H. Paetow, *ibid.*, **111**, 770 (1939); A. F. Kip, *Phys. Rev.*, **55**, 554 (1939); H. Raether, *Zeits. f. Physik*, **110**, 611 (1938); H. Costa, *ibid.*, **113**, 531 (1939).

[10] L. B. Loeb, *Fundamental Processes of Electrical Discharge in Gases*, pp. 372 ff.

[11] L. B. Loeb, *ibid.*, p. 410.

[12] L. B. Loeb, *ibid.*, pp. 420 ff.

[13] G. Holst and E. Oosterhuis, *Phil. Mag.*, **46**, 1117 (1923); R. Seeliger, *Naturwissenschaften*, **16**, 665 (1928); *idem*, *Physik. Zeits.*, **33**, 273, 313 (1932); R. Seeliger and R. Hirchert, *Ann. d. Physik*, **11**, 817 (1931); R. Holm, *Zeits. f. Physik*, **75**, 171 (1932).

[14] J. S. Townsend, *Electricity in Gases* (Oxford, 1915), pp. 327, 380.

[15] R. N. Varney, H. J. White, L. B. Loeb, D. Q. Posin, *Phys. Rev.*, **48**, 818 (1935).

[16] L. B. Loeb, *Rev. Modern Phys.*, **8**, 278 (1936).

[17] L. B. Loeb, *Fundamental Processes of Electrical Discharge in Gases*, pp. 418 ff.; also D. H. Hale, *Phys. Rev.*, **55**, 815 (1939); *ibid.*, **56**, 1199 (1940).

[18] L. B. Loeb, *Fundamental Processes of Electrical Discharge in Gases*, p. 416.

[19] P. O. Pedersen, *Ann. d. Physik*, **71**, 371 (1923); J. W. Beams, *Jour. Franklin Inst.*, **206**, 809 (1928); J. J. Torok, *Trans. Amer. Inst. Elect. Engrs.*, **47**, 177 (1928); **48**, 46 (1930); O. Burawoy, *Archiv f. Elektrotechnik*, **16**, 14 (1926); R. Tamm, *ibid.*, **20**, 235 (1928); W. Rogowski, *ibid.*, **20**, 99 (1928); E. O. Lawrence and F. G. Dunnington, *Phys. Rev.*, **35**, 396 (1930); F. G. Dunnington, *ibid.*, **38**, 1535 (1931); J. C. Street and J. W. Beams, *ibid.*, **38**, 416 (1931); L. von Hamos, *Ann. d. Physik*, **7**, 857 (1930); R. Strigel, *Wiss. Veröffent. aus dem Siemens-Konzern*, **11**, 52 (1931); 11, **53** (1932); A. Tilles, *Phys. Rev.*, **46**, 1015 (1934); H. J. White, *ibid.*, **46**, 99 (1934); **49**, 507 (1936); M. Newman, *ibid.*, **52**, 652 (1937); R. R. Wilson, *ibid.*, **50**, 1082 (1936).

[20] R. Schade, *Zeits. f. Physik*, **104**, 487 (1937).

[21] W. Rogowski, *Archiv f. Elektrotechnik*, **20**, 99 (1938); J. Franck and A. von Hippel, *Zeits. f. Physik*, **57**, 695 (1929); W. O. Schumann, *Zeits. f. Technische Physik*, **11**, 194 (1930); N. Kapzov, *Zeits. f. Physik*, **75**, 380 (1932); R. N. Varney, L. B. Loeb, H. J. White, and D. Q. Posin, *Phys. Rev.*, **48**, 818 (1935).

[22] J. Franck and A. von Hippel, *Zeits. f. Physik*, **57**, 695 (1929).

[23] J. S. Townsend, *Electricity in Gases* (Oxford, 1914), chapter viii; L. B. Loeb, *Fundamental Processes of Electrical Discharge in Gases*, pp. 358 ff.

[24] A. von Engel and M. Steenbeck, *Elektrische Gasentladung* (Julius Springer, Berlin, 1934), **1**, 89, 184, 192; L. B. Loeb, *Fundamental Processes of Electrical Discharge in Gases*, pp. 367 ff.

[25] H. Paetow, *Zeits. f. Physik*, **111**, 770 (1939).

[26] A. Tilles, *Phys. Rev.*, **46**, 1015 (1934); L. B. Loeb, *Fundamental Processes*, pp. 441 ff.

[27] H. Raether, *Zeits f. Physik*, **107**, 91 (1937).

[28] K. Zuber, *Ann. d. Physik*, **76**, 231 (1925); M. von Laue, *ibid.*, **76**, 261 (1925).

[29] W. Rogowski and A. Wallraff, *Zeits. f. Physik*, **102**, 183 (1936); W. Rogowski and W. Fuchs, *Archiv f. Elektrotechnik*, **29**, 362 (1935); W. Fuchs, *Zeits. f. Physik*, **98**, 666 (1936); W. Rogowski and A. Wallraff, *ibid.*, **108**, 1 (1938).

[30] H. J. White, *Phys. Rev.*, **48**, 113 (1935); W. Rogowski and A. Wallraff, *Zeits. f. Physik*, **97**, 758 (1935).

[31] L. B. Loeb, *Rev. Modern Phys.*, **8**, 267 (1936).

[32] L. B. Loeb, *Science*, **69**, 509 (1929).

[33] L. B. Loeb, *Fundamental Processes of Electrical Discharge in Gases*, p. 415.

[34] L. B. Loeb, *Rev. Modern Phys.*, **8**, 280 (1936); L. B. Loeb, *Fundamental Processes of Electrical Discharge in Gases*, p. 407.

[35] L. B. Loeb, *ibid.*, p. 407.

[36] W. Holzer, *Zeits. f. Physik*, **77**, 676 (1932); R. Strigel, *Wiss. Veröffent. aus den Siemens-Werken*, **15**, 68 (1936); T. E. Allibone and J. M. Meek, *Proc. Roy. Soc.*, **A, 166**, 97 (1938); **A, 169**, 246 (1938).

[37] H. Raether, *Zeits. f. Physik*, **96**, 567 (1935); E. Flegler and H. Raether, *ibid.*, **99**, 635 (1936); **103**, 315 (1936); H. Raether, *ibid.*, **107**, 91 (1937); **110**, 611 (1938); **112**, 464 (1939).

[38] F. G. Dunnington, *Phys. Rev.*, **38**, 1535 (1931); L. von Hamos, *Ann. d. Physik*, **7**, 857 (1930); H. J. White, *Phys. Rev.*, **46**, 99 (1934); R. R. Wilson, *ibid.*, **50**, 1082 (1936).

[39] A. F. Kip, *ibid.*, **54**, 139 (1938); **55**, 549 (1939); G. W. Trichel, *ibid.*, **55**, 382 (1939); L. B. Loeb and A. F. Kip, *Jour. Applied Phys.*, **10**, 142 (1939).

[40] H. Raether, *Zeits. f. Physik*, **112**, 464 (1939).

[41] J. M. Meek, *Phys. Rev.*, **57**, 722 (1940); L. B. Loeb and J. M. Meek, *Jour. Applied Phys.*, **11**, 438, 459 (1940).

[42] J. M. Meek, *Proc. Phys. Soc.*, **52**, 547, 822 (1940).

[43] W. Braunbek, *Zeits. f. Physik*, **39**, 6 (1926); **107**, 180 (1937).

[44] G. Hertz, *Zeits. f. Physik*, **106**, 102 (1937).

Chapter II

THE STREAMER THEORY OF SPARK DISCHARGE

1. Anode Space-Charge Field Due to an Avalanche

One may begin by considering a plane-parallel gap of $\delta = 1$ cm length in which the cathode is illuminated by ultraviolet light to such an extent that one electron per microsecond leaves one square centimeter of cathode area. Assume that in air at atmospheric pressure the potential across the plates is 31,600 volts, which is the *conventionally* observed sparking potential V_s. The ratio $X/p = 41.6$ volts/cm per mm Hg.

Let us then calculate what happens in the field to one of these electrons. It starts across the gap, quickly acquiring an average random energy of some $E = \frac{1}{2}mC^2 = 3.6$ electron volts and a drift velocity v in the field direction of about 1.5 to 2×10^7 centimeters per second as measured by White[1] and Raether.[2] As it moves it creates new electrons at the rate of α per centimeter in the field direction so that in a distance x it and its progeny amount to $e^{\alpha x}$ electrons, forming what is called an *electron avalanche*. Therefore, $e^{\alpha x}$ positive ions have been left behind by the electron group, virtually where they were formed in the 10^{-7} second of advance for the electrons in the distance $x = \delta$ across the plates. (The mobility of the positive ions is of the order of 10^{-2} to 10^{-4} that of the electrons.) As the electron avalanche advances, its tip is spreading *laterally* by the random diffusive movement of the electrons. The rate of diffusion of such an avalanche has been experimentally measured by Raether[2] and is found to be about what one would expect from theory based on the velocity v. The average radial distance of diffusion can be calculated from Raether's equation giving $\bar{r} = \sqrt{2Dt}$, where $t = x/v$ is the time of advance of the avalanche and D is the coefficient of diffusion which may be esti-

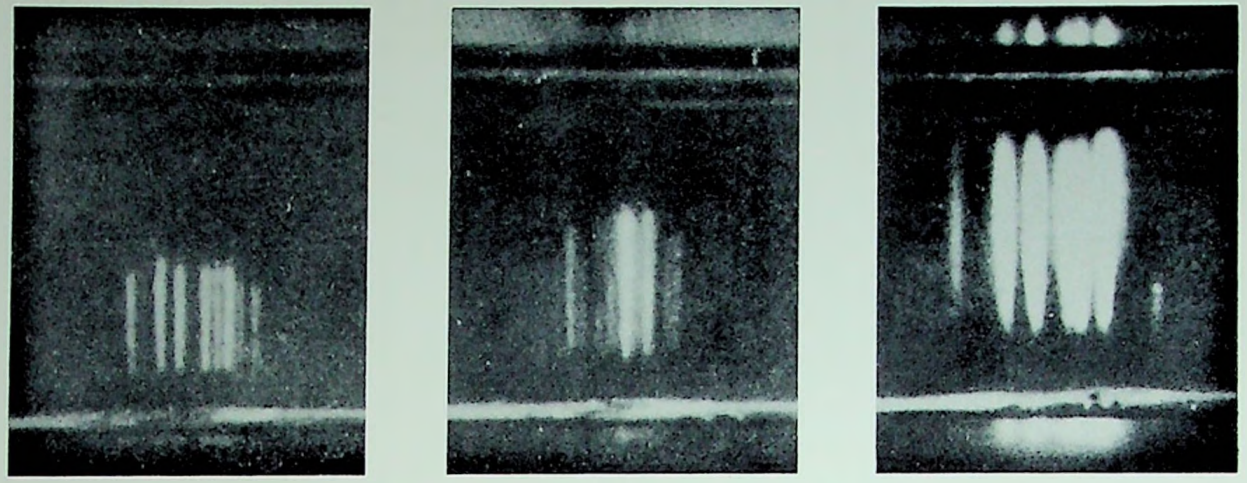

FIG. 6.—Tracks of electron avalanches photographed in a cloud chamber by Raether. Electrode spacing 3.6 cm. The upper electrode is the anode. The gas is H_2 in both *a* and *b* at 525 mm Hg. Field strength 11,000 volts/cm. In *c* the pressure is 275 mm Hg and the field strength is 7000 volts/cm. Note the greater diffusion width of the channel at lower pressures. The duration of the applied impulse voltage is $a = 1.07 \times 10^{-7}$ second, $b = 1.74 \times 10^{-7}$ second. $c = 2.6 \times 10^{-7}$ second. The difference in length between the tracks in *a* and *b* represents 6.4×10^{-8} second travel, which enables the velocity to be computed directly.

mated from v.* From these data it is possible to compute the density of positive-ion space charge left behind at any point x. The value of α under these conditions is about 17, making $e^{\alpha\delta} = e^{17}$ or 2.4×10^7. The first ion pair is created at 0.0407 cm from the cathode. At 0.5 cm from the cathode there are 4914 ions, at 0.75 cm there are 3.66×10^5 ions, and within 0.0407 cm from the anode there are 1.2×10^7 ions. Most electrons will be drawn to the anode except for some few that are bound by the positive ions, making a sort of a conducting discharge plasma in the avalanche path. Cloud-track pictures of such avalanches as they proceed across the gap with time intervals of 10^{-7} second between pictures are shown in Figure 6 as taken by Raether.[2] A schematic diagram of this is shown in Figure 7.

Such a distribution of ions does not make a conducting filament of charges across the gap, and hence in itself an avalanche that has crossed does not constitute a breakdown of the gap. In some 10^{-5} second, the positive ions created could cross the gap and these could lead by secondary mechanism at the cathode to the beginning of a Townsend form of breakdown. However, long before this time interval, the spark has passed and the discharge is nearly over. Thus one must look further for the mechanism of the spark.

Let us calculate the field due to the positive ions at the anode where they are most densely packed after the electrons have entered the anode. While the ions are not in a spherical volume (they are in a nearly conical channel with an apex of maximum density at the anode), it is, however, simpler for purposes of calculation to assume that the ions are largely in a sphere of radius r, to be defined, at the end of the avalanche and to compute the space-charge field at the surface from the density of the charge. The field strength X_1 due to this space charge is $4\pi q\epsilon/4\pi r^2$, where ϵ is the electronic charge and q is the number of charges in the sphere. Now $q = \frac{4}{3}\pi r^3 N$, where N is the ion

* According to G. Jaffé $\bar{r}$ is more properly $\sqrt{4Dt}$. The numerical error introduced by the use of 2 in what follows is not of great importance.

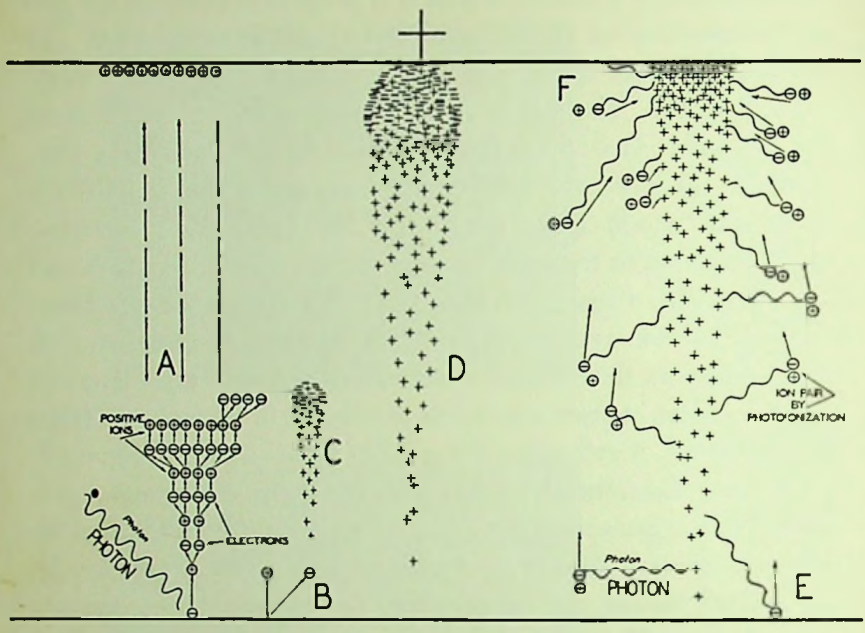

FIG. 7.—Schematic figure showing, *A*, the electron multiplication of electrons by the cumulative ionization of a single electron liberated from the cathode by a photon; *B*, illustrating a secondary electron emitted from cathode by a + ion, which has a chance of occurrence γ; *C*, the development and structure of an avalanche, with + ions behind electrons at the tip; *D*, the avalanche has crossed the gap, spreading by diffusion; *F*, the later history of an avalanche. Electrons have disappeared into anode. Positive space-charge boss appears on cathode at *F*. Ion pairs out from the trail indicate the appearance of photoelectric ion pairs *in the gas* produced by photons from the avalanche. These were omitted from *C* and *D*; they are denser in the channel from which they are omitted for the sake of clarity. *E* shows a photoelectron from the surface of the cathode produced by the avalanche.

density. Thus $X_1 = \frac{4}{3}\pi r N\epsilon$. In a distance dx at the end of a path x, the number of ions resulting from cumulative ionization is $ae^{ax}dx$ and

$$N = \frac{ae^{ax}dx}{\pi r^2 dx} = \frac{ae^{ax}}{\pi r^2} \tag{17}$$

Hence

$$X_1 = \frac{4}{3}\epsilon a e^{ax}/r \tag{18}$$

Now r is the value of $\bar{r}$ caused by electron diffusion in crossing the gap which is $\bar{r} = \sqrt{2Dt}$. Hence

$$X_1 = \frac{4\epsilon a e^{ax}}{3\sqrt{2Dt}} = \frac{4\epsilon a e^{ax}}{3\sqrt{2D(x/v)}} = \frac{4\epsilon a e^{ax}}{3\sqrt{\left(\frac{2D}{k}\right)\left(\frac{x}{X}\right)}} \tag{19}$$

where v is the electron velocity and k is the mobility. For rough calculation r as observed by Raether is $r = 0.013$ cm, which makes $X_1 = 6{,}000$ volts per centimeter, or $X_1/X = 0.20$. Thus the field caused by the space charge is 20 per cent of the applied field near the cathode. Had an overvoltage of 5 per cent been applied, making $X/p = 43.6$, α would have been 20 and X_1 would have been 140,000. Thus part of the electron swarm would not have crossed the gap completely, for it would have been held back by the heavy space charge some 0.9 of the way across from the cathode unless other actions, to be discussed, take place.

2. Photoelectric Ionization in Gas as a Secondary Mechanism

Accompanying the cumulative ionization there is produced by the electrons from four to ten times as many excited atoms and molecules. Some are excited to an energy exceeding the ionizing potential of some of the atoms and molecules present, either by excitation of an inner shell, by ionization and excita-

tion, or in a mixed gas like air by the excitation of molecules of higher ionizing potential, e.g., N_2. These excited atoms or molecules emit radiations of very short wave length in some 10^{-8} second. This short ultraviolet radiation is *highly absorbed* in the gas and leads to ionization of the gas. In fact, the whole gas and the cathode as well are subjected to a shower of photons of all energies traveling from the region of dense ionization with the velocity of light. Thus nearly instantaneously in the whole gap and from the cathode new photoelectrons are liberated which almost at once begin to ionize cumulatively. Such photons have been observed in corona discharge by Cravath and Dechene,[3] in Geiger counters by Greiner,[4] in parallel gaps with sparks by Paetow,[5] and at the cathode in high-pressure positive corona by Kip,[6] as well as by means of cloud tracks by Raether and Costa.[7]

3. The Mechanism of Positive Streamer Formation

The photoelectrons created at points in the gas and at the cathode at any great radial distance from the avalanche axis will merely create other avalanches. Those in the gas will be short and those coming from the cathode region will be long and like that of the initial avalanche. Being smaller and, in any case, later in creation than the parent avalanche, such avalanches will be of no interest in breakdown. However, those photoelectrons created near the space-charge channel of positive ions, and especially near the anode, will be in an enhanced field which exerts a directive action drawing them into itself. If the space-charge field X_1 is of the order of magnitude of the imposed field X, this action will be very effective. In addition the values of α in this region will be much enhanced.

The electrons from the intense cumulative ionization of such photoelectron avalanches in the combined fields X and X_1 which are drawn into the positive space charge feed into it, making it a conducting plasma which starts at the anode. The added fields will be most effective along X and so will the ionization. The

positive ions they leave behind will therefore extend the space charge toward the cathode. These electrons also create photons which produce electrons to continue this process. *In this fashion the positive space charge develops toward the cathode from the anode as a self-propagating positive space-charge streamer.*

Such streamers have been observed and studied in positive-point corona discharge by Trichel, Kip and Loeb.[8] They have also been photographed in cloud tracks by Raether,[9] as shown in Figures 8 and 9. The way in which these streamers progress is shown schematically in Figures 7 and 10. Their velocity of propagation, dependent as it is on photo-ionization in the gas and photon propagation with the velocity of light as well as *short-distance motion of electrons in high fields near the space charge*, is rapid. It is probably distinctly more rapid than the velocity of 2×10^7 cm/sec of the initial electron avalanche,[9] being of the order of 1.3×10^{-8} cm/sec as observed by Raether in one case.

As the streamer advances toward the cathode it produces a filamentary region of intense space-charge distortion along a line parallel to the field, the potential distribution along which is shown in Figure 11. The conducting streamer of a plasma consisting of electrons and ions extending to the anode thus makes a very steep gradient at the cathode end of the streamer tip. As this advances toward the cathode the photoelectron avalanches produced by radiation at the cathode, especially at the intercept of the extended streamer axis at the cathode, begin to produce an intense ionization near the cathode. Hence positive ions created there may increase the secondary emission. Thus, as the space-charge streamer approaches the cathode a cathode spot is forming which may become a source of visible light. These are seen in Dunnington's Kerr cell pictures[10] in Figure 12. *When the streamer reaches the cathode there is a conducting filament bridging the gap.* As the streamer tip reaches the cathode the high field produces a rush of electrons toward the end of the streamer. This, if followed by a current of elec-

trons, gives a high-potential wave which passes up the pre-ionized conducting channel to the anode, multiplying the electrons present by a large factor. The channel is thus rendered highly conducting. If the metal can emit a copious supply of electrons because of the formation of an efficient cathode spot, the current of electrons continues up the channel maintaining its high conductivity and even increasing it. This current, unless limited by external resistance, will then develop into an arc. It is, however, the intense increase in ionization by the potential wave which gives the highly conducting channel characterizing the spark. The velocity of propagation of the returning wave of ionization up the pre-ionized channel may be exceedingly great. It reaches 10^8 to 10^9 cm/sec in stepped leader strokes and 10^{10} cm/sec in the return stroke in lightning discharge.[11] Similar velocities have been observed by Allibone and Meek[12] in long sparks. This mechanism was first invoked by Cravath and Loeb[13] in an attempt to explain the velocity of the stepped leader strokes. It was later developed by Schonland,[14] who showed that the velocity of propagation depended on the ion density in the pre-ionized channel and on the gradient of the potential wave.

4. The Quantitative Criterion for Streamer Formation

It was seen above that the action of the radial field X_1 of the positive space-charge residue left by an avalanche that had crossed a gap could be such as to draw into itself photoelectrons and propagate as a positive-anode streamer to the cathode. It was shown that such a streamer that had crossed the gap short-circuited the electrodes by means of a conducting filament of plasma, thus being in a condition to discharge the plates and so giving a spark. It was further seen that the positive-ion space-charge fields at the anode of a gap at the sparking potential were of considerable magnitude. The presence of the proper kind of photo-ionization in the gas was indicated to have been observed ex-

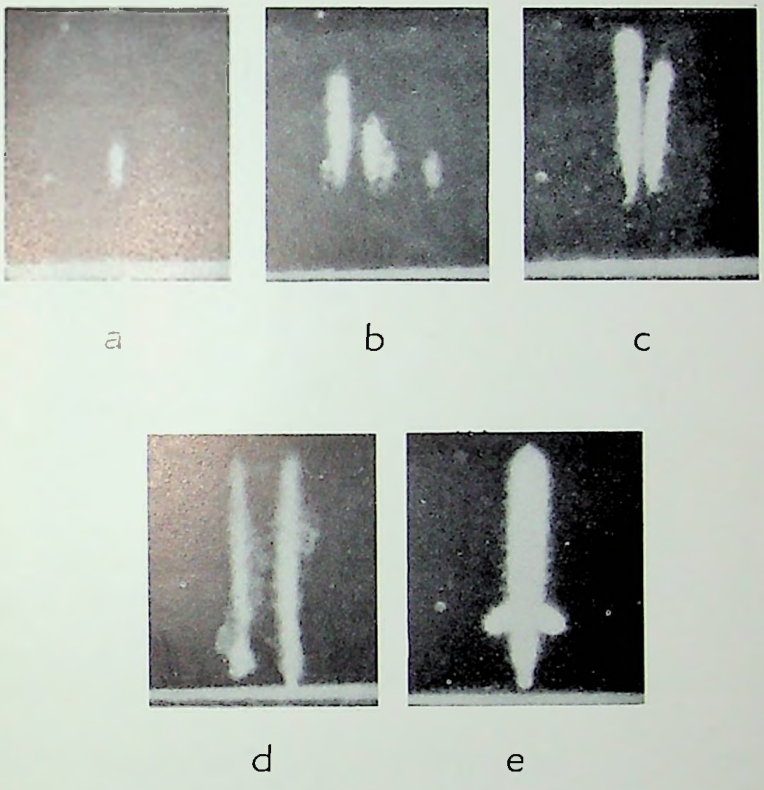

FIG. 8.—The development of an avalanche into a streamer as photographed by Raether at about 260 mm Hg at 20° C. in H_2O-alcohol air mixtures, expansion ratio 1.13. The field strength was initially 11.800 volts/cm in *a*. The field strength increases in *b* and *c* and at about 12.200 volts/cm it causes the return streamers to cross the gap as they do in *d* and *e*. Note the branching in *e* and the cathode spot that developed in the right-hand streamer in *d* and the streamer in *e*. The low expansion ratios cause condensation on chemical products in the avalanche so that only the *core* of the discharge is seen without its mass of diffused ions and electrons.

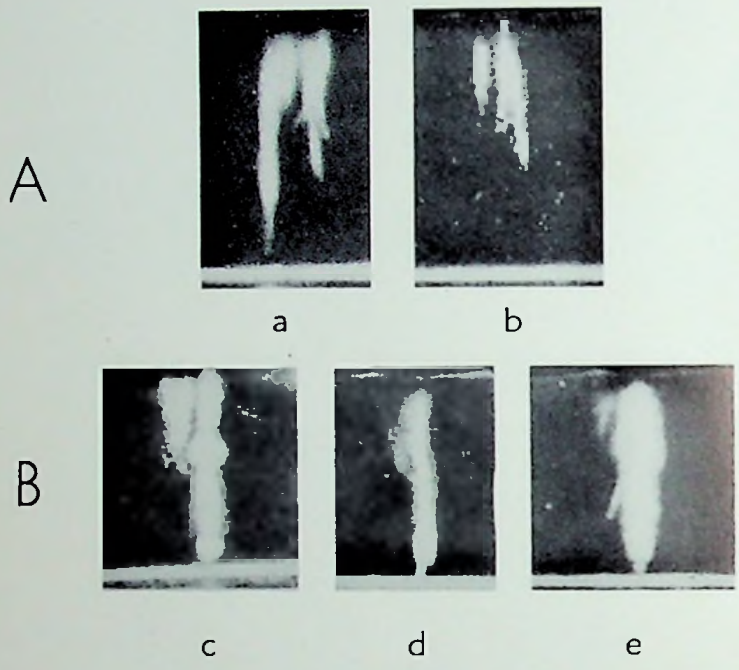

FIG. 9.—Discharge streamers observed by Raether

A (*a*, *b*). conditions similar to those in Figure 8 with only the time of the impulse field increased so that the streamer could progress farther toward the cathode. The streamer velocity observed was 1.1 to 1.3×10^8 cm/sec. Note the advance of the streamer well past midgap in *a*, while in *b* it has not advanced as far. Note also the avalanche that has not developed to a streamer to the left in *b*. Note the evidence of branching in these streamers.

B (*c*, *d*, *e*). discharge streamers crossing the gap observed by Raether in longer time intervals. In these cases a distinct cathode spot has formed and the bright return stroke is taking place. The discharge in *c* has developed farther than the others. The wedge at the left of *c* is the core of the head of an avalanche that came too late to form a streamer.

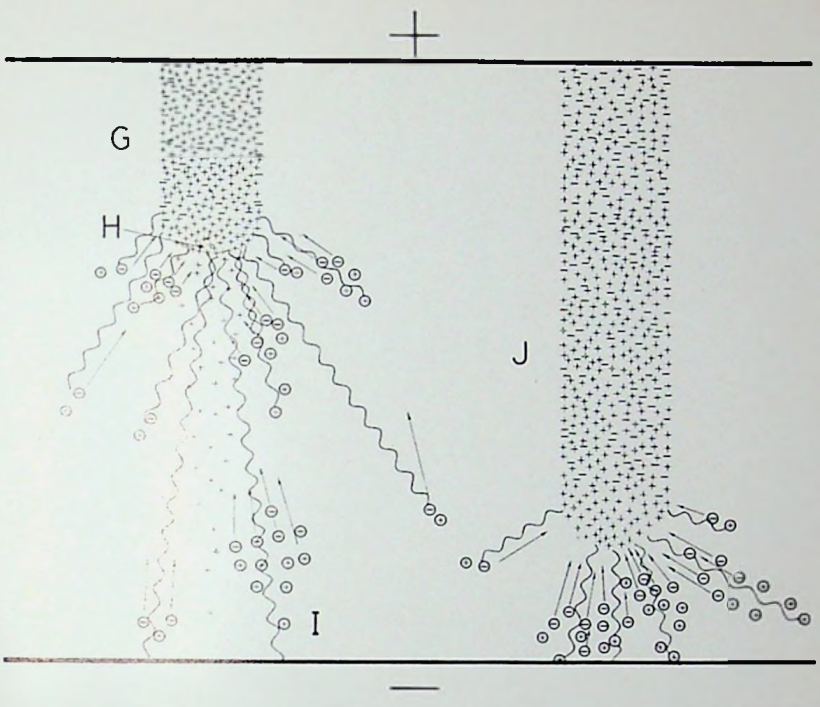

FIG. 10.—This figure carries further the schematic diagram of Figure 8, showing the growth of a streamer. In Figure 8 at *F* one sees the positive space-charge boss ready to move toward the cathode by photo-ionization. At *G*, in Figure 10, one sees the channel of *plasma* which has advanced one-third the way across the gap with its positive tip at *H*. The photo-ionization about the tip is shown with some ionization at the cathode at *I*. In *J* we see the streamer as it approaches the cathode. The intense photo-ionization and photoelectric liberation from the cathode is indicated. It is perhaps not emphasized sufficiently, for Raether's pictures show a strong cathode spot at this stage.

FIG. 11.—Space potential of streamer

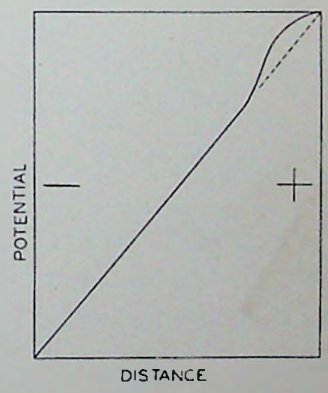

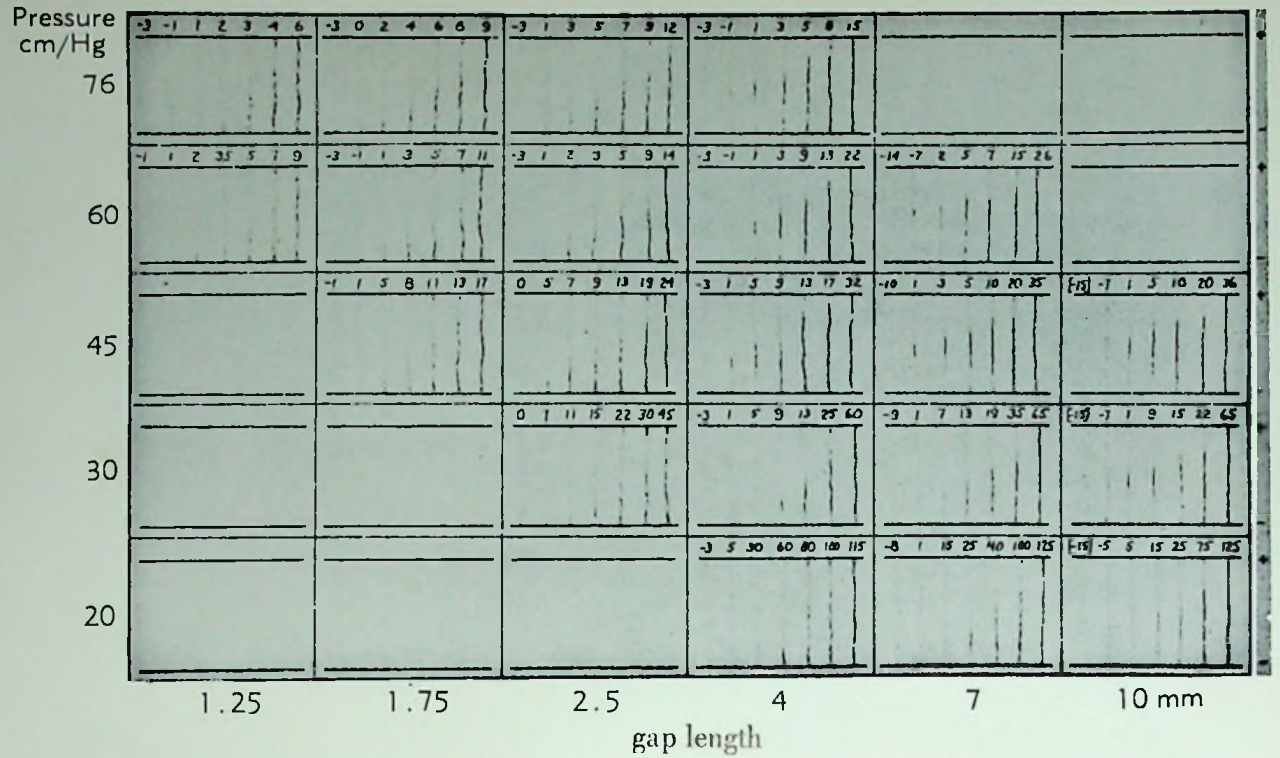

FIG. 12.—Dunnington's Kerr cell photographs

perimentally. Finally the existence of such streamers has been amply demonstrated in positive-point corona discharge and some of their characteristics have been established. Thus the possibility that at higher $p\delta$ the plane-parallel spark gap may break down by a positive-streamer mechanism has been demonstrated. It now remains to determine under what conditions such a streamer formation can occur and whether or not such conditions as are needed do exist.

First it is clear that an adequate density of photo-ionization must exist in the gas near the space charge to insure a continuous supply of electrons. This will depend on the diffusion in the electron avalanche (i.e., concentration of the space charge and photon production in a small volume) and on the absorption coefficients of the molecules or atoms for the active photons produced in the avalanche. If the space-charge channel is broad and the absorption of the photoelectrically active radiations is small, streamer formation cannot occur. Thus at low pressures streamer formation would be unlikely.

Secondly, the positive space-charge field must be such as to insure that those photoelectrons produced are drawn into the channel and that in being drawn in they sufficiently increase so as to produce an adequate supply of electrons to advance the tip.

Thus streamer formation requires adequate photo-ionization and adequate fields at the streamer tip. The necessary magnitude of both these quantities for streamer propagation must be established. The question of the density of ionization needed will be discussed at a later point. Suffice it to say that in air at atmospheric pressure it is more than adequate for gaps under 10 cm length. There are, however, conditions where this is not the case.

The question of the magnitude of the field required for streamer propagation was the question which remained unanswered until Meek[15] proposed the following simple solution. In order that the electrons needed feed into the space-charge

tip, the radial field X_1 at the surface of the hemispherically considered positive space charge must equal the impressed external field X. Applying this criterion, Meek at once obtained reasonable values of the sparking potential in air. This criterion was thus adopted for practical purposes. Further study has indicated that the field X_1 need not exactly equal the impressed field. In fact, as will later be seen, the numerical results are quite insensitive to the criterion set and we should more properly set the condition as $X_1 = KX$. Here K is a factor lying between the limits $0.1 < K < 1$ for air. It may conceivably even vary slightly with changing conditions. The physical significance of the criterion is obvious. If $X_1 = KX$, then those photoelectrons created near the tip of the space-charge avalanche will be quite certain to feed into it. Whereas, if $K \ll 1$ the chance for this is small. Physically a more complicated and esoteric criterion is required. Such a condition would be that the combined field $f(\overline{X}_1 + \overline{X})$, at the distance of a certain number of ionizing free paths, must be of such magnitude that for n photoelectrons produced in this volume, the $ne^{\int a dx}$ positive ions produced are enough to maintain the space-charge density as it advances. In our ignorance of the photon production, photoelectric ionization, absorption coefficients for photons, etc., the more appropriate criterion above would be hopelessly complicated and we could derive no theory. The very simple criterion of Meek, rough and loose though it be, owing to the nature of the processes involved, appears to be sufficiently successful to warrant its future use as a criterion. For the purposes of the present considerations we will set $K = 1$. At a later point an attempt will be made in view of existing numerical data to fix a more satisfactory value for K.

We are now in a position to apply the Meek condition, that the radial tip field X_1 equal the impressed field X when the gap length has reached a value $x = x_1$, such that a spark can pass, to the equations deduced for the field produced by an avalanche after an advance of x_1 cm.

It has been shown in Equation 19 that

$$X_1 = \frac{4\epsilon a e^{ax}}{3\sqrt{\left(\frac{2D}{k}\right)\left(\frac{x}{X}\right)}},$$

and here we set $X_1 = X$ at $x = x_1$ in order that a streamer form at some distance x_1. Before doing so, however, it is necessary to make certain transformations essential for evaluation of the constants. The ratio of D/k for electrons in a field has been shown by Townsend[16] to be expressed as

$$\frac{D}{k} = \left(\frac{P}{N\epsilon}\right)\left(\frac{c_1^2}{c^2}\right).$$

Here P is the gas pressure in dynes per square centimeter where there are N molecules per cubic centimeter, so that $P/N\epsilon$ is the gas pressure in dynes per square centimeter divided by the Faraday constant per cubic centimeter. The ratio of the *average* energy of the electrons to the average energy of the gas molecules defining P is c_1^2/c^2, which is also the ratio of electron temperature T_e to that of the gas T. Now Townsend[17] has shown how to evaluate $T_e/T = c_1^2/c^2$ when fields are so low that ionization and excitation by electron impact do not occur. Druyvesteyn[18] and Smit[19] have shown how to evaluate c_1^2 or T_e when elastic or elastic and inelastic impacts occur. In the high-energy region, however, the problem is extremely difficult and data needed for molecular gases are missing, so that the solution has never been worked out. Karl T. Compton[20] gives an approximate equation for c_1^2,

$$c_1^2 = 1010\frac{\epsilon X \lambda_0}{mp\sqrt{f}} \qquad (20a)$$

Here λ_0 is the electron-free path at 760 mm, f is the average fraction of energy lost per impact, and p is the pressure in millimeters of Hg. Below the ionization and excitation potentials in inert gases, $f = 2.66\ m/M$. For molecular gases, and above

excitation energies, f is greater but unknown. From Ramsauer's curves λ_0 can be obtained if the electron energy is roughly known. The expression for X_1 becomes

$$X_1 = \frac{\frac{4\epsilon a e^{ax}}{3}}{\left(\frac{2Pc_1^2 x}{N\epsilon c^2 X}\right)^{1/2}} = \frac{\frac{4\epsilon a e^{ax}}{3}}{\left(\frac{2Px}{N\epsilon X}\right)^{1/2}\left(\frac{1010\epsilon X\lambda_0}{mc^2 p\sqrt{f}}\right)^{1/2}}$$

$$= \frac{\frac{4\epsilon a e^{ax}}{3}}{\left(1010\frac{2Px\lambda_0}{3NkTp\sqrt{f}}\right)^{1/2}} = \frac{\frac{4\epsilon a e^{ax}}{3}}{\left(1010\frac{2x\lambda_0}{3p\sqrt{f}}\right)^{1/2}} \qquad (21)$$

In view of the unknown character of the term $\lambda_0/\sqrt{f}$, one must attempt to find data with which to evaluate this quantity. Now, as is well known from studies of electron mobility, the electron velocity

$$v = 0.815\frac{\epsilon\lambda_0 X}{mc_1 p} \qquad (20b)$$

Since c_1 is given in terms of $\lambda_0/\sqrt{f}$, an experimental evaluation of v under sparking conditions such as those made by White[1] or Raether[2] will give $\lambda_0\sqrt{f}$. Using the value of $v = 1.25 \times 10^7$ cm/sec as given by Raether at $X/p = 41$, one finds $\lambda_0\sqrt{f} = 5.7 \times 10^{-6}$. Brose and Saayman[21] give the electron free path in air at about 3 volts energy as $\lambda_0 = 3.6 \times 10^{-5}$ cm. This makes $f = 0.025$ and $\lambda_0/\sqrt{f} = 3.6 \times 10^{-5}/(0.025)^{1/2} = 2.28 \times 10^{-4}$. Actually, both λ_0 and f are functions of electron energy so that $\lambda_0/\sqrt{f}$ will change somewhat with electron energy, i.e., with X/p. Therefore, the use of a constant value of $\lambda_0/\sqrt{f}$ over an extended range of X/p is not exact. However, it will not change by more than a factor of 2 or 3 in the range of X/p for high-pressure sparks, from 20 to 45. Thus we write approximately,

$$X_1 \simeq \frac{\frac{4\epsilon a e^{ax}}{3}}{\left(0.133\frac{x}{p}\right)^{1/2}} \simeq \frac{1.76\times 10^{-9} a e^{ax}}{(x/p)^{1/2}} \text{ e. s. u.}$$

or

$$X_1 \simeq 5.27\times 10^{-7}\frac{a e^{ax}}{(x/p)^{1/2}} \text{ volts/cm} \qquad (22)$$

5. The Meek Equation for Spark Breakdown at Atmospheric Pressure

Now if $x=\delta$, the gap length for a plane-parallel gap, the condition for the sparking *threshold* is that $X_1 = X_s$, with X_s the sparking field, for this insures a streamer crossing the gap and giving a spark. Then

$$X_s\left(\frac{\delta}{p}\right)^{1/2} = 5.27\times 10^{-7} a e^{a\delta}, \frac{X_s}{p}\left(\frac{\delta}{p}\right)^{1/2} = 5.27\times 10^{-7}\frac{a}{p}e^{\frac{a}{p}(p\delta)} \qquad (23)$$

so that

$$\frac{a}{p}(p\delta) + \log_e\frac{a}{p} = 14.46 + \log_e\frac{X_s}{p} - \tfrac{1}{2}\log_e p\delta + \log_e\delta \qquad (24)$$

For an overvolted gap at $X_1 = X_s + \Delta X_s$, $x = x_0 < \delta$. Here midgap streamers form and breakdown proceeds rapidly and effectively.

For any other field distribution, streamer formation will follow when for $X_1 = X_s$, with X_s the sparking field, the electron avalanche has traversed a length x_s such that

$$X_1 = X_s = \frac{\frac{4}{3}\epsilon a_{x_s} e^{\int_0^{x_s} a\,dx}}{\left(1010\frac{2x_s\lambda_0}{3p\sqrt{f}}\right)^{1/2}} =$$

$$5.27\times 10^{-7}\frac{a_{x_s} e^{\int_0^{x_s} a\,dx}}{(x_s/p)^{1/2}} \text{ volts per cm,} \qquad (25)$$

provided that enough density of ionization is achieved to insure photoelectrons. Here, since the field and thus X/p varies with x, α depends on x and α_x, is the value of α at the end of the avalanche x_s where great multiplication occurs. This permits a more general application of streamer formation to break down as will later be seen.

Consider again the plane-parallel gap at the sparking threshold. Since we have values of α/p as a $f(X/p)$ it is clear that, given δ and p, X_s/p can be determined by the values of X/p and α/p which satisfy the equation above. The evaluation of X_s/p can be achieved only by trial and error, but with practice it becomes relatively easy as will be shown in chapter iii. A solution by Meek gave $X_s/p = 42.2$ (when $\alpha = 18.6$) for the spark in air. This makes $X = 32.2$ kilovolts per centimeter, which is close to the conventional value of 31.6 kilovolts per centimeter. More accurate data for $\lambda_0/\sqrt{f}$ may give a value slightly below the *conventional sparking potential,* for the criterion sets the *threshold for a spark* and conventional values of V_s are slightly above the threshold value. However, as stated, the criterion that $X_1 = X_s$ is in itself only very rough. This question, in its relation to the sparking threshold, will later be discussed in detail. It suffices here to note that approximately correct values of V_s can be computed with no assumed value of γ and with no arbitrary constants.

6. Meek's Equation and Paschen's Law

It is to be noted that Equation 24 expresses X_s/p as a function of α/p and of $p\delta$, except for the term $\log_e \delta$. In other words, except for this term, X_s/p is a function of $p\delta$. The experimentally observed relation that X_s/p, and hence the sparking potential V_s, varied with the value not of δ or p independently, but with the product $p\delta$, is called Paschen's law.[22] It has been tested extensively and verified at lower pressures. It is usually assumed to hold at higher pressures, though no careful test has

been made of it for large values of δ at atmospheric pressure. It is doubtful, in view of the considerable differences used in setting criteria for evaluating the *conventional* sparking potential, with the consequent variation of the values given, whether the accuracy of the results of the past is adequate to test the question. There is no doubt, however, but that such a study should be made, since on its result the proof of this theory depends.

As previously indicated, Paschen's law has been deduced by numerous workers in a general way on the mechanism assumed by Townsend.[23] Its validity rests not on Townsend's mechanism in detail, but on the circumstance that in the theory the coefficients a/p and γ are both assumed to be functions of X/p. The physical meaning of the law is that *the sparking potential and the value of* X_s/p *are determined by the total number of molecules which an electron encounters in a linear path across the gap*, i.e., on the number of ions created. For it is on such encounters that the number of ions is conditioned and it is on the *total ion production* that the mechanism depends. We are now, however, dealing with a new mechanism in which we picture as the essential criterion, *not the total number of ions* formed in a linear succession of processes, but the *density of ions.* This density is achieved in a distance of travel δ without reference as to how many secondary electrons are produced, except that these must be adequate. If there are gases in which, when $X = X_s$, photo-ionization is not adequate, the theory must be modified as will later be seen. It is probable, however, that in all gases at the value of X_s operative for sparks up to 10 cm, enough photoelectrons will be produced. Thus the criterion set requiring a certain *density* of ions produced by primary process introduces a new element into the theory irrespective of the secondary process. Under these conditions, as pointed out by Varney,[24] who studied spark breakdown as a result of ionization by collision in a gas with positive ion space-charge production by ion movement, the use of ion densities instead of

numbers of ions formed leads to a small deviation from Paschen's law.

At low values of $p\delta$, where the Townsend theory applies, Paschen's law is strictly obeyed, as numerous investigators have found.[22, 36] The deviations from Paschen's law due to the space-charge factor in Meek's theory are shown in the table below. The sparking potentials V_s in kilovolts are calculated for various values of $p\delta$ and δ. If Paschen's law held, then the values of V_s would be constant for a given $p\delta$.

TABLE I

$p\delta$ mm × cm	V_s in kilovolts		
	$\delta = 0.1$	$\delta = 1.0$	$\delta = 10.0$
7,600	245	248	249
760	31.5	32.3	32.9
380	18.0	18.6	18.9

The computed deviations are within the limits of uncertainty of the existing sparking potentials.

7. Comparison of Meek's Equation as a Function of Pressure with Experiment

The curve of sparking potential V_s in air against $p\delta$ plotted to logarithmic scale is shown in Figure 13 using Sanders' values[25] of α/p as a $f(X/p)$ up to $X/p = 160$ in air, and for higher values Posin's data[26] on N_2 are used. The experimental curve shown as dotted is that given by Whitehead[27] as the mean of the data of a number of workers. Theory and experiment agree from $p\delta = 10^4$ down to nearly $p\delta = 10^2$ mm × cm. For values of $p\delta \sim 100$, the calculated values are higher than those observed and the deviation increases steadily with decreasing $p\delta$ and thus with increasing X/p. The deviation becomes notable at the values of X/p where the abrupt termination of the curves *giving an α without a γ* are being replaced by curves with a measurable value of γ. In other words, the deviation of the theoretical V_s from experiment on the new theory occurs at

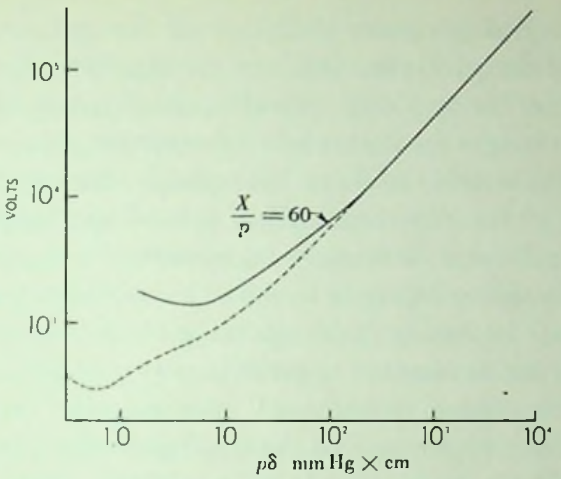

FIG. 13.—Meek's $V_s - p\delta$

just the values of $p\delta$ where streamer formation ceases to be possible and the Townsend theory of the mechanism of low-pressure sparks becomes applicable. This means that as $p\delta$ becomes very low the space-charge densities of positive ions in avalanches, owing to attenuation of the density of molecules, become less efficient in causing spark breakdown than the mechanism of Townsend probably because of inadequate photo-ionization in the gas. At this point, the formative time lags of sparking begin to be materially higher than is the case with high-pressure sparks, as seen in chapter i. It is not inconceivable that the Meek equation at lower pressures could be followed to lower values of $p\delta$ by using square wave pulses of high potential less than 10^{-6} second long. In these the Townsend breakdown would be suppressed and the value of V_s would continue along Meek's curve.

8. Streamer Formation and Sparking Threshold

It was noted on page 42 that there is some uncertainty in the exact value of K to be used in setting Meek's criterion for a spark. This question must now be further studied and is a particularly involved one. It comprises: First, the question of

the efficiency of the photo-ionization of the gas; secondly, the question of statistical time lags and the significance of a threshold value for the sparking potential; thirdly, the effect of considerable changes in the values of constant terms in Meek's equation on the value of X_s or V_s; fourthly, the significance and reliability of the experimentally observed sparking potentials.

a) As will later be seen, in air except at low pressures and for gaps exceeding 10 cm in length at atmospheric pressures the photoelectric ionization under sparking conditions appears adequate at the fields required to produce the spark when $X_1 = KX$. Thus in this discussion one need have no great concern about the approximate adequacy of the density of photo-ionization.

b) In the development and progress of the streamer the number of photons effective for propagation within regions about the tip where multiplication is effective is not great. Of the photoelectrons produced, the most effective ones will be those along the streamer axis within a distance s of the tip surface such that $\int_0^s \alpha dx$ is a maximum. This is because along the axis the fields X_1 and X add such that $X_a = X_1 + X$. At a point at right angles to the streamer axis at its tip the field is $X_p = \sqrt{X_1^2 + X^2}$. This field is much less and will not be very effective in feeding the streamer. Since in this region of X/p, α is very sensitive to changes in the total field (X_a or X_p), this circumstance is most important. This may explain why, for shorter sparks near atmospheric pressure, the spark channels are nearly straight.[1,10] Here adequate electrons are present along the axis. Where paths are longer or the pressure is low, the density of photoelectrons is not as great. Hence, the channel may have to develop by any photoelectrons produced in the active volume, as we shall see. This will increase the chance of crooked or branched sparks as is experimentally observed.[12]

Since there are so few photoelectrons involved in streamer propagation, these must be subject to a considerable statistical fluctuation in the advance of a streamer. If this fluctuation is such at one point of the advance as to give too few electrons,

propagation ceases and the avalanche does not produce a spark. Now the larger X_1, relative to X, i.e., the larger K, the more effective any photoelectrons become. Hence, as K is increased the fluctuations due to the photo-ionization are decreased in their effectiveness in interrupting the streamer advance. It is thus clear that at some low value of K it is *possible* for an avalanche to give a streamer that crosses the gap. It is, however, *not probable* that one will do so. There are thus, under any given set of conditions, values of K below which the chance of the development of an avalanche to a streamer is so small that the value of K under these conditions constitutes a sparking threshold. Above these values of K a greater and greater proportion of the avalanches yield streamers that cross the gap as K increases. Hence, with a constant number of electrons initiating avalanches, the number of sparks observed depends on K.

From this, one can conclude that for a given number of electrons per second, i_0, starting avalanches from the cathode the chance of a spark appearing within a stated time interval, T, after applying a given potential, V_s (number of electrons $\frac{i_0 T}{\epsilon}$), depends on the value of K corresponding to that value of V_s. If one considers that a spark appearing within $T = 30$ sec constitutes a reasonable working basis for fixing a sparking potential, then, as we vary the photoelectric current, i_0, from the cathode, the value of K and V_s must shift correspondingly to observe a spark. Thus the statistical time lag of sparking, T, the photoelectric current, i_0, at the cathode and either the sparking potential, V_s, or the constant K in Meek's equation, are inextricably linked together. This would appear to make the definition of the sparking potential most indefinite.* And, in fact, theoretically this is true. It allows us, therefore, to set as

* The indefinite character is, however, not as serious as would seem, since in Townsend discharges W rises very rapidly with V_s as seen on page 23. It is likely that in photo-ionization with streamers the chance W also rises exponentially with V_s or K. In this event the variation will extend over values of V too limited to observe with certainty.

a definition of V_s a purely arbitrary condition. For example, we might choose as a definition for V_s one in which the potential would be set as that value of V_s or K which, with a photocurrent $i_0 = 10^{-12}$ ampere, will give an *average* time lag T of say 30 seconds. By convention such a condition could be chosen and it may eventually become necessary to set such a condition as accuracy of control improves.

c) Despite the uncertainties of this character which apply both to the filamentary type of Townsend discharge at low $p\delta$ and to Meek's equation at high $p\delta$, the sparking potentials give the illusion of being quite definitely fixed. If one is content to accept an agreement between reported values within less than 3 per cent the foregoing statement is valid. The rather wide differences within the 3 per cent limit mentioned have in the past been largely attributed to experimental uncertainties, especially to lack of steadiness of the potential source. This condition, however, no longer holds and the differences are real. Of these more will be said later.

The immediate question at present is how is it that with a quantity $\lambda_0/\sqrt{f}$ varying by a factor perhaps of 2 or 3 and a K that varies by a factor of possibly 10, the value of V_s observed is constant within 2 to 3 per cent? The question is answered very simply and the answer has in part been indicated on pages 10 and 118 in connection with Townsend's equation. The equation of Meek, as do all equations which involve the cumulative ionization, depends on certain constant, or nearly constant, factors such as $\lambda_0/\sqrt{f}$, K, etc., and a term $e^{\alpha\delta}$ or $e^{\int \alpha dx}$. Thus small changes in α will compensate for large changes in the constants. Furthermore the value of V_s comes directly from the value of X_s/p corresponding to a certain α/p needed to satisfy the relation. Now for sparks in the region of atmospheric pressure in air, N_2 and H_2, α/p has the form of $e^{BX/p}$ as Sanders[25] was the first to show. Thus, if p is constant, α increases as $e^{BX/p}$. Accordingly the equations, such as those of Meek or Townsend, have constants multiplying into a term $e^{e^{BX/p}}$. Hence, it takes

but a minute change in X to compensate for very large changes in the values of the constant terms. For example, Meek finds that using the same value of $\lambda_0/\sqrt{f}$, we have a value of $V_s = 32{,}200$ volts for $K = 1$, one of $V_s = 31{,}800$ for $K = 0.2$, and one of $V_s = 31{,}600$ volts for $K = 0.1$. This change in V_s by a tenfold change in K is less than 2 per cent. The conclusion is that the equations are so insensitive to the value of K that one has considerable latitude in the choice of K to be applied.

Now it is not certain how much difference in K or V_s is needed to make the average spark lag $T = 30$ seconds with a variation say of perhaps 10^4 in the value of i_0 or n_0, i.e., $t_s = \frac{1}{n_0 W}$. In a Townsend discharge such a change in W or n_0 occurs for 0.3 per cent change in V_s. Since again a change in K affects the field active in multiplying photoelectrons by a factor $(1 + K)$ and since small changes of $1 + K$ in this region cause large changes in α, the changes in K to give adequate ions to insure a streamer need not be too large. Thus, while the chance of a streamer forming as one varies i_0 may vary from 1 to 10^4, the changes needed in K may not need to be more than by a factor of 2 to 4 in the region of values considered. Hence, the actual observed sparking threshold need not vary by more than 1 per cent for considerable changes in i_0, or keeping i_0 constant for considerable changes in time lag, T. The extent to which this is true is now under investigation by Haseltine,[28] whose results at present indicate that the changes are less than 1 per cent.

d) When one comes to an experimental test of the conclusions above, one is confronted with a mass of data in the literature from which it is impossible to draw any definite conclusions. V_s in air at atmospheric pressure in plane-parallel gaps has been determined by a number of observers, none of whom agree by better than 1 to 2 per cent. For sphere gaps the data are equally poor. The causes for this may be listed as follows:

(1) Inadequate control of potential sources in the past.

(2) Inaccuracies in the measurement of the potentials applied.

(3) Different criteria as to what spark-lag period to use.

(4) No control whatsoever of the photoelectric current i_0 at the cathode. These have varied from $i_0 = 0$ to an i_0 of 10^{-11} ampere.

(5) No adequate control of the constancy of the purity of the gas or its absolute purity. The presence of water vapor, Hg, or of nitric oxides produced by previous discharges in varying amounts in air, may alter the value of V_s by far more than the 3 per cent mentioned above. In fact, as Ehrenkrantz[29] has shown, purity control in spark discharge studies, even in pure gases like A, H_2, and N_2 is very difficult. Recent results of Haseltine[28] for sparks in pure dry air and by Fitzsimmons[30] for corona streamers in air have shown that a continuous flow of clean dry air is needed over a gap to prevent changes of many percent in V_s due to nitric oxides.

The effect of nitric oxides in air is to *lower* the threshold. This is due to the fact that the ionization potentials of N_2 and O_2 are in the neighborhood of 15.5 and 12.5 volts respectively, whereas that of NO is 9.5 volts and other nitrogen oxides are still lower. This implies a much higher yield of photoelectric ionization when these substances are present, in addition to changes in α/p as a $f(X/p)$. Thus, both K, and through changes in α and K, V_s can be materially decreased.

In attempting to evaluate the quantity K in terms of observed sparking data Meek has, therefore, been considerably hampered by the uncertainty as to the values to use. High values of V_s may mean improper technique, low values may be ascribed to impurities. The value 32,200 volts for air at n.t.p. was initially assumed. Probably a value of $V_s = 31{,}600$ volts is more nearly correct. Subsequently the analysis of the sparking between concentric spheres and the onset of corona streamers recently determined in ventilated paraboloid gaps in *dry* air by Fitz-

simmons[30] has indicated the value of 31,600 volts to be the better value. This makes $K = 0.1$ if one accepts the value of $\lambda_0/\sqrt{f}$ given on page 44 as sensibly correct. For the bulk of the calculations so far made, the value of $K = 1$ has been used. In the more recent work the value of $K = 0.1$ corresponding to the newer data has been resorted to. In chapter iii of this book the use of both these values is discussed in connection with the applications of the theory to specific problems.

9. The Effect of Intense Photoelectric or Other Currents from the Cathode on the Sparking Potential

In discussing the statistical time lags of sparking, it was indicated that *intense* ultraviolet illumination of the cathode not only reduced the statistical time lags of sparking but lowered the sparking potential of the gap V below the conventional value V_s. It was further indicated that this lowering was due to the effect of space charges built up by cumulative ionization in the gap *preceding* the discharge. Let us consider a gap at a potential $V < V_s$ and suddenly create an intense ultraviolet illumination of the cathode surface lasting for some 10^{-5} second by means of a light from a condensed spark focused on it with a quartz lens. This experiment is precisely one carried out by H. J. White[31] in 1935 and some months later carried out independently by Rogowski and Wallraff.[32] Under these conditions the gap is found to break down at a value of V some 10 per cent below V_s. For a current density j_0 estimated as about 10^5 times that from the quartz mercury arcs usually used, the maximum lowering observed at atmospheric pressure was about 10 per cent. As j_0 was decreased V rapidly approached V_s. The values of the current densities used are highly uncertain as are the times of exposure to the current. Thus the quantitative data are somewhat unsatisfactory for calculation.

Now, except for the Townsend mechanism as studied by Schade[33] at low pressures, the theory of sparking should give V_s independent of i_0 or j_0 except as this is influenced by time

lags. That is, i_0 or j_0 has nothing to do with V_s where the spark is initiated by avalanche processes set free by *one* electron. Hence, the filamentary Townsend processes at pressures above where Schade worked and the new streamer theory both require V to be V_s and independent of i_0 or j_0 where there are no statistical time lags. The phenomenon observed by White and Rogowski and Wallraff thus requires explanation. Rogowski and Fuchs[34] have developed an elaborate theory of the spark based on the Townsend theory. They envisage a space-charge distortion produced by the current density, j_0. The theory contains certain assumptions concerning the mobility of positive ions of a questionable sort. On the basis of this theory, approximate agreement with observation, as to the lowering of V below V_s by j_0, is obtained. It is probable that the considerations of Meek[35] to be discussed later would yield the same result with Townsend's theory without the assumptions as to positive ion mobilities made by Rogowski and Fuchs. For the basic considerations of Meek as regards the effect of j_0 in the gap are independent of sparking mechanism. In any case, it is clear that the phenomenon falls into the region of $p\delta$ to which Townsend's theory is not applicable. Thus one may inquire as to whether the phenomenon can be brought into line with the streamer theory.

Now when V is below V_s for any period of time, the photocurrent i_0 will build itself up to its equilibrium value i as given by Townsend's classical theory either with or without a γ. The time for reaching 99 per cent of its steady-state value, whether γ is present or not, can be calculated as Schade[33] has done, provided V, p, and δ are not such as to lead to a field distortion of the gap by positive-ion movement. The times will obviously be well in excess of 10^{-5} of a second required for positive ions to cross the gap. In the event that V, p, and δ are such as to lead to a space-charge distortion of the gap, then one may apply the theory of Varney[24] to the calculation of the steady-state conditions in the gap, where γ is not active. If γ were active the

calculations would become very much involved indeed and no solution exists, except that of Rogowski and Fuchs.[34] These space-charge distortions of Varney, in theory, take infinite time to achieve. In practice the field distribution is nearly always reached in convenient times. Thus, when a V less than V_s is applied with a current density j_0, there can well be built up a space-charge distribution without the influence of a γ, as envisaged by Varney, which can lead to a streamer formation. Meek has calculated the space-charge distortions to be expected for various values of V near V_s, using a 1-cm gap and different values of j_0. From these one may apply the condition for streamer formation as given in Equation 25. If then the condition is fulfilled, a spark will ensue. The involved character of the functions even under ideal conditions indicates that well below V_s streamers will form that in some cases can lead to a spark. Since the criterion for streamers that yield sparks in low fields is as yet indefinite, no accurate V_s can be fixed. The lowering is definitely indicated in considerable measure and at relatively low values of j_0. Since these are the steady-state field distortions, the lowering of V below V_s will be greater than that observed by White and Rogowski and Wallraff. There the lowering corresponded to the field distortion set up by j_0 in the 10^{-5} second during which the spark illumination permitted j_0 to act.

Meek also calculated the approximate field distortion and the corresponding sparking potential at various values of j_0, using successive waves of positive ions for successive electron avalanches which crossed the gap. For a few waves of these positive ions, equilibrium fields were not reached but the time of building up the space charges corresponded more nearly to the times observed by White[31] and by Rogowski and Wallraff.[32] Here definite thresholds can be obtained.

The comparison of experimental data with these theoretical calculations shows that: (1) The lowering of V_s by j_0 is less than that observed; and (2) the lowering becomes significant at

somewhat higher values of j_0 than those observed. The cause of the first discrepancy was that, in the experimental cases, the lowering was due to several waves of positive ions instead of to the single wave computed. The failure of the calculated and observed values of j_0, at which the deviations become notable, to agree is in part to be ascribed to the uncertainty in the experimental estimates of j_0. These estimates depend on the measurement of the number of photoelectrons liberated and an estimated duration of spark illumination. They may easily be off by a factor of 10. Again the increase in the number of ion waves would reduce the value of j_0 at which lowering becomes appreciable.

10. Effects of Overvoltages, Branching, and the Properties of Streamers

a) *Overvoltages.*—By overvoltages we mean potentials in excess of the value of V_s experimentally observed and termed hereafter the *conventional* sparking potential. The conventional sparking potential may possibly be a per cent above the minimum possible value.[28] In theory it is the potential at which, with a reasonable number of electron avalanches starting from the cathode per second, one may expect a spark to occur in a reasonable time, T. If we place $T = 30$ seconds and $i_0 = 10^{-13}$ ampere, this would represent the value of K or V_s at which one avalanche in some 2×10^8 resulted in a streamer. As we increase V above V_s, the electron multiplication goes up very rapidly. Thus an increase of V from $V_s = 31{,}600$ to $V = 32{,}200$ increases $\alpha e^{\alpha\delta}$ by a factor of 10. Hence, the space-charge field strength, X_1, at the anode for a gap 1 centimeter long would be increased tenfold. Such an increase in X_1 has the immediate result of making the efficiency of streamer propagation far higher. Hence, instead of perhaps one in 10^8 avalanches leading to a streamer and a spark, perhaps one in a hundred or less avalanches succeeds in causing sparks. Thus the first increases in

potential above the threshold, i.e., even very low overvoltages, wipe out statistical time lags. For very short gaps Tilles[60] found that except at high n_0 appreciable overvoltages were needed.

If one increase V still more, the electron avalanche will no longer need to cross the gap to give a streamer. With sufficient overvoltages this will occur despite the fact that the electron swarm at the avalanche tip has not been swallowed up by the anode. Hence, in such cases, long before the electron avalanche has reached the anode, the streamer has started for the cathode from *midgap*. This produces a sharp axial field distortion along the streamer axis and in the field direction. Such a distortion is indicated schematically in Figure 14 (p. 60). This enhanced field, both at the anode and at the cathode along the streamer axis, has an even greater influence on the values of α. Hence, as the midgap streamer approaches lengths approximating $\delta/2$, with overvoltages, the electron avalanches going to the anode from the anode end of the streamer and those started by photoelectrons launched from the cathode by streamer photons will build up space charges and even streamers in very much reduced distances of travel. Thus, it would not be strange in overvolted gaps when streamers approach lengths $> \delta/2$ to see anode streamers beginning to form and advancing toward the anode end of the avalanche. Likewise the intense fields at the cathode can begin to produce a cathode spot. Accordingly the appearance of cathode spots and anode streamers even in the slightly overvolted gaps used by Dunnington[10] and by White[1] in their Kerr cell studies of the early stages of spark discharge need not surprise one. When, however, these phenomena were first observed their appearance was the cause of considerable concern as considered in the light of the Townsend theory. Dunnington's sketches of the sparks as observed in the Kerr cell studies within 10^{-7} second are shown in Figure 12. Most of these were made at a $p\delta$ in the Townsend regime and developed outward from the cathode. In this region Dunnington[10] remarks that the channels were diffuse compared to those at higher $p\delta$. Those

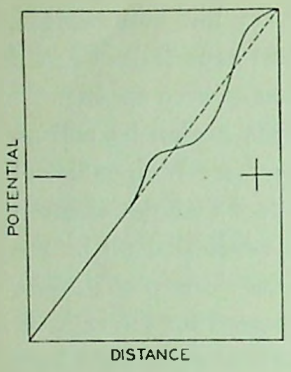

FIG. 14.—Midgap streamer and space potential

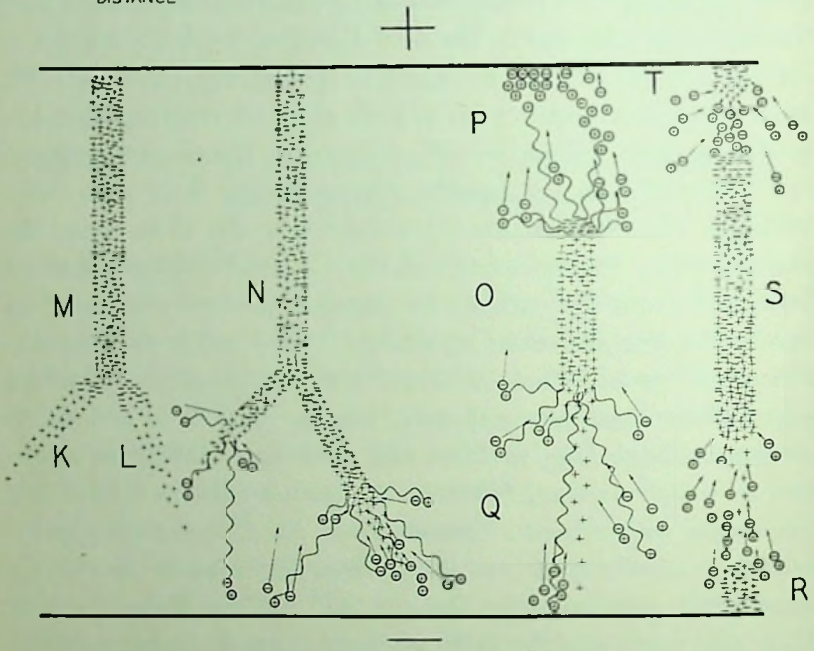

FIG. 15.—Schematic diagram showing the mechanism of streamer branching. *M* is a streamer channel drawing in two avalanches *K* and *L* simultaneously. In *N* one sees the two branches developing independently as separate streamers by photoionization.

At *O* one sees a midgap streamer that advanced as an avalanche two-thirds of the way across the gap and then sent a retrograde streamer back toward the cathode at *Q*. The electrons at the anode end can clearly be seen and the cumulative ionization in the enhanced field near the anode by photons from the tip can be seen at *P*. At *T* the later stage shows an incipient anode streamer, the long midgap streamer with the cathode spot and streamer building up at *R*.

made at larger $p\delta$, however, clearly show the midgap and anode streamers and the cathode spot. White[1] also notes that for N_2 gaps above 3.5 mm length show the midgap streamers. In He the spark is preceded by a glow discharge. That is, in He at higher $p\delta$, we still have the Townsend mechanism. For the purposes of study all of these gaps were definitely overvolted. The growth of a midgap streamer in an overvolted gap is schematically shown in Figure 15.

Another effect of overvoltage in a gap is a measurable reduction in formative time lags. In the gap at V_s the formative time lag is the time for the avalanche to cross the gap plus the time of the crossing of the anode streamer. The order of magnitude of the time of electron crossing is 5×10^{-8} to 10^{-7} second for a gap of about 1 cm, and the time of passage of a streamer is less, but of the same general order of magnitude (about 2×10^{-8} second). This is evidenced by the fact that in cloud-track pictures[9] of gaps the streamer can be caught relatively frequently in its passage. Were the time of streamer crossing very fast compared to the avalanche the streamers would only rarely be observed. In an overvolted gap the breakdown proceeds by midgap streamer and a nearly simultaneous anode streamer. The electron avalanches do not have to proceed across the whole gap and the midgap streamer has to cross less than the whole gap. The increased fields also slightly increase the velocities. Thus, as White,[1] Wilson, and Newman[37] have shown, formative lags are materially reduced in overvolted gaps. Wilson and Newman observed breakdown in the order of less than 5×10^{-8} second for gaps with 200 per cent overvoltage.

It is thus seen that overvoltage acts in gaps to wipe out statistical time lags, to cause breakdown by means of midgap, anode and even multiple streamers, and materially to reduce the formative time lags.

b) *Statistical time lags and ionization in the gap.*—The study of the sparking threshold has already indicated that unless overvoltages are used to insure effective multiplication of the

photoelectrons only a rare electron avalanche will end in a streamer and thus a spark. Hence the time required after the application of the sparking voltage, V, before a spark materializes must depend on the number of electrons liberated in the gap, n_0, the chance, P_s, that at V an avalanche will give a breakdown streamer (which depends on $V - V_s$) and the chance, P_c, that the electron is so liberated in space that ultimately it can lead to a streamer-producing avalanche. The average statistical time lag, T, will then be $T = 1/n_0 P_s P_c$.

The quantity, n_0, depends directly on i_0, the ion or photoelectron current formed in the gap by an external agent, or by agents existing after some previous discharge. Let us consider some possible values of n_0 or i_0 occurring under different conditions and estimate their effect on the spark lag.

(1) Free air at atmospheric pressure has normally from 10 to 20 ions produced per cubic centimeter per second by means of α particles from the walls, radon in the air, γ rays from the earth, and cosmic rays. These, together with recombination, lead to the permanent existence of some 1,000 to 3,000 *ions* per cubic centimeter.[38] For the purposes of most discharges at $X/p \sim 40$ such ions are useless, since X/p must be about 90 in order to detach electrons from negative ions,[39] for negative ions do not ionize by impact in gases. Hence, without external ionization, the 10 or so electrons created per cubic centimeter per second are the only initiating electrons. Now these electrons are produced anywhere in the cubic centimeter. For plane-parallel electrodes of 1 cubic centimeter effective volume, the most propitious case, an electron produced near the *anode* if $V \sim V_s$ is practically useless. An electron produced very near the cathode will have a good chance of giving a spark. It will at once be seen that with $n_0 \sim 10$, $P_s \sim 0.01$, we must make $P_s \sim 3 \times 10^{-1}$ to give T the reasonable value of $T = 30$ seconds. This means that $V - V_s$ must be rather high. If we make n_0 very much less as for a spark-plug gap, it is seen that $V - V_s$ may really have to assume very high values. This means that

even with $P_s = 1$, T must be very long. Edwards and Smee[40] record values of $(V - V_s)/V_s$ of some 50 per cent or more with mean deviations of 30 per cent for small gaps. In fact it is surprising that spark gaps in gasoline engines, even though operated at considerable overvoltage, fire at all regularly unless there are other sources of i_0.

The value of n_0 is increased almost in proportion to the pressure of the gas so that higher pressures help decrease the lag. As the volume of the gap is increased in air the quantity n_0 increases and the lags go down. Thus for sphere gaps of several centimeters separation the effect of T is to increase the spread of sparking potential to some 7 per cent with the average $(V - V_s)/V_s$ some 4 per cent. It is thus clear that to get reliable values for the threshold of sparking, one cannot use gaps under these conditions.

(2) Illumination of the cathode with ultraviolet light furnishes a photocurrent i_0 from the cathode. For plane-parallel gaps under 10 centimeters in air at atmospheric pressure and for smaller-sphere gaps, this source of current furnishes the most satisfactory arrangement. Here $P_e = 1$, and $n_0 = i_0/\epsilon$, so that T depends largely on n_0 and P_s. Using ordinary electrode surfaces with a quartz Hg arc focused by a quartz lens, diaphragms and absorbing screens, i_0 can readily be varied from 10^{-16} ampere per square centimeter to 10^{-12} ampere per square centimeter. More intense illumination can be obtained from naked condensed sparks.[31, 32] Here values of i_0 estimated at 10^{-9} ampere per square centimeter and perhaps more can be obtained for intervals of 10^{-4} or 10^{-5} second. With 10^{-12} ampere the value of n_0 is 6×10^6 electrons per second. With values of the current density from the cathode less than 10^{-12} ampere per square centimeter, for a 1-centimeter gap, space charges will not distort the gap before the spark passes. Thus, except for the effect of illumination on the statistical time lag, V will not be lowered below V_s and measurements of V with $T \sim 30$ seconds will give V_s. For longer gaps, values of $i_0 > 10^{-11}$ ampere per

square centimeter may lower V below V_s by space-charge distortion as Meek[35] and Varney[24] have shown.

(3) Ionization by α or γ rays in the volume of the gap is sometimes resorted to. In this case the quantity n_0 is distributed through the gap volume. Hence, for many sparks P_c is far less than 1. The values of n_0 usually achieved are less than with ultraviolet light. In many cases 3 to 5 mg of radium will give γ radiation enough to yield reasonable values of n_0. For sphere gaps the radium is placed inside the sphere in a hole going nearly to the surface of the sphere and separated from the gap by as thin a layer of metal as possible.[41] This makes the ionization a maximum without distorting the field. The values of the current, i_0, under these conditions will not be much above 10^{-15} to 10^{-14} ampere at most. Thus time lags may be considerable, leading to high values of V.

It must be noted that with Ra the ionization n_0 is not distributed uniformly in *time* as with light. For in 10^{-8} second one α particle or γ ray liberates 10^4 or 10^2 ions with no more until the next particle arrives. These bursts of ionization may be spaced with considerable time intervals between. Thus the real n_0 will be given by the number of α or γ rays per second.

There is one case where theory indicates that ionization of the gas in a gap near the *anode* is the most favorable region for reducing P_c. This is in sphere gaps where the gap length is large compared to sphere radius. In this case avalanches from the cathode sphere do not cross the gap. The breakdown proceeds as a streamer from the anode. To initiate such a streamer the n_0 electrons, to be in a position to be effective, must be created in the gas a few millimeters or a centimeter from the anode. Electrons in this position give the avalanches that form the streamer.

(4) There are many cases, especially for gases confined in vessels, where the statistical time lag, T, will be very large until the first spark has passed. Thereafter this time lag may become small[33] or even go to 0. The effect is greatest in He and Ne but can occur in all the inert gases, in N_2 and H_2, and possibly in

all gases. This phenomenon may be due to a rather large number of causes. Where metastable atoms are present these can persist up to seconds. They disappear in part by collisions with walls, electrodes, atoms, or molecules of lower ionizing potentials. In many cases these reactions liberate electrons or photons that can liberate electrons. In electrodeless discharge in some cases chemical products are formed which can be frozen out in an activated state by liquid air.[42] As they warm up they emit light and doubtless produce ions. Chemical reactions in gases liberate photons and sometimes electrons. These can all furnish the electrons for starting a discharge some time after the discharge created them. Active nitrogen can produce excitation and ionization of impurities of ionization potentials below 7 volts as much as 20 seconds after formation. These photons can cause photo-ionization in the gas or at the electrodes. The ions occluded but not neutralized on dry glass walls of a discharge tube can be released by surface leakage on the outside of a tube, as Locher[43] has shown, and may later liberate an electron from an electrode. Finally Paetow[44] has shown that specks of oxide of submicroscopic size on an electrode surface can be charged by ions or photoelectric action by previous sparks. These form small units ($\sim 10^{-5}$ cm) of enormously high potential difference with the surface on either cathode or anode. The fields across these specks may suffice to cause local sparks through the specks of dielectric, to cause high-energy photons to be emitted on neutralization or decay as do the phosphorescent zinc sulfides, or even to cause a local field emission of electrons. These effects will last minutes after the first discharge. They are particularly bad with supposedly clean surfaces with insufficient outgassing, or with dust of MgO, Al_2O_3, etc. They can be removed in He and Ne only with the most rigorous cleaning and outgassing. Again, if surfaces are hot and have low work functions (such as some spark-plug electrodes), enough thermionically liberated electrons may leave the electrode to insure a spark. Initiating electrons may also come from fine

points in the field if high enough. These factors are often forgotten in the study of discharges. They undoubtedly contribute to the operation of spark plugs in internal combustion engines and are thus of value. On sparking and time lag studies they must be guarded against at all times.

It is seen that in the case of the streamer mechanism one can readily account for the presence of statistical time lags and indicate the fashion in which these may be controlled. These considerations also throw much light on the significance of sparking potential data taken under various conditions. With Townsend's theory where the breakdown operates by means of a filamentary channel the considerations above also apply. They do not apply to the Townsend form of breakdown observed by Schade[33] to nearly the same extent.

c) *Branched and crooked spark channels.*—From what has been said of the chance nature of photo-ionization near the tip of the advancing streamer, owing to the relatively small number of photoelectrons created, it is clear that this leads to spatial as well as temporal fluctuations. With ample photo-ionization about a streamer tip the sensitive volume for streamer advance about the field axis ahead of the tip will have adequate electrons. The streamer advance will then be fairly well along the axis in the field direction. Where, however, the photoelectric ionization begins to be inadequate, then photoelectrons from other parts of the volume ahead of the tip will also be utilized. Under such conditions the less axial electrons bring in avalanches that tend to divert the advance of the streamer along their direction of advance, which is that of the vector sum of the fields X_1 and X. If a particular avalanche feeding in from a more radially created photoelectron happens to be especially long and intense, the advance will, for a while, proceed along that streamer. If two strong avalanches feed into the streamer tip simultaneously, then the tip will be branched. In many cases, branching will reduce ionization so as to stop streamer advance; in others, one branch or both may succeed in crossing the gap.

FIG. 16.—Photograph of spark channel

FIG. 17.—Branching in lightning

The conditions for branching and crooked streamers can thus be determined from circumstances which produce inadequate density of photo-ionization. These conditions, as will be seen, are low pressures, long gaps, and the use of certain gases. Allibone and Meek[12] found a distinct increase in branching when pressures were reduced in longer gaps. The effect of long gaps in producing crooked and branched sparks has long been known. In these, the attenuation of density of photo-ionization is caused by electron diffusion in the avalanche path and to the reduced values of X_s for the longer sparks. Gorrill[45] has observed considerable branching in the corona streamers in the regions of weaker fields. Unfortunately, little is known about the photo-ionization in CO_2 and hence the reason for branching in this case is largely conjecture. Photographs of crooked and branched sparks are shown in Figures 16 and 17. A schematic diagram of branching in streamer formation is shown in Figure 15. Actual photographs of cloud-track streamers are shown in Figures 8 and 9. Figures 8 and 9 give cloud-track photographs of Raether[9] showing branching of streamers and crooked streamers.

d) Some properties of breakdown streamers.—There are no direct observations of breakdown streamers except those by Kerr cell shutter,[1,10] showing simultaneous midgap and anode streamers, and the cloud tracks of Raether.[9] The overvolting of Kerr cell shutter gaps made observations of the anode streamers alone impossible in the studies of Dunnington[10] and White.[1] Raether's photographs[2,9] of avalanches are exceptionally clear. Using impulse waves of potential of different duration, Raether's photographs giving the velocity of advance of, and the electron diffusion in, the avalanches are invaluable for the theoretical analyses needed in a quantitative study. When it comes to a study of the avalanches in higher fields and the transitions of these to streamers by cloud-track photographs the situation becomes very complicated. The intense ionization and the multiplication of photoelectrons about the discharge in the portions

of the declining potential wave make the photographs so diffuse that they are unintelligible. Analogous situations were encountered by Gorrill[45] in his cloud-track studies of corona. By reducing his expansion ratios to a point where condensation set in only on the chemical products in the more intense regions of the avalanches and streamers, Raether[9] got the tracks of the streamers shown in Figures 8 and 9. Even these are far from satisfactory.

It is seen, however, that the breadth of the streamer tracks are slightly larger but of the same order of magnitude as the heads of the initiating avalanches. In the case of White[1] and Dunnington's[10] midgap streamers, the widths can be seen to be of the magnitude of spark channels. It should be noted also that these streamers emit sufficient light to be photographed. Aside from this, we have no direct evidence concerning the streamers in spark discharge.

The study of positive point-to-plane coronas by Kip[8] has revealed the presence of streamers and allowed quite a bit to be inferred concerning their properties. They originate when the fields at the positive electrode fulfill Meek's condition for streamer formation in air. Positive space charges about the point, from preceding streamers or burst pulse corona, reduce the fields about the point so that streamer formation cannot occur. The pre-onset streamers range from a few millimeters to a centimeter or two in length in short gaps. The pre-onset streamers, therefore, do not normally cross gaps which exceed 1 cm length. Where they cross to the anode they have a high probability of making a cathode spot and giving a spark. At higher fields where space charges are cleared from the point and where the lowering of the field near the point by space charge is overcome by the added impressed potential, streamers again appear. At slightly higher fields these cross the gap and then lead to sparking. The pre-onset streamers can be started in a cleared gap by a single electron.[6]

The streamers in air are visible to the dark-adapted eye as

fine bright blue processes that quickly disappear. Their extinct tracks lead to local fields giving a lavender or purple glow discharge.[40] The branching of the streamers, which is not visible to the naked eye but is revealed by cloud tracks and streamer photographs in mass, causes them to have a brush-like appearance. Single streamers cannot be photographed by a fast Leica camera with ordinary film. They were photographed as midgap streamers by White[1] and Dunnington[10] with special optical arrangements and plates. Some 40 or more streamers in a confined region can, however, be photographed. Spectroscopic study with a small quartz-prism spectrograph revealed largely the conventionally observed glow discharge spectrum in air. The bright blue of the streamer, however, indicates the presence of high tip fields and the presence of the spark spectrum of N_2. The purple haze represents the arc lines of air and N_2 due to excitation by electrons in the fields of extinct channels.

The streamers produce a large electrostatic disturbance[8] and are capable of shock-exciting neighboring systems, owing to considerable values of di/dt of the order of 0.1 ampere per second. They cause the noisy corona discharge which is so troublesome in radio reception.

In the spark-streamer channels, behind the advancing head of the streamer tip, there is a conducting plasma of positive ions and electrons. During the short time of advance in the usual gaps the electrons remain free and there appears to be little recombination. Whether there are any high-potential gradients down this channel of plasma is doubtful. There may be some fall of potential maintaining a small current of electrons to the anode. The fall cannot be great since the potential gradient at the tip must be maintained. That there is some current follows from the fact that the plasma must be neutral electrically. Now, ahead of the tip all photoelectrons and their progeny leave behind positive ions that will later be incorporated as part of the streamer channel plasma. On the other hand, photoelectrons at some distance from the axis channel may be drawn into the

tip, leaving their positive ion partners *outside* of the future plasma-streamer channel. Hence, more electrons enter a streamer than positive ions. These excess electrons constitute a current up the streamer to the anode. It may be considerable in some cases. One may regard the streamer mechanism at the tip somewhat as a potential wave propagating itself in the gas in the field direction by means of advance photo-ionization and electron multiplication. It leaves behind a filament of conducting plasma with a small gradient extending to the anode.

In the oscillograph the corona streamers produce a considerable disturbance when inductively picked up.[8] The disturbance is due to sudden changes in charge distribution in the static fields about the point. The time of transit of the ions produced by streamers has been measured across the low field portions of the gap[6] and corresponds to what would be expected of a cloud of positive ions in such gaps, being of the order of 10^{-3} second. The pre-onset corona streamers, it must be remembered, do not cross the gap and thus yield a positive space charge in the gap after the electrons are removed. The number of positive ions in such streamers, after the electrons have gone to the anode, has been determined by Kip from the oscillograph records as lying between 10^{9} and 10^{10} ions per centimeter length of streamer.[6] The diameter of the streamer channels is visually less than the 10^{-2} cm calculated for the 1-cm gap with a uniform field from Raether's data.[2] This is doubtless because these streamers form in intense field regions of short length where diffusion is small. Thus, while streamers in a 1-cm gap in air may have a radius of 1.5×10^{-2} cm, in the corona they may be more nearly 0.5×10^{-2} cm. The ion densities in these streamers are of the order of 10^{13} to 10^{14} ions per cubic centimeter. The time for the corona streamers to develop is exceedingly short. They can well be less than 10^{-7} second.

When a streamer attached to the anode by a conducting filament of plasma approaches the cathode and is suddenly met by a stream of electrons from the cathode spot, a potential wave

of negative sign sweeps up the pre-ionized channel with its 10^{13} ions per cubic centimeter. The velocity of such a wave can be estimated on classical grounds but on account of its difficulty has not as yet been attempted. It depends on the ion density. In the case of lightning discharge the velocity of the return stroke has been measured as close to 10^{10} centimeters per second.[11] In the spark channels it can be of an equal magnitude. If the gradient is sufficiently steep in this wave it multiplies the density of charges by causing each electron to multiply itself many times by collision. Thus the return stroke after the streamer has reached the cathode sweeps up the pre-ionized channel at high speeds multiplying the ionization and excitation by many fold. Then follows a further flow of the electrons up the channel equalizing the charges between the electrodes and ionizing the channel until the potential difference between the plates begins to fall. This process produces the brilliant and noisy phase of the spark. The process continues for perhaps some 10^{-6} to 10^{-5} second, depending on the circuit conditions. From the Stark effect broadening of the Zn lines in the later stages of the spark Dunnington[10, 47] estimates the final ion densities in some of his overvolted sparks as being as high as 10^{19} ions per cubic centimeter. Thus the transition from a filament of streamer plasma into an intensely noisy luminous spark can readily be understood.

11. The Spark Breakdown in Long Gaps

As has been amply seen, there is a lower limit of $p\delta$ below which the streamer mechanism, owing to insufficient density of photo-ionization, is replaced by the more efficient Townsend mechanism. One may next inquire as to whether there is not an upper limit of $p\delta$ above which the streamer mechanism and Meek's equation do not apply. The question is not an idle one, since, in long sparks in air[12] and in lightning discharges,[11] one observes not only streamers from the positive electrode, but what appear to be streamer-like processes emanating from the cathode

or negative cloud masses. The appearance of such negative processes seems at first sight to be incompatible with the mechanism of breakdown thus far presented. It will, however, appear on more careful study that such processes are not only not inconsistent with the streamer mechanism, but that they are in fact dependent on it. Thus it is clear that the matter requires further analysis. To do this one must at first review existing knowledge concerning sparks in long gaps.

Plane-parallel gaps have thus far been investigated for values of $p\delta$ only up to about 10^4 mm $\times$ cm with steady potentials. The steady high potentials, as well as the large plate areas needed for such studies, have not until recently been available for convenient study. What data we have on hand include gaps up to 10 cm at atmospheric pressure and smaller gaps up to 20 atmospheres. Paschen's law appears to be obeyed to within 3 per cent, which is the limit of experimental accuracy. At higher densities, where density ρ is not proportional to pressure, the law must be tested in the form $V_s = F(\rho\delta)$.

There is a wealth of data on sparking potentials for air at atmospheric pressure using 60-cycle alternating potentials, especially on short-sphere gaps with large electrodes. There is also one set of data with A.C. potentials on a large plane-parallel gap.[48] In theory and to some extent through experiment, the 60-cycle A.C. sparking potentials should not differ much from the steady potential values unless corona precedes breakdown. The best data of interest is that on large-diameter spheres placed at gap lengths small compared to their diameter, i.e., approaching the parallel-plane arrangement. The values of various observers are pretty well in agreement here and the values may thus be reliable. The values of V_s should, for such gaps, lie near, but if anything slightly below, the values of plane-parallel gaps. Ishigura and Gosho[18] made a study using A.C. on a poorly contoured plane-parallel gap of 6-meters diameter and up to 60-centimeters maximum gap length. Their values for V_s, however, lie well *below* the sphere gap data. This causes one to question

their data. The validity of their data is completely ruled out, however, when one calculates the sparking field, X_s for their 50-centimeter gap as being 12,000 volts per centimeter, a value at which Townsend's α has immeasurably small values. Were the conditions for long gaps the same as for shorter ones, their value of V_s would be 1,100,000 volts instead of the value 640,000 volts observed. Of the character of these A.C. results more will be said at the appropriate place. Suffice it to say that our data on steady D.C. potentials is limited to values of $p\delta \sim 10^4$ mm $\times$ cm and that there are data that might be equivalent which are fairly reliable out to about 20 centimeters on sphere gaps with alternating current.

While the curves for V_s with steady potentials plotted against $p\delta$ appear to give a linear relationship at high values of $p\delta$, this relation is an illusion resulting from the scale of plotting. In reality all curves for V_s plotted against $p\delta$, starting from above the minimum sparking potential, rise more rapidly than $p\delta$ at first and gradually flatten out. Thus at higher $p\delta$ their slope is less than that of the line drawn from the point through the origin. Up to the limit of the present observational data with *steady potentials*, the slope of the curve is still decreasing, at, however, a low rate. With the sphere gaps which are equivalent to plane-parallel gaps using alternating current potentials, the slope of the curve at $\delta = 15$ cm at 760 mm *increases* so that the curve tends to extrapolate through the origin beyond $\delta = 20$ cm. The fields with larger spacings are no longer uniform. Curves which have tangents intercepting the axis of ordinates above 0 at high $p\delta$ are given by Meek's theory. They are also given by Townsend's equation fitted with an *empirical* γ as mentioned on page 10. This latter agreement is entirely fortuitous.

The trend of V_s with $p\delta$ means that the sparking potential V_s is increasing more slowly than $p\delta$. This circumstance may be more clearly illustrated by plotting the sparking-field strength $V_s/\delta = X_s$ at constant p against δ. Under these conditions it will be seen that the very important parameter X_s, the sparking-

field strength, falls at first rapidly with δ and then more and more slowly. An analogous result is obtained if $V_s/p\delta$ is plotted against $p\delta$. This is shown in Figure 18 where $V_s/p\delta = X_s/p$ is plotted against $p\delta$. The quantity X_s/p decreases at first rapidly and then more slowly, reaching a value of about 33 with X_s about 25,000 volts per centimeter, at the largest values of $p\delta$ observed in plane gaps. How much below this the values fall as $p\delta$ increases beyond the present data in plane gaps with steady potentials, one cannot say. The sphere-gap data with alternating current shows a decrease to a value of $\delta \sim 15$ cm at atmospheric pressure. Thereafter the *slope increases*, tending to a value that passes through the origin beyond $\delta = 20$ cm.

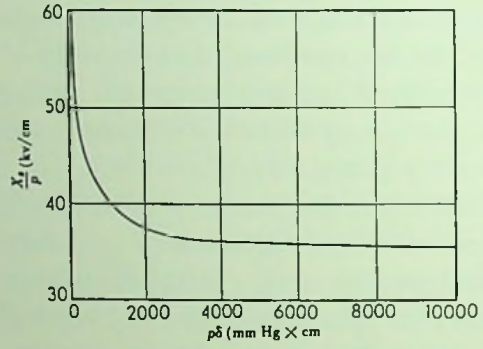

FIG. 18.— $\frac{X_s}{p} - p$

The course of the trend of the sparking-field strength below $\delta = 15$ cm at atmospheric pressure is to be ascribed to the exponential increase of the electrons in an avalanche and the nearly exponential increase of α/p with X/p in this region of X/p. Such a trend can be expected as long as Meek's theory is applicable in the form given and is a consequence of the character of the equation.

It is thus clear that if there is a change in trend of the $V_s - p\delta$ curve at longer gap lengths it will be related to a failure of Meek's equation for the spark at larger values of $p\delta$. Hence it

is necessary that we examine the influence of long gaps on the conditions essential for the fulfillment of Meek's sparking criterion. These conditions, one may recall, are (1) that the avalanche must be of such a length $x \leqq \delta$ that the space-charge field X_1 set up by an avalanche equals K times the impressed field; and (2) that at this time there must be enough density of photo-ionization about the streamer tip to insure propagation.

a) If the necessary length δ of the gap is less than the path length x to make $X_1 = KX$, the avalanche can produce no spark. If $x = \delta$, the avalanche crosses the gap and a spark follows. If $x < \delta$, then the avalanche achieves a midgap streamer and the spark may follow. Now, owing to the cumulative nature of electron multiplication in an avalanche, it seems unlikely that by increasing δ one cannot achieve a value of the space charge sufficient to make $X_1 = KX$. The one condition opposing an ultimate fulfillment of this is by electron diffusion at a rate of $\bar{r} = \sqrt{2Dt}$. The effect of this term on Meek's criterion is to put the expression $(\delta/p)^{1/2}$ in the denominator of the equation

$$\frac{X_1}{p} = 5.27 \times 10^{-7} \frac{\left(\frac{a}{p}\right) e^{(a/p)p\delta}}{\left(\frac{\delta}{p}\right)^{1/2}}$$

It is seen that the increase of the denominator as δ increases is small compared to the exponential term above. Thus it is not surprising to find on calculation that even for the longest gaps down to the lowest values of a, condition 1 is satisfied.

b) One must now inquire as to the density of ionization necessary for the development of a streamer. For it is here that one can run into difficulties. The reason lies in the fact that as δ increases at constant p the lowered values of X_s reduces the value of a needed. Hence, while large numbers of ions can be produced by a large δ, even when a is low, the *rate of production of photons along the track with the low value of* a *and large* $\bar{r}$ *is continually decreasing.* It is thus not inconceivable that

eventually the photon production near the positive space charge may become inadequate for the propagation of a streamer. One must then consider the photon and ion density necessary for streamer production.

12. Photon and Ion Densities Necessary for Streamer Propagation

About the photon production and the photoelectric ionization in electron avalanches, we know virtually nothing. Although attempts at such a study are under way in the Berkeley laboratory, the problem is technically such a difficult one that its solution is not near. It is certain that there are many more photons produced by electron impact than there are ions. The ratio between the number of photons and the number of ions produced changes with the average electron energy and thus with the value of X/p. At lower X/p the photon/ion ratio is much larger than at large X/p. However, the number of photons capable of photoelectric ionization in the gas is low at low X/p and rises as X/p increases. Even though we do not know the ratio of these two quantities we can be sure that there will be a fairly close relation between the photon density and the ion density at any given region of values of X/p. Thus one can use the ion density as a criterion for estimating the density of production of photons photoelectrically active in the gas. This is particularly true as the photon/ion ratio will not materially change in the range of X/p from 35 to 25 in which we are interested, especially since photoelectrically active photons in the gas are more efficiently produced at higher electron energies. Now, the only streamers about which we have any knowledge as regards ion densities are the corona streamers studied by Kip.[6] Here the ion densities are of the order of 10^{13} per cubic centimeter for the whole streamer. It is doubtful if the ion density is as high in the tip of a spark streamer. It is still more doubtful that this represents the *minimum density* necessary for propagation. This datum, therefore, does not give the needed information.

It is possible to achieve more information from a study of Meek's equation. We are, by it, in a position to calculate the ion densities at the streamer tip for any p and δ that are compatible with Meek's theory. To do this one solves the Meek sparking equation

$$X_1 = KX_s = \frac{\frac{4\epsilon a e^{a\delta}}{3}}{\left(1010\frac{2}{3}\cdot\frac{\delta\lambda_0}{p\sqrt{f}}\right)^{\frac{1}{2}}} \tag{21}$$

with the values of p and δ set. This solution gives not only X_s but the value of α appropriate to the gap. From X_s and δ one fixes the value of $\bar{r}$ from $t = \delta/v_x$ and D. The ion density given is then found at once from the relation

$$N = \frac{ae^{ax}}{\pi r^2} \tag{17}$$

Thus one can make a table of values of N appropriate to any gap length δ and pressure p for which Meek's equation holds.

It is of interest to combine these two equations in order to see how N must vary with p and δ in the limits where Meek's equation holds. Combination leads to the relation

$$KX_s = \frac{4}{3}\pi\epsilon\left(1010\frac{2\delta\lambda_0}{3p\sqrt{f}}\right)^{\frac{1}{2}}N \tag{26}$$

If p is low as at the point where the Townsend equation begins to replace the streamer mechanism, then if δ is not too low, the value of N becomes relatively small. This merely means that at a low pressure p, increasing x to δ to get a spark results in a reduced ion density N. If N is reduced below some critical value N_0 needed to insure photo-ionization for streamer propagation, there will be no streamer. If p is higher, the value of δ at which the density N reaches N_0 will be greater. Thus, at any given pressure, such as atmospheric pressure, there will always be a

value of the gap length, $\delta = \delta_0$ at which N is reduced to N_0. At pressures p well above 760 millimeters the value of δ_0 at which $N = N_0$ may be considerable so that Meek's equation will hold for very large gaps. It is, therefore, essential to establish the value of N_0.

Since we have no other basis for fixing the value of N_0, we may proceed as follows. The reason why, at low $p\delta \sim 200$ in air, the streamer mechanism is replaced by Townsend's mechanism with a low γ is that at this value the density of photo-ionization is too low for certain streamer propagation. Hence, we can choose as a working value for N_0 the value of N_0 at which at $p\delta \sim 200$ the Townsend mechanism replaces streamer formation. This value computed as above is $N_0 = 6.9 \times 10^{11}$ ions per cubic centimeter. Now at $p = 760$ millimeters, Meek's equation still holds at $\delta = 10$ centimeters. The value of N at this point is 8.8×10^{11} ions per cubic centimeter. For a gap of $\delta = 15$ centimeters, at 760 millimeters pressure, $N = 7.2 \times 10^{11}$ ions per cubic centimeter. This value is fairly close to the lower limit $N_0 = 6.9 \times 10^{11}$ ions per cubic centimeter at $p\delta \sim 200$. Thus, we will arbitrarily choose as the critical limiting density for streamer formation an ion density N_0 of 7×10^{11} ions per cubic centimeter.

An interesting consequence of this reasoning is that, while as usually studied on gaps with $\delta \sim 1$ centimeter Meek's equation fails and gives way to Townsend's mechanism at $p\delta \sim 200$, the value of $p\delta$ for this phenomenon will not always be 200. For, if we decrease δ, the value of p at which $(\delta/p)^{1/2}N$ permits the same limiting N_0 will also be decreased. Thus, the $(p\delta)_0$ for which $N = N_0$ will be smaller at shorter gap lengths than at longer ones. Hence, Meek's equation and the streamer mechanism will persist at lower values of $p\delta$ the shorter the gap. This condition will, however, be limited by the efficiency of the Townsend process as $p\delta$ varies. We can then proceed to state that at 760 millimeters there is a gap length $\delta \sim 15$ centimeters at which we can again expect streamer formation to begin to be

uncertain. The value of the sparking-field strength at δ_0 and $p = 760$ millimeters is $X_s = 24{,}000$ volts per centimeter.

Adopting this situation, one must conclude that at 760 millimeters pressure, for gaps exceeding $\delta_0 \sim 15$ centimeters, Meek's sparking criterion ceases to apply and that something is happening to the $V_s - p\delta$ curve at this point. Now it is precisely in this region that our only data on longer gaps at atmospheric pressure with alternating current in large-sphere gaps shows a change in slope of the $V_s - p\delta$ curve. With this situation in mind we may try to formulate a new sparking criterion or mechanism for long sparks. Since, with different pressures, the value of δ_0 for which $N = N_0$ will vary, we will proceed to formulate the theory on a more general basis applicable to any pressures.

13. Sparking Criterion for Long Sparks

To establish the sparking criterion one may proceed as follows. It will be assumed that sparking in long gaps still depends on streamer formation. However, for large values of δ it is clear that the ion densities at the head of the avalanche will fall below the critical value, N_0, adopted for air near atmospheric pressure as $N_0 = 7 \times 10^{11}$ ions per cubic centimeter. Hence, the condition *that the avalanche cross the gap* and produce a positive space-charge field $X_1 = KX_s$ at δ cannot be applied. Thus the sparking-field strength cannot be calculated from Meek's equation. What must take place as one reaches such gap lengths is that *the spark will require values of X_s greater than those computed by Equation 24.* Assuming that streamer formation requires a minimum concentration N_0 we can compute a field strength X_{s_0} and path length δ_0 which satisfy Equation 24 for a given p and when applied to Equation 17 give a concentration $N = N_0 = 7 \times 10^{11}$ ions per cubic centimeter. The calculation of the values of X_{s_0} and δ_0 satisfying these conditions can be achieved only by trial and error. Thus one selects a value of δ at a fixed p and from Equation 24 and α/p as a $f(X/p)$ evalu-

ates X_s. From these data, a, $x = \delta$ and r in Equation 17 can be fixed and N evaluated. One may then plot N as a $F(\delta)$ and evaluate the point δ_0 for which $N = N_0$. From δ_0 one can then evaluate X_{s_0}.

With this information it is clear that at p, for values of δ greater than δ_0 a streamer cannot form unless $X_s = X_{s_0}$. In this case the avalanche will progress to δ_0, *a streamer will form in the gap and progress back to the cathode*, allowing the avalanche to proceed anew as will be seen in detail later. Hence, for gaps longer than δ_0 *the value of* X_s *will not decrease for increasing* δ as before but will assume a higher value X_{s_0} adequate for streamer propagation. The value of X_{s_0} and δ_0 will change with p. The sparking potential V_s will then no longer be given by $X_s\delta$ but instead will be given by $V_s = X_{s_0}\delta$.

The effect of this change on the characteristic curve for sparking will then be as follows. At low values of δ for a constant p the slope of the sparking curve $dV_s/d\delta$ is greater than X_{s_0} as is well known. The slope gradually decreases until, in conformity with Meek's theory in a limited range, it is slightly less than X_{s_0} for air. *As the gap length approaches and exceeds* δ_0 *the slope must again increase up to* X_{s_0} *and then remain constant.* The new values of V_s above δ_0 must lie on a line of slope $(dV_s/d\delta)_0 = X_{s_0}$, and this line must pass through the origin. This is shown schematically in Figure 19, where V_s is plotted against δ.

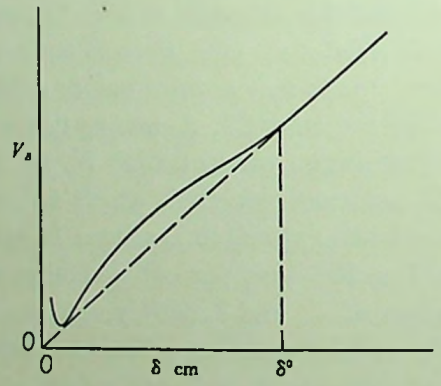

FIG. 19.—$V_s - \delta$ in air at 760 mm

This change in the slope of the curve near δ_0 will doubtless be gradual. So far no curves of this character have been observed for plane gaps at steady potentials. It is, however, precisely what is observed in the case of the sphere gaps where, at 760 millimeters, $\delta > 15$ centimeters. The difficulty of obtaining long gaps with uniform fields has in the past precluded the necessary measurements in regions where the change could be observed. That this is so can be seen by computing the values of X_{s_0} and δ_0 at a few values of p. They are shown in Table II.

TABLE II

p in mm	X_{s_0} volts/cm	δ_0 cm	X_{s_0}/p	$V_{s_0} = X_{s_0}\delta_0$
1520	38,000	88	25.0	3,340,000
760	24,000	15	31.8	363,000
380	15,050	3.3	39.6	49,700

It is to be noted that the values depend somewhat critically on the value of N_0 chosen and are not to be regarded as more than orienting magnitudes.

It is seen that above atmospheric pressure Meek's theory is applicable to almost any measurements we are able to make. At atmospheric pressure it is applicable beyond any measurements made to date. Below atmospheric pressure the change in the curves is open to experimental study. This has not been undertaken until now because no one thought it worth while to study long gaps at lower pressure. Such a study is now in progress in the Berkeley Laboratory.

The influence of the new sparking criterion on Paschen's law is to introduce a further deviation beyond that inherent in Meek's theory. This deviation is one which increases V_s by an increase in δ more than by an increase in p at such values of δ that Meek's law holds at the higher p and not at lower p. The deviation in any case will not exceed a few per cent.

It will thus in what follows be assumed that for gaps in excess of δ_0 in length, at any pressure, the Meek criterion is no

longer applicable; that *sparks progress by avalanche advance and retrograde streamers;* and that the sparking potential is given by $V_s = X_{s_0}\delta$. For air at atmospheric pressure $N_0 = 7 \times 10^{11}$ ions per cubic centimeter, $\delta_0 \sim 15$ centimeters and $X_{s_0} = 24{,}000$ volts per centimeter. With this assumption one must now analyze the retrograde streamer mechanism.

14. The Mechanism of Avalanche-Retrograde-Streamer Advance in Long Gaps

At atmospheric pressure, if X is less than X_{s_0}, or if $X = X_{s_0}$ but δ is less than δ_0, avalanches will leave the cathode and cross the gap. No streamers will form and *the gap will not break down.* If $X = X_{s_0}$ and $\delta = \delta_0$ avalanches cross the gap, streamers form at the anode and breakdown is possible. If $X = X_{s_0}$ and δ is greater than δ_0 breakdown will occur. The sparking potential V_s will be fixed by $X_{s_0}\delta$ but the avalanche will not cross the gap at once. What will happen is that the avalanche will advance to δ_0. At this time *a streamer will propagate in the retrograde direction* back to the cathode at a speed of some 10^8 centimeters per second. Before it is well advanced, the positive space charge at δ_0 will exhibit some retarding action on the advance of the electron cloud until the incoming electrons up the streamer channel reduce the positive space-charge field. Once the streamer tip reaches the cathode and the supply of electrons runs up the channel, making it a conducting filament of plasma, the negative electrode will have extended itself to the distance δ_0 in the midgap. In the meanwhile the avalanche has again begun to proceed at its normal velocity until it reaches a distance $\delta_0 + \delta_1$ from the cathode.

The condition for streamer formation is that with X_{s_0} fixed, the electron avalanche or avalanches proceeding from δ_0 must advance a distance δ_1 such that the combined space-charge density at the end of δ_1 is $N_0 = 7 \times 10^{11}$ ions per cubic centimeter. Now at the cathode there was one electron initiating the avalanche. Hence, the value of $\delta_1 = \delta_0$. After the first advance of

δ_0 there may be more than one electron in the electron space charge so placed that it progresses in the field X_{s_0} to multiply effectively and thus lead to the density N_0 needed for a streamer. In this case with n such electrons the distance δ_1 traversed before the second streamer completes this channel will be fixed by $N_0 = nae^{\alpha\delta_1}/\pi r^2$. Hence, the later distances of avalanche travel before retrograde-streamer formation will not of necessity be δ_0 but distances δ_1. This circumstance will merely have the effect of making the distances of avalanche progress between streamers shorter, thus only reducing the value of r. After advancing $\delta_0 + \delta_1$ the avalanche again suffers some retardation, while a new streamer advances toward the cathode from $\delta_0 + \delta_1$ to join the filament of plasma with its tip at δ_0. This continues until the avalanche approaches the anode, when, as is the case in the overvolted gap, the anode streamer finally closes the gap, giving breakdown. If in such a long gap an electron is initially created in midgap, as is usually the case for long sparks, then after traversing the distance δ_0 toward the anode the avalanche pauses while the streamer not only propagates backward the distance δ_0 *but proceeds all the way back to the cathode;* from then on it proceeds as before.

The breakdown process is thus seen to be essentially an avalanche advance combined with a streamer action. It is thus in keeping with the streamer theory of spark discharge and is in fact a modified streamer theory. It yields, however, a different value of the sparking potential than that given by Meek's criterion. This follows since streamer formation is limited by the decreased ion densities involved. This in turn requires a fixed field strength X_{s_0} so that one computes the sparking potential on a different basis.

The streamer propagates in a retrograde direction with an initial diameter equal to the value of r given by the avalanche cross section at δ_0 or δ_1. It may spread somewhat as a result of the ionization by the incoming electron avalanches. The low diffusion coefficient for positive ions in the 3×10^{-7} second of

retrograde travel to the cathode, however, keeps the channel relatively narrow. The electron avalanche cloud is by its rapid diffusion tending to broaden the channel as it advances. On the other hand, the strong axial component of the space-charge field of the positive streamer tip and of the avalanche tip exert a conservative action in reducing the lateral diffusion of the electron cloud, thus tending to keep the avalanche from spreading as it would were it unrestricted. There is, however, a greater tendency toward crooked streamers and branching in the longer sparks. Since in such long avalanche-streamer processes there is a slight diffusive loss of electrons from the avalanche tip, one may expect that a small electron current flows from the cathode up the streamer channel to supply the loss.

15. Sparks in Long Gaps with Nonuniform Fields

In nonuniform fields the equation for streamer formation is the modified equation of Meek, which takes into account the fact that the field strength X and hence also α varies over the gap. This equation reads

$$X_1 = KX_{x_s} = \frac{\dfrac{4\epsilon a_{x_s} e^{\int_0^{x_s} a\,dx}}{3}}{\left(1010\dfrac{2x_s\lambda_0}{3p\sqrt{f}}\right)^{1/2}} \tag{25}$$

In this equation, x_s is the distance of avalanche travel in the divergent field necessary to make the positive ion space-charge field $X_1 = KX_{x_s}$ so that a streamer may propagate, while a_{x_s} is the value of α at the vital portion of this avalanche where the ionization is cumulatively increasing most rapidly and X_{x_s} is the strength of the electrical field at the point x_s. That is, the derivation of the equation requires that α multiplying into the exponential term to be the value a_{x_s} in the last increment of path dx where the space charge is building up. It may be noted

that the value of the integral $\int_0^{x_s} a dx$ is independent of the order in which the limits are imposed relative to the increase or decrease of a with x so that $\int_0^{x_s} a dx$ is independent of polarity in the high-field region. On the other hand the polarity of the high-field region changes the value of X_{x_s} and hence alters V_s (see page 142). It is essential in addition that at the pressure existing, the distance of travel and the field X_{x_s} are adequate to insure the density N_0 of ions required for streamer propagation.

In writing this equation nothing has been said as to the values of X across the gap. It is clear that *a streamer is initiated* if, either at the positive or negative electrode, the fields X_{x_s} are such that a streamer can form. If the electrode is the positive electrode then the avalanche proceeds from an origin $x = 0$ at a distance x_s away from the electrode surface in the field direction and ends at the surface at $x = x_s$. The streamer then advances outward from the electrode toward the negative electrode. Whether it reaches this is a matter to be discussed later. If the electrode is negative an avalanche proceeds outward from the surface at $x = 0$ to a distance $x = x_s$. If at this point $KX_{x_s} = X_1$ for the positive space charge, a retrograde streamer moves back to the cathode essentially extending the potential of the electrode out into the gap a distance x_s. The process then again repeats itself. The question as to how far this process proceeds out into the gap is again one which needs further discussion.

Now, in many unsymmetrical and otherwise nonuniform gaps the fields at the electrodes are very high while those in midgap are very low, lower than the potential difference divided by the gap length. They are so low in fact that a has a value zero in these regions. While it is absolutely correct to infer that the streamer process carries with itself a considerable field distortion and thus extends the electrode fields out into the gap, it is possible that the midgap fields may be so low as to

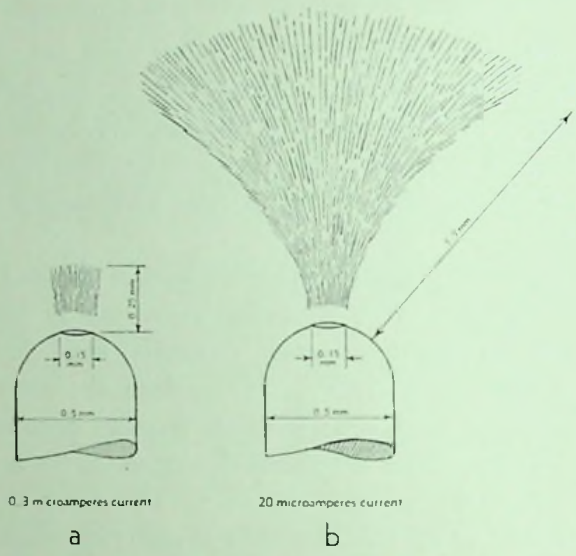

FIG. 20.—Trichel's corona

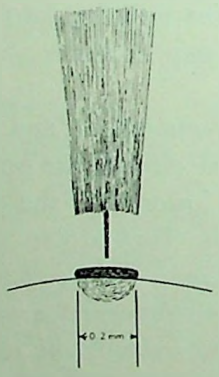

FIG. 21.—Kip's corona

prohibit further streamer propagation. This situation is actually frequently encountered in very long gaps and gaps that are fouled by ionic space-charge accumulations from antecedent discharges in the weak midgap regions. In such cases we have *local and partial breakdown in the form of corona discharges from one or even both of the electrodes.*

Where the small electrode is positive we in fact see the development of pre-onset streamers which cannot cross the gap. These are eventually choked off by their own space charges and lead to a modified form of corona known as the burst pulse corona of Trichel.[8] Where the positive points are too small and the fields are too concentrated, even the pre-onset streamers fail to develop.[6,8]

For larger negative points against positive planes the avalanche-retrograde streamer mechanism is observed. Where the fields become too restricted, owing to the small radius of curvature of the point, the corona localizes at the point surface. Here γ becomes prominent and *a characteristic glow-like discharge operating on Townsend's mechanism materializes.* In some cases this periodically throttles itself by space charges. Electrodes of intermediate size show a combination of the glow-like discharge together with an incipient negative avalanche-retrograde streamer process.[50] The Townsend-like glow discharge and the incipient streamer are shown in Figures 20*a*, *b* and 21, drawn by Trichel[49] and Kip[50] from telemicroscopic studies.

Where the electrodes, despite large spacing, are sufficiently large to insure either positive or negative streamer formation, breakdown may proceed by one or the other mechanism or both. There will, in general, be a significant difference between the two forms of breakdown in long gaps. For fine negative points the character of the space-charge formation differs from that for the fine positive point.* For the positive point the elec-

* The points must not be so fine that the $\alpha_{x_s} e^{\int_0^{x_s} \alpha dx}$ fails to give an adequate space charge for streamer formation. This leads to the suppression of streamers for both signs of points and replacement by other mechanisms.

trons of the initiating avalanche are swallowed up by the point and the positive streamer advances into nearly virgin air without much space charge to hinder it. It carries the high ion density from the electrode surface with it. It advances to a point where the field is too low to permit further advance. Until the space charge of such a streamer which did not cross the gap is cleared from the weak-field regions of the gap, it may, however, prohibit a further streamer formation. Where the field about the negative point attenuates rapidly an avalanche proceeds outward from the point into a weak-field region. The electrons at the avalanche tip then find themselves in a weak-field region *which is still further attenuated by the positive space-charge field of the avalanche.* Thus *the positive space charge in the rear of the avalanche increases the field between itself and the cathode,* while in the weak and declining field ahead of the electron avalanche the field to the anode is not enhanced in equal measure. In a uniform field this action of the positive charge does not occur, as it is dense only *near* the anode or at an avalanche head. Where the field diverges rapidly the difference may be significant. Thus the negative avalanche-retrograde streamer mechanism may in divergent fields be inhibited from materializing until fields at the electrode surface are achieved that are much higher than those for the positive point. This action is further enhanced, since X_{x_i} for the negative point is less than for a positive point, so that α_{x_i} is much lower for the negative point and V_s must be increased, as seen on page 142. This situation leads to a tendency of the small-point mechanism to utilize a γ which becomes appreciable in the high-field region and so favors Townsend's mechanism.

For larger electrodes the high fields extend out farther. Here the positive point can again yield streamers as soon as Meek's equation is satisfied. In the case of the negative point given a sufficiently long high-field region the negative avalanche-retrograde streamer mechanism can materialize. However, the length of advance of such streamers in a nonuniform gap for the same

field strengths as for the positive streamers will not be nearly as great. This is nicely seen in Figure 22, discussed on page 92. For, while both processes advance into low-field regions, the positive streamer carrying with it the high-field gradient at the electrode surface will find advance easy. On the other hand the fact that the negative avalanche-retrograde streamer mechanism is already operating at a density limit of N_0 makes progress into low regions of X much less likely on the basis of the attenuation of ion densities in low fields. That is, such a mechanism cannot send a negative avalanche-retrograde streamer process far into fields $X < X_{s_0}$. Hence, breakdown by means of negative-streamer processes will take place at higher electrode potentials and less readily at lower potentials than will those by positive-streamer processes. This is a well-known experimental observation.

That minimum fields for the progress of streamers and avalanche-retrograde streamer processes exist was amply indicated above. As to the magnitudes of these minimum fields little is known. It is possible that they will in part depend on the previous history of the streamer or avalanche-retrograde streamer and on pressure. That is, it is possible that they will depend on the electrode conditions from which the processes originate and on the density of effective photo-ionization. Probe measurements[51] in a gap with positive point-to-plane corona discharge indicate that near breakdown with an average gradient between the points and plane of 5,500 volts per centimeter the minimum measured field about halfway across the gap of 4,000 volts per centimeter is low enough to prohibit streamer advance. The field required for propagation estimated from the breakdown potentials where streamers crossed the gap may then be as high as 4,400 volts per centimeter. More studies of this sort can well be carried out and may lead to considerable light on the subject.

The fact that there is a marked difference in the conditions for streamer advance and avalanche-retrograde streamer ad-

vance leads us at once to expect that there should be a difference in the breakdown potentials from positive and negative points. This is in fact the case. It is difficult to express the degree of the difference quantitatively. The best one can do is to state that the average field strength (potential difference divided by the gap length) for a spark with the positive point to plane is of the order of 4,400 volts per centimeter, compared to the value of 9,000 volts per centimeter for the negative point to plane. As indicated before, when the fields in the gap with a positive point reach such a value that the streamers can traverse the gap, breakdown is likely. With the negative points it is clear that the fields must be higher before avalanche-retrograde streamer processes can advance very far into the gap. In gaps such as this it is doubtful whether the negative point-to-plane breakdown ever takes place by means of the negative avalanche-retrograde streamer mechanism alone, owing to the low value of the midgap fields.* In fact the moving-film camera photographs of Allibone and Meek[12] show that the sparks consist of avalanche-retrograde streamers which advance from less than one-third to one-half way across the gap where they are met by a positive streamer from the anode. That this must be the case was postulated by Loeb and Kip[8] in their study of the negative corona. To account for the positive streamer from a plane electrode where the field is assumedly low, it was proposed that in breakdown with steady negative-point corona *the space-charge density of negative ions at the anode* might produce fields that could yield streamers. Actual measurements made by Waithman and Baker,[51] using probes in positive- and negative-point corona gaps of about 4 centimeters length at atmospheric pressure in air, indicate that fields of this character and probably adequate magnitude can occur. The occurrence

* Lightning discharge is the nearest exception to this statement. In this case the low conductivity of the ground and the ultra-long gaps favor negative-streamer advance. Still the stroke is usually completed by a positive streamer from the ground.

of such fields can also be demonstrated on the basis of actual data as the following simple calculation shows.

Assume a negative point-to-plane gap of 4 centimeters length. Just before breakdown the current is 15 microamperes. In a time of t seconds the current i gives $q = 3 \times 10^9\ it$ e.s.u. of negative charge in the gap in transit, where t is the time of transit of the ions across the gap. Now the field strength X at the anode will be $X_a = 4\pi\sigma$, where σ is the surface density of *induced positive ions* at the anode. If the current to the anode is uniformly distributed over its area A, the value of X_a can be computed as follows: Assume, as is the case for the negative point, that the point is effectively screened by the positive space charge

$$X_a = \frac{4\pi \times 3 \times 10^9 it}{A} \times 300 = 1.13 \times 10^{13} \frac{it}{A} \text{ volts/cm} \quad (27)$$

Now t has been measured by Kip[6] for the positive ions and is not essentially different from that for negative ions. Hence, in Equation 27, $t = 2 \times 10^{-3}$ second and $A = 10$ square centimeters. Thus $X_a = 34{,}000$ volts per centimeter. With the concentration of the discharge at the center of the anode the field will be materially higher and will thus enable the positive streamer to propagate from the anode.

In the case of impulse breakdown from the negative point the situation is somewhat different. Space charges at the anode do not form in the short times. The potential of the negative point must be raised to values sufficiently high to launch an avalanche-retrograde streamer process that can advance well toward the anode. The impulsive change in the field distribution in the gap can then be shown to lead to field gradients at the anode of sufficient magnitude to launch an anode streamer. This will meet the cathode streamer process near midgap and complete the spark. Such breakdowns photographed with the moving-film camera by Allibone and Meek[12] are shown in Figure 22. Analogous breakdowns photographed for positive-

point breakdown with only positive streamers are shown in Figures 23*a*, *b*.

To show that breakdown occurs in this fashion we proceed as follows. The negative avalanche is projected into the gap and introduces a charge of Q coulombs into the gap at the negative point before it is propagated across the gap. Now Jeans[52] shows that the field induced at a conducting-plane electrode a distance l directly below a quantity of Q coulombs at a point is given by

$$X_a = \frac{2Q \times 3 \times 10^9}{l^2} \text{ e.s.u.} = 1.8 \times 10^{12} \frac{Q}{l^2} \text{ volts/cm} \qquad (28)$$

To make $X_a = 3 \times 10^4$ volts/cm, Q must equal $1.67 \times 10^{-8}\ l^2$ coulombs. Thus $\int_0^t i\,dt$ must equal $1.67 \times 10^{-8}\ l^2$ coulombs in the time t of streamer formation at a current i. For $l = 3$ cm, $Q = 1.5 \times 10^{-7}$ coulomb, which means that the avalanche in its time of growth t must give 9.4×10^{11} ions. This is just about the number of positive ions and therefore of electrons in the avalanche to permit streamer formation. Hence, for this gap, where streamer formation is just beginning, a positive streamer may start. This picture is perhaps oversimplified. For there are periods before the streamer elements reach the cathode where there is a dipole acting instead of the volume charge Q. There will, however, be times when Q alone acts, and this *with the advance of Q into the gap* can give adequate fields at the anode. For longer gaps l^2 is increased. Hence $\int_0^t i\,dt$ must be larger. This requires merely that the time t must be greater, which has the consequence that the negative streamer *must* advance further into the gap, decreasing l and increasing Q. Thus one clearly sees why with impulse breakdown for small negative electrodes the observed negative-streamer advance into the gap is longer and meets the positive streamer more nearly in midgap.

Before leaving a discussion of the breakdown of long gaps

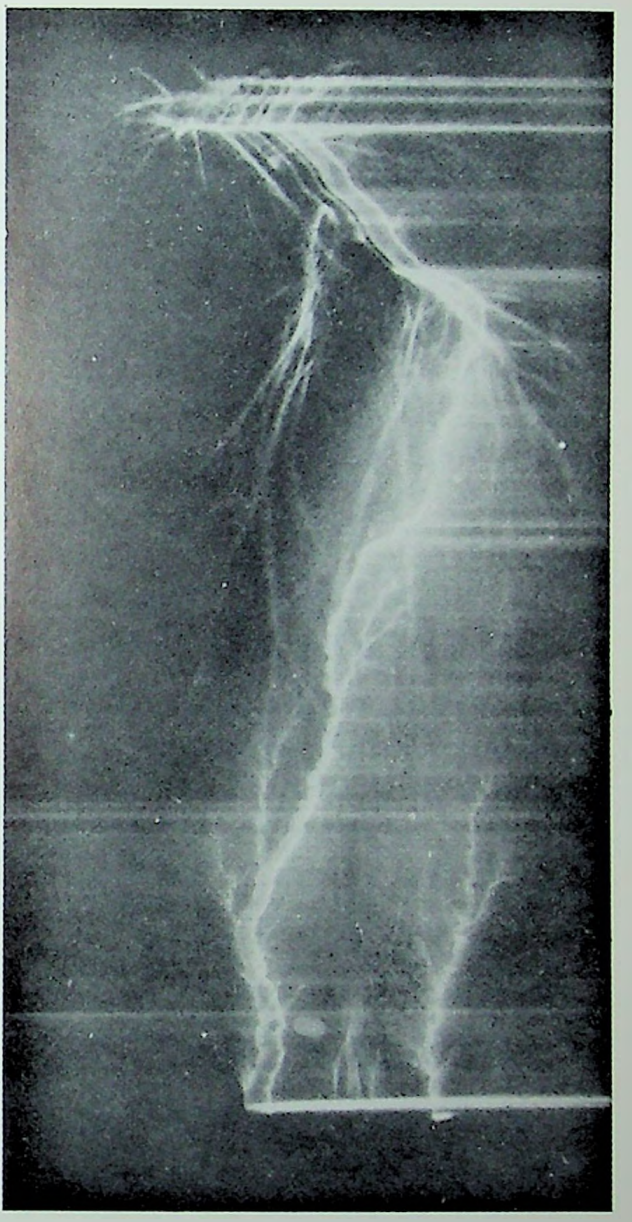

FIG. 22.—Discharge in a long gap photographed by Allibone and Meek with a rotating camera. The voltage source was an impulse generator connected to the gap through a resistance of 6×10^5 ohms. The negative point is at the top. The anode is an earthed plane. The high resistance causes a negative stepped-leader stroke consisting of an avalanche retrograde-streamer mechanism to proceed one-third the way across the gap. This causes a high field distortion at the earthed plate which starts a positive streamer. The streamer proceeds to meet the negative leader stroke at a point ⅔ the gap length up from the plate. The final return discharge from cathode to anode after junction of the two streamers is seen to the right of the initial positive streamer. The passage of time is indicated by displacements to the right. Note the unsuccessful negative leader strokes to the upper left, which did not produce a positive streamer and the second positive streamer to the lower right that started too late to join the negative leader.

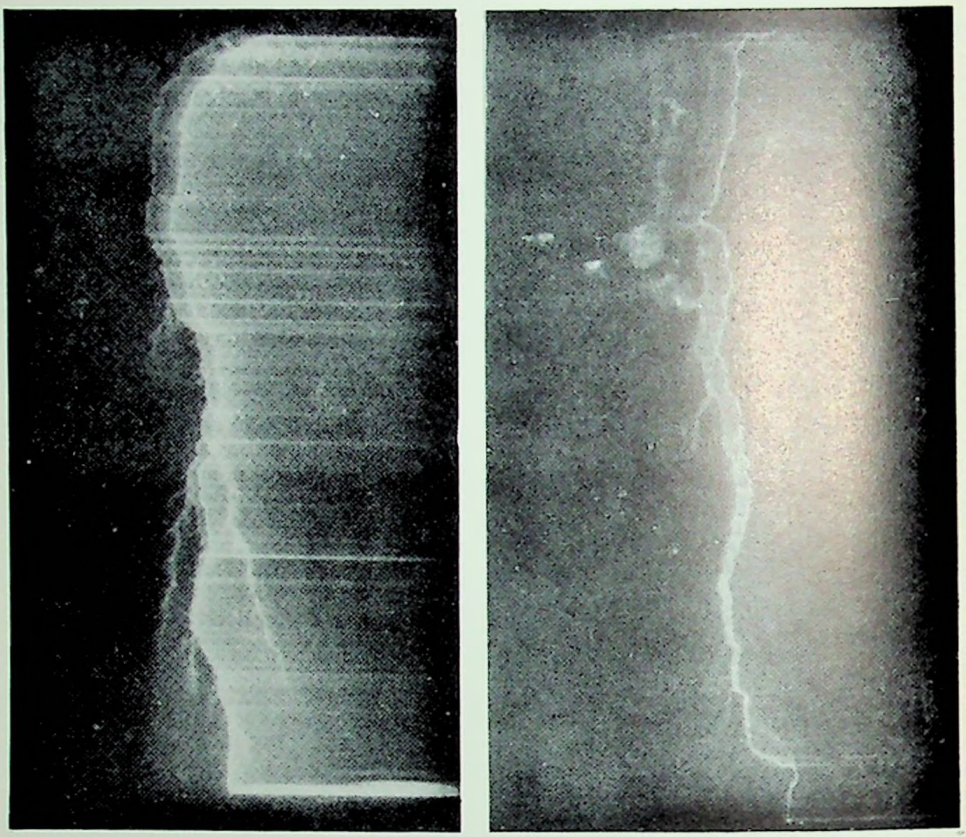

FIG. 23.—Photographs taken with a rotating camera to show the breakdown of a 100 cm gap in air at atmospheric pressure between a positive point and an earthed plane. The voltage source is an impulse generator, which is connected to the discharge gap through a resistance R, where (*a*) $R = 100.000$ ohms; (*b*) $R = 1.000.000$ ohms. The film movement is such that the leader stroke appears on the left, the main stroke on the right. The point electrode is at the upper end of the photograph. The discharge progresses along the trace at the left to strike the ground and then returns as a brilliant flash depicted by the right-hand trace, which follows in general contour the leader stroke. The speed of the main stroke is much greater than that of the leader stroke, so that the distance between the two traces at any position in the gap enables the time of passage of the leader stroke, and thus its velocity, to be determined. In *b* the very faint parallel lines to the left probably represent the first two steps of the leader-stroke advance. Note the downward branching, particularly in *a*.

with nonuniform fields, attention must be called to the quantitative discussion of the breakdown of sphere gaps. This is treated at length in chapter iii. Here only a few matters cogent to the questions under discussion will be pointed out. For sphere gaps of large radius with gap length that do not give too low a field in the midgap region, breakdown usually starts, as in the plane-parallel case, from the cathode as a negative avalanche process and proceeds across the gap to the anode, giving a breakdown streamer. The field, X_{sm}, in midgap must, however, be great enough so that the field at the streamer tip along the axis, $X_1 + X_{sm}$, will give enough photo-ionization to yield the N_0 ions per cubic centimeter needed for a streamer. On this basis one can calculate V_s for the gap on Meek's theory from Equation 25. The total value of V_s is slightly less than for a plane-parallel gap of the same length but the field at the cathode X_{s_c} is greater than X_s for a plane-parallel gap. If, now, the gap length be increased so that the midgap field falls, the picture changes. When the field at midgap falls so low that α ceases to have adequate values, the avalanche ceases to increase across the gap and disperses as it advances in the low-field region. The avalanches from the cathode may advance to near midgap and perhaps even send back a streamer, but they can usually advance no farther. On the other hand, an avalanche starting at midgap will advance to the anode. This will give a streamer that can propagate from anode through the midgap region (if $X_1 + X_{sm}$ is not too low) and produce a spark in this fashion. In this event δ is one-half as great as for the avalanche crossing from the cathode. The value of V_s for this gap is still slightly below the value for the plane-parallel gap. It is, however, higher than that for a process where the avalanche *could cross the whole gap length* δ *and produce a streamer.* Again Meek's theory can be applied to this process of breakdown and leads to values of V_s in agreement with experiment. At gaps whose length is just on the borderline between the two mechanisms, sparks will take place on either mechanism, but those

initiated by avalanches from the cathode will have a lower value of V_s than those from avalanches which start in midgap. Hence, the observed potential V_s in this region will show an abnormally high scattering of values dependent on the point of origin of the initiating electron. This was observed but could previously never be explained.[53]

There is finally another phenomenon which has been observed in the spark breakdown of corona gaps at various pressures which had defied understanding until recently. Inasmuch as it throws a great deal of light on the question of the progress of positive streamers in weak-field regions, it will be discussed.

If the characteristic curves for sparking potential and the potential for positive-corona onset are plotted as a function of pressure, the onset potentials for corona will be observed to be well below the spark-breakdown values of the gap for lower pressures. As the pressure increases, however, a value is reached where the sparking potential begins to decrease. It decreases with increase in pressure until the sparking-potential curve reaches the curve for onset of corona. Thereafter, as pressure increases *there is only one curve which is the breakdown and corona-onset-potential curve.*[54] Thus it is clear that above a certain pressure range the corona onset and sparking potential coincide.

Now it was indicated above that positive-corona onset was preceded for all but the finest points by the appearance of pre-onset streamers. These proceeded away from the anode but a short distance. If the gap was fouled by positive space charge they could not develop at all.

It is clear that low-field strengths must prevent streamer propagation. The reason for this is clear. The advance of a streamer depends on the supply of photoelectrons in the gas and their effective multiplication by ionization by collision in advance of the tip space charge of the streamer. Now the field multiplying the electrons in the effective region ahead of the streamer is some function of X_1, the tip field of the streamer,

plus X_x, the field at the point x in the gap. The tip field of the streamer X_1, emanating as it does from the high field at the anode, may initially be high and in midgap greater than X_x. As the streamer advances some of this field, X_1, goes to maintaining the iR drop which keeps the excess electrons (see p. 104) going to the anode. Thus the tip field is falling as the distance from the anode increases. It may also decline for other causes connected with ionization. In any gap, if X_x is low enough, there must come a time when the photoelectronic density and the electron multiplication ahead of the streamer fail to maintain the ion concentration N_0 because of the low value of $X_1 + X_x$ and the advance field $f(X_1 + X_x)$. Now as pressure increases, while α may be decreased somewhat by the increase in p, two other conditions are being much ameliorated. First the density of photo-ionization about the tip is being increased and, what is more, the increased density of photoelectrons is brought much closer to the strong portion of the space-charge tip field. At the higher pressure the efficiency of ionization in short distances of travel is also increased. Hence, the effect of attenuation of the imposed field X_x is no longer as serious as pressures are increased, for the ionization processes feeding the streamer tip are brought much closer to the tip where the fields are higher. It is thus not unexpected to see at higher pressures the point reached where even in attenuated fields, X_x, the tip field, can propagate a streamer across the gap. Thus, at this point, the onset potential, which marks the initiation of streamers at the anode, suffices to give streamers that propagate across the gap and cause a spark. This accounts for the observations and again emphasizes the importance of pressure in facilitating streamer advance, which was nicely illustrated by Meek's equation.

16. The Mechanism of Lightning Discharge

When one considers the case of the longest discharges observed, namely the lightning discharge, it is again clear that the mechanism will be based on the propagation of streamers,

or, where conditions warrant, on an avalanche advance and retrograde streamer formation. The observations on lightning discharges have shown that, wherever it is possible for positive streamers to form and propagate, this mechanism will predominate. However, the observations of Schonland and others[55] on lightning discharges from cloud to ground indicate that since, in the majority of the thunderstorms, the negative cloud predominates in its proximity to ground, a considerable fraction of the discharges propagate from highly localized concentrations of negative charge in the cloud and move toward the ground. The exact nature of the way in which the electrification leading to a stroke accumulates and concentrates is not known. The excellent studies of Simpson and Scrase[56] made on gradients at the ground, in the air, and in the clouds by means of balloons indicate the existence of either mild field gradients of 300 volts per centimeter or less or else gradients that caused a spark to pass in their apparatus. They correctly conclude that either the gradients leading to strokes are exceedingly localized in space or else that they arise very suddenly as a result of turbulent convection in localized areas. Doubtless both effects are present. But when such an accumulation in a negative cloud yields gradients capable of giving avalanches or streamers, a breakdown begins, much as is the case for smaller negative electrodes.

a) Progress of a typical lightning discharge.—The typical lightning discharge has been extensively studied by Schonland, Malan, and Collens[55] by means of the Boy's camera. It is illustrated by Figure 24, where the steps in the leader stroke are seen at the right, the time axis going from right to left. Schonland[57] has analyzed the progress as follows. The discharge from the negative cloud is preceded by an invisible pilot streamer advancing into virgin air at the rate of about 1×10^7 centimeters per second.* After an advance of some 5 meters, or in an

* Schonland[57] finds that for the majority of pilot streamers the velocity lies between 1.0×10^7 and 5×10^7 centimeters per second, though higher velocities,

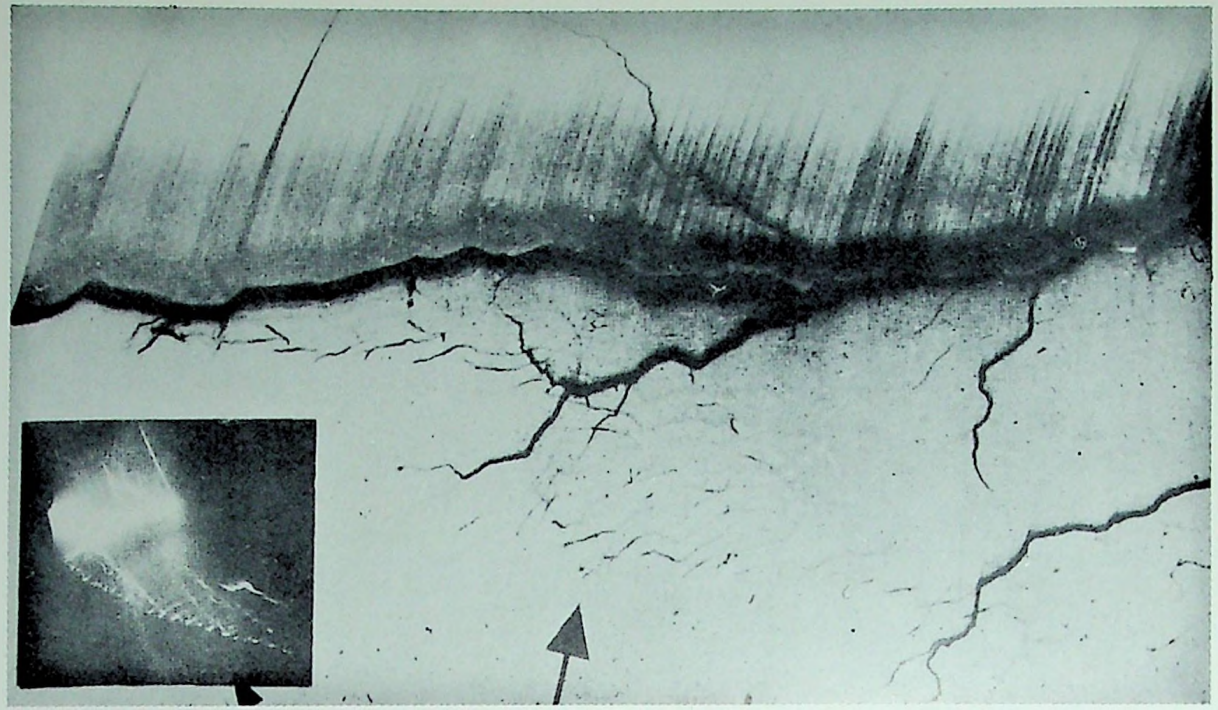

FIG. 24.—Photograph taken by Schonland, Collens, and Malan with a Boys camera to show the development of the stepped-leader stroke for the lightning discharge. The direction of motion of the lens which recorded the stroke is from right to left, as shown by the arrow, so that the steps are seen on the right of the subsequent brilliant return stroke. The time interval between each of the steps represents approximately 50 μ secs. Notice also that the leader stroke corresponding to the branch on the right is well to the right near the arrow while the leader stroke corresponding to the main stroke can be discerned more to the left.

average of 50 microseconds of travel, a *stepped-leader stroke*, moving at the speed of 2×10^9 centimeters per second advances from the cloud to the tip of the pilot streamer down the pre-ionized pilot streamer and slows down to the pilot-streamer speed. Then after another interval of 50 microseconds, if the stroke is long enough, it is caught by a second stepped leader and so on. For strokes in excess of 2 kilometers as many as 2 stepped leaders may be proceeding down the channel at once. As the pilot streamer approaches the ground, field distortions such as those calculated on page 92 may lead to the initiation of one or more positive streamers from appropriate conductors. These, as in Allibone and Meek's long sparks,[12] eventually join the pilot streamer. Then over the pre-ionized streamer channel the brilliant return stroke, operating through ionization by a potential wave traveling up an ionized channel, follows at a speed of 10^{10} centimeters per second, completing the discharge. Later successive strokes (up to 40 have been observed) from the cloud follow down the first spark channel, with its ionization decaying as a result of recombination, as the more distant elements of the cloud release their charge. These discharges consist of what Schonland terms *dart leaders proceeding from cloud to ground* at the rate of 2×10^8 centimeters per second, through the decayed ionization in the old channel, followed by a rapid return stroke from the ground.

b) *Meek's theory of the stepped-leader stroke.*—Meek[58] has investigated the details of the progress of the pilot streamer and shown the origin of the stepped leader without considering the mechanism of the pilot streamer.

In order that the pilot streamer could advance continuously, he assumed that there must be a minimum current, *i*, flowing

up to 2×10^8 centimeters per second are observed. The higher velocities occur for streamers whose behavior indicates that they may be traveling in fields of abnormal strength. In his calculations Meek[58] uses the value of 2×10^7 centimeters per second for the velocity. However, since we are considering here the minimum fields necessary for streamer advance, we will use the lowest value for the velocity as observed by Schonland, viz. 1.0×10^7 centimeters per second.

into the streamer tip to provide the charge. To calculate this current he also assumed that the field at the streamer tip was 30,000 volts per centimeter, a field capable of giving streamers with 1 centimeter of travel of the avalanche. If the pilot-streamer channel has a radius of r centimeters, then the current i, according to Schonland,[57] has the value $i = \frac{1}{2}Xvr$. Now r was chosen as the diffusion radius of the electron avalanche in 5 to 10 meters of advance, or in 50 microseconds of travel. This was calculated to be about 0.3 centimeter from Raether's equation,[2] giving the current i as 0.1 ampere, a not unlikely value. The ion density at the tip is then

$$\rho = \frac{i}{(\pi r^2 \epsilon v)} = 1.1 \times 10^{11} \text{ per cm}^3$$

for $v = 2 \times 10^7$ centimeters per second. It is seen here that the values were not quite properly chosen, since the ion density is too small to cause streamer formation. Of this more will be said later.

Having determined these conditions, Meek showed that in the 50 microseconds of travel the initial density of ions at the cloud end of the channel had decayed to 10^{10} ions per cubic centimeter by recombination. With a resistance, R, of 4.6×10^5 ohms per centimeter, in the spark-path channel calculated from the electron mobilities, the iR drop of 4.6×10^4 volts is sufficient to launch a stepped-leader stroke from cloud to pilot-streamer tip at the speed of 5×10^9 centimeters per second. This increases the ion density to 10^{14} ions per cubic centimeter in the channel and re-establishes the conductivity. In the next 50 microseconds the density has, by recombination, again fallen to 10^{10} ions and a new stepped leader proceeds. The calculations are consistent with the observed data on lightning-discharge propagation. The high velocity of the return stroke comes from the density of 10^{14} ions per cubic centimeter in the stepped-leader stroke process which, on the Schonland-Loeb and Cravath[13,14] mechanism, makes such velocities possible. The

fact that the decay of ionization by recombination in 50 microseconds to 10^{10} ions per cubic centimeter is so insensitive to the initial ion density N_0, above 10^{11} ions per cubic centimeter, comes from the recombination equation, $N = N_0/(1 + N_0 a_1 t)$. It lies in the fact that with the coefficient of recombination a_1 in air $= 2 \times 10^{-6}$, $N_0 a_1 t = 2 \times 10^{-6} \times 1 \times 10^{11} \times 50 \times 10^{-6} = 10$ is greater than 1, and thus N is nearly independent of N_0 but depends on time only.

c) Modification of Meek's theory in conformity with avalanche-streamer mechanism.—One must now consider the mechanism of the pilot-streamer advance. In the light of the mechanism of long sparks one can assume that, when a gradient due to the cloud of $X_{s_0} = 25{,}000$ volts per centimeter or more is created over a length of some 15 or more centimeters, a chance electron at the cloud starts an avalanche which proceeds toward the ground at a speed of about 1×10^7 centimeters per second. After 15 centimeters travel, this avalanche has built up a density of positive ions of 7×10^{11} charges per cubic centimeter. At this point a retrograde streamer moves to the cloud, establishing a conducting channel at its arrival in some 5×10^{-8} second or thereabouts. This conducting path is somewhat increased in radius beyond the radius of the avalanche tip, which in 15 centimeters travel is $r = 0.052$ centimeter, owing to the character of the process of streamer formation as shown in Raether's photographs. The avalanche then forges ahead again for a distance of δ_1 centimeters, and a new streamer propagates backward, lengthening the channel of conducting plasma to $15 + \delta_1$ centimeters from the cloud. This process of advance of the pilot streamer continues for some 50 microseconds until a stepped leader starts and reaches the end of the pilot streamer. The arrival of the stepped leader doubtless increases the tip field of the pilot streamer, which forges ahead with a somewhat enhanced speed and perhaps shorter steps before retrograde streamers form, but eventually settles down to the initial procedure.

If, then, this picture is the correct one for the mechanism of advance of a pilot streamer, the reasoning and figures given above must be altered in detail but not in principle. In principle, Meek's theory assumes that there must be a current i flowing down the streamer channel. It assumes that, owing to decay of ionization, the resistance of the streamer channel increases so much that after 50 microseconds the potential gradient caused by the iR drop in the channel reaches values initiating a stepped leader. This proceeds down a pre-ionized channel having a density of 10^{10} *electrons* per cubic centimeter. It is now necessary, in view of the mechanism of streamer advance developed, to reconsider the conditions existing. The first of these lies in the criterion for the propagation of the stepped leader. Since recombination is taking place in the channel *the negative carriers present must, in a large measure, be negative ions;* otherwise the density would not fall to 10^{10} ions per cubic centimeter in 50 microseconds. While the energy of the electrons and the field strengths in the channel are not known, one can make certain statements. During the early part of the travel of the streamer, it is clear that the fields in the channel will be low, since the iR drop is small. If decay by recombination is to proceed, the potential gradients must furthermore be well below that corresponding to an $X/p = 20$ at which electrons can ionize by impact. Just before the potential wave starts down as a stepped leader, however, both ionization by collision and high electron energies must begin to occur. Under these conditions it is probable that in the early stages electrons will be attaching to molecules to give negative O_2 ions, and the data on rate of attachment indicates that possibly 0.9 of the negative carriers are ions and the rest electrons. Before, however, the step can advance, *all the negative ions must suffer electron detachment* which requires an X/p of from 70 to 90.[39] Thus in the channel as the ion density falls the carriers are mostly ionic, the iR drop increases, and gradients build up leading to ionization by collision, with an attendant sudden increase of gradient

between that section and the adjacent region toward the advancing end. In this way quite suddenly fields of the order of 53,000 to 65,000 volts per centimeter appear at the cloud end of the streamer channel, and the stepped leader starts its advance at a velocity of 2×10^9 centimeters per second.

It now becomes essential to consider the value of the current which gives the iR drop needed in the streamer channel. It is, at first, obvious that the general equation used by Meek[58] and Schonland[57] has no significance in this particular mechanism. One must consider the character and nature of the mechanism in the ionized column set up by streamer formation. As a result of the field X_{δ_0}, which must equal 25,000 volts per centimeter over the δ_1 centimeter of avalanche travel, the avalanches create $e^{\alpha\delta_1}$ ions for each of the electrons which advance a distance δ_1. At the end of the $\delta_0 = 15$ centimeters of travel, if only one avalanche starts, that one electron avalanche has created an ion density of 7×10^{11} ions per cubic centimeter and a retrograde streamer forms, making a plasma in the channel of radius $r \sim 5.2 \times 10^{-2}$ centimeter with about 10^{13} or more ions per cubic centimeter. Now such a mechanism does not require a current of electrons to maintain itself. All it requires is a potential pulse or wave which moves at about 1×10^7 centimeters per second toward the ground. The plasma must have equal numbers of positive ions and electrons plus negative ions. Hence, no current other than a displacement current is needed. This does not contribute to the iR drop as it advances with the tip. If, however, in the advance of the electron-avalanche tip, there is a loss of electrons as a result of the radial field and lateral diffusion so that the electrons do not remain in the channel later to be occupied by the streamer, negative charges are lost. *These charges must be replenished* to give a neutral plasma and can do so only if they follow down the streamer channel as a current i from the cloud. It is this current that provides the iR drop and leads to the stepped-leader mechanism. Thus, to calculate i, we must calculate the $n = n_1 e^{\alpha\delta_1}$ electrons created in

the travel of δ_1 before the streamer propagates and calculate the current i_0, of which a fraction, f, is lost by diffusion such that $i = fi_0$.

Now it is difficult to evaluate the quantity n_1, which represents the electrons in the avalanche tip which are moving in the field, so that they multiply and form the avalanche. Owing to the space charge of the electron-avalanche cloud, but few of these electrons will be in such a position as to produce the avalanche. For the sake of simplicity assume that *only one electron has the good fortune to form the avalanche.** Setting $n_1 = 1$, $X_s = 24{,}200$ volts/cm, $X_s/p = 31.85$, $\alpha = 1.47$, $\delta_0 = 15$ centimeters, $\alpha\delta_0 = 22.05$, we calculate $n = 3.86 \times 10^9$. This charge is produced in $t = 15/v = 15/10^7 = 1.5 \times 10^{-6}$ second. Hence $i_0 = 3.86 \times 10^9 \times 4.8 \times 10^{-10}/1.5 \times 10^{-6} = 1.24 \times 10^6$ e.s.u., and $i = 1.24 \times 10^6 f$ e.s.u., where $f \ll 1$. To get the potential gradient down the channel we can proceed as follows. The current $i = \pi r^2 N_e \epsilon v$, where r is the streamer radius, N_e the electron density, and v the electron velocity. The value of N_+, the *positive ion density*, is given by recombination as $N_+ = N_0/(1 + N_0 a_1 t)$, with $a_1 = 2 \times 10^{-6}$, and t the time of advance of the streamer before stepping, i.e., ~ 50 microseconds. Now again, owing to the electron attachment and the required rate of recombination $N_+ = N_- + N_e$, with N_- several times (about 9) N_e. Hence, if we take N_e as a fraction f_e of N_+, we have

$$i = fi_0 = \pi r^2 f_e N_+ \epsilon v \tag{29}$$

The value of v, however, is fixed by the electron-mobility equation which reads $v = 1.23 \times 10^6 \sqrt{X}$ centimeters per second

* In conformity with what has been said before (see page 83), the effect of the N_1 electrons is merely to shorten δ_0 to δ_1 before the next streamer forms. It will increase i in the measure that a shorter δ_1 gives a shorter time of travel to provide the needed ion density $N_0 = 7 \times 10^{11}$ ions per cubic centimeter. It will also reduce r for the streamer somewhat if $\delta_1 < \delta_0$. However, with smaller r the value of N to give N_0 is less, so that for convenience one avalanche may be used.

per e.s.u. per centimeter for air at 760 millimeters as given in conformity with data in Equation 20. Inserting this for v in Equation 29 and evaluating the constants, the field

$$X = 8.73 \times 10^7 \frac{(fi_0)^2}{(f_e N_+)^2 r^4} \text{ volts/cm} \qquad (30)$$

Inserting the values for $i_0 = 1.24 \times 10^6$, $r = 5.1 \times 10^{-2}$ centimeter, $N_+ = 10^{10}$, we find

$$X = 2.01 \times 10^7 (f/f_e)^2 \qquad (31)$$

If $f = 0.05$ and $f_e = 0.1$, the gradient in the channel for streamer advance is $X = 50{,}250$ volts per centimeter. This makes the loss of electrons by diffusion from the avalanche very small. It is, however, not inconceivable that this is the case in view of the fields existing. In any case, these data are sufficient to indicate the character of the changes needed to bring Meek's theory of the stepped-leader stroke into conformity with the present discharge mechanism.

Before leaving the question of lightning discharge, there is one more point which requires analysis. McEachron,[59] in his studies of lightning discharges from the Empire State Building in New York, observed numerous strokes that emanated as *positive strokes* from the metal parts of the building to the cloud. These strokes were obviously the result of *positive pilot streamers* set up by high fields induced on the sharp points of the conducting metal. In this case, also, the discharge showed stepping. There is no difficulty in explaining the appearance of *positive pilot streamers*. They are to be expected where positive points have adequate fields. There is also no difficulty in explaining the decay of the ionization in the positive leader-stroke channel by recombination as in the negative case. The only question arises as to the nature of and reason for an electron current up the channel to the anode to give the iR drop. In the case of the negative-avalanche process this current was needed to make up

for the loss of ions produced by diffusion of the electrons from the head of the avalanche. In this case electrons are being drawn into the head of the positive space charge. If the electrons drawn in exactly equal the positive ions produced, then the stem of the streamer remains neutral and *no current is needed.* However, the more remote of the photoelectrons ahead and to the side of the streamer are drawn in from regions perhaps distant from the future streamer channel. Hence, while they move in to the channel, their nearly immobile equivalent positive-ion partners remain well apart from the space-charge channel. Thus it is not unlikely that quite a few excess electrons flow into the streamer channel beyond those needed to make a neutral plasma. This will necessitate a current flowing up the streamer to the anode and thus give the *iR* drop requisite for the stepping process.

REFERENCES TO CHAPTER II

[1] H. J. White, *Phys. Rev.*, **46**, 99 (1934).

[2] H. Raether, *Zeits. f. Physik*, **107**, 91 (1937).

[3] A. M. Cravath, *Phys. Rev.*, **47**, 254 (A) (1935); C. Dechene, *Jour. de Phys. et Radium*, **7**, 533 (1936).

[4] E. Greiner, *Zeits. f. Physik*, **81**, 543 (1933).

[5] H. Paetow, *Zeits. f. Physik*, **111**, 770 (1939).

[6] A. F. Kip, *Phys. Rev.*, **55**, 554 (1939).

[7] H. Raether, *Zeits. f. Physik*, **110**, 611 (1938); H. Costa, *ibid.*, **113**, 531 (1939).

[8] A. F. Kip, *Phys. Rev.*, **54**, 139 (1938); **55**, 549 (1939); G. W. Trichel, *ibid.*, **55**, 382 (1939); L. B. Loeb and A. F. Kip, *Jour. Applied Phys.*, **10**, 142 (1939).

[9] H. Raether, *Zeits. f. Physik*, **107**, 91 (1937); **112**, 464 (1939).

[10] F. G. Dunnington, *Phys. Rev.*, **38**, 1535 (1931).

[11] B. F. J. Schonland, D. J. Malan, and H. Collens, *Proc. Roy. Soc. (London)*, **A, 152**, 595 (1935).

[12] T. E. Allibone and J. M. Meek, *Proc. Roy. Soc. (London)*, **A, 166**, 97 (1938); *ibid.*, **A, 169**, 246 (1938).

[13] A. M. Cravath and L. B. Loeb, *Physics*, **6**, 125 (1935).

[14] B. F. J. Schonland, *Proc. Roy. Soc. (London)*, **A, 164**, 132 (1938).

[15] J. M. Meek, *Phys. Rev.*, **57**, 722 (1940); L. B. Loeb and J. M. Meek, *Jour. Applied Phys.*, **11**, 438, 459 (1940).

[16] L. B. Loeb, *Fundamental Processes of Electrical Discharge in Gases* (Wiley and Sons, 1939), pp. 169, 170, 179.

[17] J. S. Townsend, *Electricity in Gases* (Oxford, 1914), pp. 122 ff.

[18] M. J. Druyvesteyn, *Physica*, **10**, 69 (1930); *ibid.*, **3**, 65 (1936).

[19] J. A. Smit, *Physica*, **3**, 543 (1937).

[20] K. T. Compton and I. Langmuir, *Rev. Modern Phys.*, **2**, 220 (1930). See also L. B. Loeb, *Fundamental Processes of Electrical Discharge in Gases*, p. 186.

[21] H. L. Brose and E. H. Saayman, *Ann. d. Physik*, **5**, 797 (1930).

[22] F. Paschen, *Wiedmann's Annalen*, **37**, 69 (1889); J. S. Townsend, *Electricity in Gases*, pp. 327, 380; W. O. Schumann, *Durchbruchsfeldstärke von Gasen* (Springer, Berlin, 1923), pp. 51, 114; J. J. Thomson, *Conduction of Electricity through Gases* (3d edition, Cambridge, 1933), **2**, 486; L. B. Loeb, *Fundamental Processes of Electrical Discharge in Gases*, pp. 410 ff.

[23] J. S. Townsend, *Electricity in Gases*, chap. x.

[24] R. N. Varney, L. B. Loeb, H. J. White, and D. Q. Posin, *Phys. Rev.*, **48**, 818 (1935); L. B. Loeb, *Rev. Modern Phys.*, **8**, 283 (1936).

[25] F. H. Sanders, *Phys. Rev.*, **44**, 1020 (1933).

[26] D. Q. Posin, *ibid.*, **50**, 650 (1936).

[27] S. Whitehead, *Dielectric Phenomena* (D. Van Nostrand, New York, 1927), p. 42.

[28] W. R. Haseltine, *Phys. Rev.*, **58**, 188 (1940).

[29] F. Ehrenkrantz, *Phys. Rev.*, **55**, 219 (1939).

[30] K. S. Fitzsimmons, *ibid.*, **58**, 187 (1940).

[31] H. J. White, *ibid.*, **48**, 113 (1935).

[32] W. Rogowski and A. Wallraff, *Zeits. f. Physik*, **97**, 758 (1935).

[33] R. Schade, *Zeits. f. Physik*, **104**, 487 (1937).

[34] W. Rogowski and W. Fuchs, *Archiv f. Elektrotechnik*, **29**, 362 (1935); W. Fuchs, *Zeits. f. Physik*, **98**, 666 (1936); W. Rogowski and A. Wallraff, *ibid.*, **102**, 183 (1936); *ibid.*, **108**, 1 (1938); W. Rogowski, *ibid.*, **114**, 1 (1940).

[35] J. M. Meek, *Proc. Phys. Soc. (London)*, **52**, 547, 822 (1940).

[36] H. Fricke, *Zeits. f. Physik*, **86**, 464 (1933); H. Büttner, *Zeits. f. Physik*, **111**, 750 (1939).

[37] R. R. Wilson, *Phys. Rev.*, **50**, 1082 (1936); M. Newman, *ibid.*, **52**, 652 (1937).

[38] L. B. Loeb, *Fundamental Processes of Electrical Discharge in Gases*, p. 90.

[39] L. B. Loeb, *Phys. Rev.*, **48**, 684 (1935).

[40] F. S. Edwards and J. F. Smee, *Jour. Inst. Elect. Engrs. (London)*, **82**, 655 (1938).

[41] R. van Cauwenberghe and G. Marchal, *Revue générale de l'électricité*, **27**, 331 (1930).

[42] L. B. Loeb, *Fundamental Processes of Electrical Discharge in Gases*, pp. 498 ff., 556.

[43] G. L. Locher; see L. B. Loeb, *op. cit.*, p. 498.

[44] H. Paetow, *Zeits. f. Physik*, **111**, 770 (1939).

[45] S. Gorrill, Thesis, University of California, 1939.

[46] L. B. Loeb and W. Leigh, *Phys. Rev.*, **51**, 149 (1937).

[47] E. O. Lawrence and F. G. Dunnington, *Phys. Rev.*, **35**, 396 (1930).

[48] Ishigura and Gosho, *Electrotechnical Journal Laboratory (Tokyo)*, September, 1938.

[49] G. W. Trichel, *Phys. Rev.*, **54**, 1078 (1938).

[50] L. B. Loeb, G. G. Hudson, and A. F. Kip, *ibid.* (1941).

[51] V. B. Waithman and W. R. Baker, *Phys. Rev.*, **57**, 252 (A) (1940).

[52] J. Jeans, *Electricity and Magnetism* (5th edition, Cambridge, 1925), p. 186.

[53] W. Dattan, *Elektrotechnische Zeitschrift*, **57**, 377 (1936); E. Hueter, *ibid.*, **57**, 621 (1936).

[54] I. Goldman and B. Wul, *Tech. Phys. U.S.S.R.*, **1**, 497 (1935); *ibid.*, **3**, 16 (1936); I. Goldman, *ibid.*, **5**, 355 (1938); A. H. Howell, *Elec. Engineering*, **58**, 193 (1939); H. C. Pollock and F. S. Cooper, *Phys. Rev.*, **56**, 170 (1939); G. G. Hudson, *ibid.*, **55**, 1122 (1939).

[55] B. F. J. Schonland and H. Collens, *Proc. Roy. Soc. (London)*, **A, 143,** 654 (1934); B. F. J. Schonland, D. J. Malan, and H. Collens, *Proc. Roy. Soc. (London)*, **A, 152,** 595 (1935); D. J. Malan and H. Collens, *ibid.*, **A, 162,** 175 (1937); B. F. J. Schonland, *ibid.*, **A, 164,** 132 (1938); K. B. McEachron, *J. Franklin Inst.*, **227,** 149 (1939).

[56] G. C. Simpson and F. J. Scrase, *Proc. Roy. Soc. (London)*, **A, 161,** 309 (1937).

[57] B. F. J. Schonland, *ibid.*, **A, 164,** 132 (1938).

[58] J. M. Meek, *Phys. Rev.*, **55,** 972 (1939).

[59] K. B. McEachron, *J. Franklin Inst.*, **227,** 149 (1939).

[60] A. Tilles, *Phys. Rev.*, **46,** 1015 (1934).

Chapter III

THE CALCULATION OF BREAKDOWN IN VARIOUS TYPES OF GAPS

1. Introduction

In chapter ii the physical basis for the streamer mechanism of spark breakdown has been given. Furthermore the basic equations for streamer formation and spark breakdown in uniform and nonuniform field gaps were developed. The results of a few calculations based on these equations were also given. In order that these computations may be carried out by other workers and applied to other gap geometries, it is essential that the methods of procedure be presented and exemplary solutions be provided.

In presenting these methods and results, one must say a few words about the equations.

α. The streamer theory of spark breakdown is not an empirical theory. It is a logical theory based on fundamental atom-physical processes and strongly corroborated by observational facts.

β. While inadequate data about the fundamental processes at work preclude an exact formulation of the breakdown conditions, a simple and mathematically adequate criterion can be set up in which the positive space-charge field at the streamer tip must be K times the imposed sparking field. The quantity, K, is a fraction between 0.1 and 1.0. This condition has a physical significance and is thus not arbitrary or empirical.

γ. The uncertain values and possibly slowly varying character of some of the clearly defined physical quantities in fields of sparking magnitude introduce some latitude in the value of a constant term. This and the undefined value of the factor, K, thus give an indefinite value to the constant terms in the equation.

δ. For purposes of calculation experimentally established values of one of the factors, $\lambda_0/\sqrt{f}$, are inserted and assumed constant. The factor, K, is, at first, arbitrarily assigned the value 1. Later comparison of the values computed assuming $K=1$ with experiment in several different phenomena indicate that the value, K, should perhaps be more nearly 0.1. In the earlier studies made, the value $K=1$ was used and, since the tedious recalculation with the later value $K=0.1$ did not seem warranted as regards greatly increased accuracy, the value of $K=1$ will be used. In later calculations the value $K=0.1$ will be used.

ϵ. To the extent that the value $K=0.1$ is used, the equations are, in a sense, semi-empirical, though based on a physical theory. Since K cannot be set more accurately on any physical basis at present, the evaluation of K from observed, though empirical, data is justified.

ζ. The fact that the wide latitude in the values of $\lambda_0/\sqrt{f}$ and of K, which contribute to constant values in the equation, cause so little variation in the sparking potentials computed lies in the exponential character of the cumulative ionization and the rapid change of α/p with X/p. Thus too much emphasis cannot be placed on the agreement of individual computed values of sparking potentials with observation.

η. On the other hand, when one observes the various modifications of the equation applied to one gap geometry after the other and utilizing the same constants, leading not only to new quantitative agreement, but also explaining previously unexplained phenomena, the remarkable power of the new theory becomes manifest.

θ. Where there are discrepancies between computed and observed values, one cannot ascribe all the discrepancies to inadequacies in the theory or the constants. For the experimental data are in many cases none too good and the very important curves for α/p as a function of X/p may be in part to blame.

a) The experimental procedure and conditions for the taking

of sparking data which can have a uniform significance have never sufficiently been worked out or adhered to. Thus

(1) Inadequate attention has been paid to the uniform purity and humidity of the air used.

(2) Very widely differing conditions have applied to the influence of alterations in the air and electrodes by antecedent discharges. Recent work in the Berkeley laboratory[1] has shown

TABLE III

SANDERS' VALUES OF X/p AND α/p FOR AIR*

X/p volts/cm × mm	p mm	α/p	X/p volts/cm × mm	p mm	α/p
20.....	380	0.000034	50.....	9.95	0.0554
22.....	380	0.000052	60.....	4.90	0.127
24.....	380	0.000134	70.....	1.00	0.224
26.....	380	0.000234	80.....	0.98	0.340
28.....	380	0.000430	90.....	0.97	0.491
30.....	380	0.000910	100.....	0.96	0.637
31.....	380	0.00136	110.....	0.975	0.806
32.....	380	0.00201	120.....	0.975	1.007
33.....	380	0.00305	130.....	0.973	1.236
34.....	380	0.00459	140.....	0.950	1.477
35.....	380	0.00605	150.....	0.990	1.602
36.....	380	0.00820	160.....	1.000	1.758
40.....	25	0.0167			

* The air was contaminated with about 1.4×10^{-3} mm vapor pressure of Hg. At values of p above 300 mm, it is probable that the values of α/p are not more than 5 per cent higher than for Hg-free air.

that the nitric oxides produced by antecedent sparks in confined spaces can lower sparking potentials by as much as five or more per cent.

(3) In many cases adequate care has not been taken to avoid field distortions in given types of gap design, so that the data are valueless.

(4) The further distortion of fields in some gaps by space-charge accumulations have been ignored.

(5) Finally, the procedures for eliminating statistical time lags, raising the potential, etc., differ so widely in different

measurements as to make results at times impossible of interpretation.

b) The only data on α/p which are extant in the important range of values of X/p for many sparks at atmospheric pressure are those of Sanders,[2] given in Table III and shown plotted in Figure 25 and for α at 760 mm in Figure 26. They have been checked above an $X/p = 30$ by the values of Masch.[3] Unfortunately, both observers worked in air which was contaminated with Hg at about 10^{-3} mm. At high X/p in N_2, Bowls[4] showed that this would raise α by 17 per cent. In the higher pressure range where most of the calculations to follow are made, it is

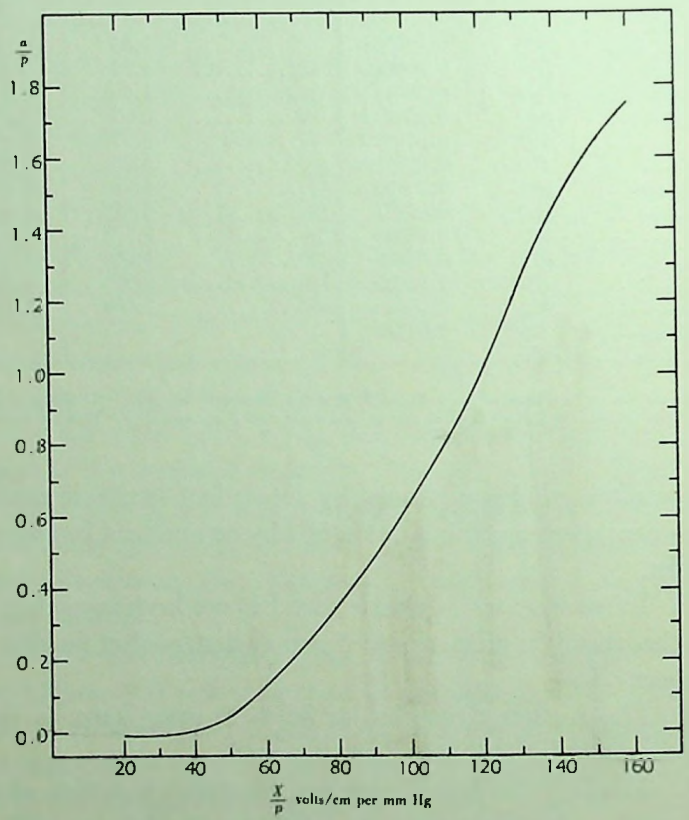

FIG. 25.—Sanders' $\alpha/p - F(X/p)$

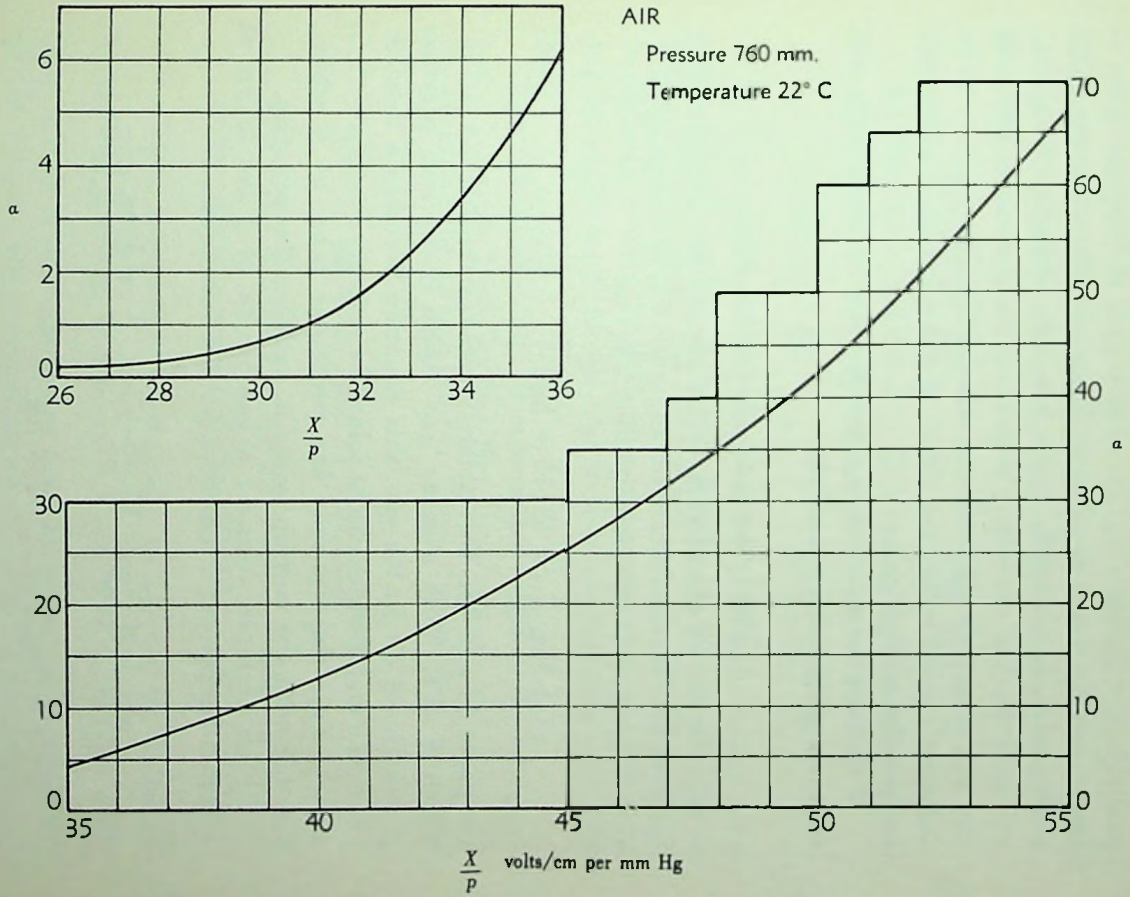

FIG. 26.—Sanders' $\alpha - F(X/p)$ at 760 mm

probable that Sanders' values of α/p as a $f(X/p)$ are good to better than 5 per cent despite the Hg vapor. When one considers that his air was dry, while other observers, whose sparking data are used, worked sometimes with room air and sometimes with dry air, it is seen that one can assume Sanders' values to be sufficiently good within the limits of the other data which will be used for comparison.

With these remarks one can now proceed to consider the calculation of sparking potentials.

2. Breakdown in a Uniform Field

a) *Method of calculation.*—The breakdown potential of a uniform field is calculated from Equation 24, in a slightly modified form as derived from Equation 23, viz.,

$$\alpha\delta + \log_e \frac{\alpha}{p} = 14.46 + \log_e \frac{X}{p} + \tfrac{1}{2} \log_e \frac{\delta}{p} \qquad (24)$$

see pages 44 and 45. This equation uses the constant 14.46 for which $K = 1$. With a given gap length δ cm and pressure p mm Hg of air in the gap, this equation becomes a relation between α and X which can be solved by reference to $\alpha/p - X/p$ curves, since there is only one particular value of X which, together with the corresponding α, satisfies the equation.

As an example, consider a gap length of 1 cm in air at 760 mm Hg pressure. The equation for breakdown is

$$\alpha + \log_e \frac{\alpha}{760} = 14.46 + \log_e \frac{X}{p} + \tfrac{1}{2} \log_e \frac{1}{760}$$

$$\alpha + \log_e \alpha = 17.77 + \log_e \frac{X}{p} \qquad (32)$$

For convenience the term $\log_e \frac{X}{p}$ is not split up into

$$\log_e X - \log_e 760.$$

The solution of the equation is now made by a process of trial and error. If we take $X/p = 42$, for which $\alpha = 17.4$, the left-hand side and right-hand side of Equation 32, respectively, become

$$LHS = 20.25 \qquad RHS = 21.52$$

An increase in the value of X/p is seen to be necessary, and for $X/p = 42.6$, $\alpha = 18.9$, we have

$$LHS = 21.84 \qquad RHS = 21.52$$

Precise agreement is obtained by plotting a curve with $LHS - RHS$ against X/p, and finding the value of X/p at which $LHS - RHS = 0$. The field strength X required for breakdown is then 32,200 volts per centimeter, and since the gap length is 1 centimeter, the breakdown potential is 32,200 volts.

As a further example, consider a gap length of 4 centimeters and a pressure $p = 190$ mm Hg, i.e., the same value of 760 for $p\delta$ as for the gap considered above. Substitution for δ and p in Equation 24 gives

$$4\alpha + \log_e \alpha = 17.77 + \log_e \frac{X}{p}$$

For $X/p = 43.0$, $\alpha = 5.0$, $LHS = 21.61$ $\quad RHS = 21.53$

$X/p = 42.9$, $\alpha = 4.9$, $LHS = 21.19$ $\quad RHS = 21.53$

The solution is seen to occur virtually for $X_s/p = 43.0$, and the breakdown potential of the gap is $V_s = \frac{X_s}{p} p\delta = 32{,}700$ volts. This voltage is little above that determined for the 1-centimeter gap at 760 mm Hg pressure, an effect which has been discussed on page 46.

It will be seen from the calculations above that the equation is critically dependent on the value of X/p. A small change in the latter causes a considerable change in the value of α and

in the value of the left-hand side of the equation, while the right-hand side is but little altered. Even if the value of the constant term in the breakdown equation is not absolutely correct and the values of α are not too exactly known, such errors are largely compensated for by the exponential character of the relation between α/p and X/p and lead to but small deviations in the value calculated for X/p.

b) *Variation of breakdown potential with gap length.*—A summary of the results of calculations for gaps of various lengths δ centimeters in air at atmospheric pressure is given in Table IV.

TABLE IV

δ cm	X/p volts/cm × mm	α	$\alpha\delta$	$\bar{r}$ cm	N/cm^3	Volts			
						V_s	V_1	V_2	V_3
0.5	48.1	35.4	17.7	0.00936	6.4×10^{12}	18,250	17,300	.....	.....
1.0	42.4	18.6	18.6	0.0132	3.7×10^{12}	32,200	31,600	.....	.....
2.5	37.05	7.9	19.7	0.0209	2.3×10^{12}	70,500	73,000	71,000	72,000
5.0	34.65	4.15	20.7	0.0296	1.5×10^{12}	132,000	138,000	134,000	136,000
10.0	32.8	2.15	21.5	0.0418	8.8×10^{11}	249,000	265,000	260,000	261,000
15.0	31.85	1.47	22.0	0.0451	7.2×10^{11}	363,000	386,000	.....	.....
20.0	31.2	1.12	22.4	0.0592	5.6×10^{11}	474,000	510,000	505,000	504,000

In the foregoing table the radius, $\bar{r}$, of the avalanche, when it reaches the anode, is included for each gap length. This radius is obtained in the manner indicated on page 37, and is given by

$$\bar{r} = \left(0.133\,\frac{\delta}{p}\right)^{1/2}$$

The ion density N per cubic centimeter is also included in the table and is determined from the relation $N = \alpha e^{\alpha\delta}/\pi\bar{r}^2$, as shown on page 77. The sparking potential V_s is that calculated from the X_s/p evaluated as in (a) through the relation $V_s = \frac{X}{p}p\delta$. V_1 is the sparking potential actually measured by

Edwards and Smee[5] for corresponding gap lengths between spheres where the ratio of sphere radius to gap length is so large that the field is nearly uniform. V_2 is the potential measured by Davis and Bowdler,[6] and V_3 is the value given by the American Institute of Electrical Engineers.[7]

Owing to inadequate control of high steady potentials, most data on the breakdown at high $p\delta$ have been taken using sphere gaps and generally 60-cycle alternating potentials. This is especially true for longer gaps at atmospheric pressure. In principle a sphere-gap breakdown potential with sufficiently large spheres should be slightly lower than the corresponding value for the plane-parallel gap. However, here care must be used in noting what is being measured to compare with the computed values in Table IV. The computed values are the *threshold values* for a spark. To get these, there must be no statistical time lag and the values of V_s must be the lowest values observed. Actually with 60-cycle A.C., there would need to be a very good value of i_0 used to insure observing threshold values of V_s. Furthermore, the measured potentials given are the average values of the observed data. Edwards and Smee[5] claim an accuracy for their average values of $\pm$ 1 per cent.

It is to be noted that the observed values of V in Table IV are initially lower than V_s, but that they gradually rise above V_s reaching a value some 7 per cent higher at $\delta = 20$ cm. That the value is initially lower comes from the use of a $K = 1$ in the equations instead of the probably more correct $K = 0.1$. The rise in the observed values of V above the calculated V_s as δ increases is to be ascribed to the change in sparking mechanism. It corresponds to the alteration in the sparking mechanism from the anode streamer to the electron avalanche-retrograde streamer mechanism discussed on page 80. Whether the change should begin to occur at gaps as short as 5.0 cm is, however, questionable. How much the way in which the data were taken alters the basis of comparison or the conclusions cannot be estimated. In any case, too much emphasis cannot be

placed on the absolute agreement in values. The value of $X_s = 24{,}800$ volts at $\delta = 15$ cm, and $N = 7.2 \times 10^{11}$ ions per cubic centimeter represents the constant sparking-field strength X_{s_0} at atmospheric pressure for all gaps with $\delta > 15$ cm computed on the basis of $K = 1$.

c) *Variation of breakdown potential with pressure.*—The variation of the calculated breakdown potential, V_s, of a 1-centimeter gap for different pressures is given in Table V. The radius, $\bar{r}$, of the electron avalanche when it reaches the anode in centimeters and the corresponding ion density N are also included.

TABLE V

p mm	X/p volts/cm × mm	$\alpha = \alpha\delta$	$\bar{r}$ cm	N/cm^3	V_s volts
7,600.....	32.6	19.5	0.0042	1.1×10^{14}	248,000
3,800.....	34.4	19.0	0.0059	3.1×10^{13}	131,000
760.....	42.4	18.6	0.0132	3.7×10^{12}	32,200
380.....	49.0	18.3	0.0187	1.5×10^{12}	18,600
200.....	55.3	18.2	0.0258	7.1×10^{11}	11,100
100.....	65.5	17.8	0.0365	2.3×10^{11}	6,550

There appear to be no experimental data for uniform gaps of the order of 1 cm in length at pressures much higher than atmospheric, so that a direct comparison between theory and experiment is not possible. However, if we consider that the measured breakdown potential for a given $p\delta$ is nearly constant (Paschen's law), comparison of the values above with those in Table IV shows that there is the same degree of agreement between measurement and calculation for the fixed gap and pressure variation as for the fixed pressure and gap-length variation. This is to be expected since the uncertainty in experimental data is greater than the expected deviations from Paschen's law on Meek's theory (see page 46). The comparison of the streamer theory with Townsend's Equation shown in Figure 13, page 49, indicates that below $p\delta = 200$ the spark proceeds by Townsend's mechanism. The value of N at $p = 200$,

$\delta = 1$ cm is 7.1×10^{11} per cubic centimeter, which is the minimum value assumed for streamer advance (see page 78).

The breakdown potentials for smaller gaps, of the order of 1 mm, have been measured by a number of different workers[8] for pressures up to about 70 atmospheres. When pressures above 10 atmospheres are employed, it is found that the measured potential begins to fall below that given by Paschen's law, and the deviation becomes considerable at higher pressures. Measurements by Hayashi[8] for a gap of 0.089 centimeter give breakdown potentials of 28,500 volts and 63,000 volts at pressures of 10 atmospheres and 40 atmospheres, respectively. In these two cases the corresponding gap lengths at atmospheric pressure to give the same value of $p\delta$ are 0.89 and 3.56 cm, for which the respective measured breakdown voltages are 28,000 and 106,000 volts. The measured values at *ten atmospheres* and at *one atmosphere* for the same $p\delta$ are thus in agreement within the bounds of experimental error, while the corresponding comparison for the measurement at forty atmospheres shows considerable deviation.

This deviation cannot be accounted for by the streamer theory, which gives calculated values of 29,300 volts and 96,200 volts for the breakdown of a 0.089-centimeter gap at 10 and 40 atmospheres respectively. While the streamer theory might be expected to hold at lower $p\delta$ with higher values of p, as seen on page 77, this disagreement with experiment must not be taken too seriously. It is doubtful whether adequate precautions were taken by the observer to avoid the lowering effect of nitric oxides[1] which were not known at that time. It is further to be noted that in these regions the sparking-field strengths are of the order of 6×10^5 to 10^6 volts per centimeter in which field emission from the electrodes can be expected from fine points of low-work function.[9] In view of such difficulties in the interpretation of the observed data, one can hardly consider the failure of the streamer or any sparking theory in this regime as significant.

d) *Reasons for the success of empirical sparking formulae.*—Reference to Tables IV and V shows that the value of $\alpha\delta$ for breakdown varies from about 18 to 22 over the wide range of values considered for both δ and p. The actual values for $\alpha\delta$ are, of course, largely determined by the constant term in the breakdown equation, which is not absolutely known. However, the fact that there should be such a small variation in the value of $\alpha\delta$ to give breakdown indicates that the breakdown potential might be calculated in an empirical manner, giving reasonable results, by the criterion that breakdown occurs when $\alpha\delta \sim 20$ or some other such value. Such a criterion for breakdown has been used at various times by different workers.[10] It must, however, be noted that such a relation is purely empirical. It has no bearing on the mechanism of breakdown except to assume cumulative ionization with the experimental values of α/p as a $f(X/p)$ which is an observed experimental fact. The character of this variation, however, shows clearly why such empirical relations give values of breakdown potential which are in fair agreement with experiment.

e) *The "corrected" breakdown equation.*—The correct value to be used for the constant term in the breakdown equation, as indicated on pages 42 and 107, is a matter open to question. Theory indicates that it will depend to some extent on pressure and field strength. For, as indicated on page 44, the original equation was derived using fixed observed values of λ_0 and $\sqrt{f}$, which correspond to conditions closely met in breakdown fields in gaps of the order of 1 centimeter in length at atmospheric pressure. Further, a certain degree of simplification was necessary in the determination of the constant, K, in the sparking criterion, $X_1 = KX_s$. In the derivation of the original equation, the criterion set for streamer formation and breakdown was that $K = 1$, whereas actually the value of K probably lies nearer 0.1 than 1.0.

The considerations suggest that to obtain a possibly more correct value of the constant term, the value of the latter should

be changed to that which gives the more generally accepted* breakdown potential of 31,600 volts for a 1-centimeter gap in air at normal temperature and pressure,[11] rather than the higher value originally used. Making this change, the resultant equation is

$$a\delta + \log_e \frac{a}{p} = 12.16 + \log_e \frac{X}{p} + \tfrac{1}{2}\log_e \frac{\delta}{p} \qquad (24a)$$

The constant term is seen to be reduced by the amount 2.3 to the value 12.16. Calculations show that the value of K which results in such an equation is $K = 0.1$.

The corrected equation yields values of breakdown potential little different from that in which the constant term is 14.46, as indicated by the fact that the reduction in calculated potential for the 1-centimeter gap is only from 32,200 volts to 31,600 volts. The calculations for both the original and the corrected equation are given in the next section on the sphere gap, and the difference between the resultant values is seen to be slight. However, it will be seen that the corrected equation gives more nearly correct values for the case of the corona discharge where recent data[12] on streamer onset are reliable, and it has been largely used in that section. More definite determinations of the constant must depend on *more reliable values for sparking potentials* under different conditions and K and $\lambda_0/\sqrt{f}$ may be found to vary with p and δ. It must also be noted that the choice of a value for K sets an *average threshold value* and, owing to chance fluctuations, a breakdown may sometimes occur at higher or lower values (see page 51). Thus it cannot be stated which of the two constants is the more correct, and particularly so since the constant term may vary under different circumstances. In general the effect of variation of the constant term will be considered for the various electrode configurations to be discussed.

* Recent careful measurements by W. R. Haseltine[1] in this laboratory avoiding the effect of oxides of N_2 show 14.46 to give excellent agreement with his observations. It is seen that the uncertainties lie as much in experiment as in theory.

3. The Sphere Gap

a) *Introduction.*—The calibration of the sphere gap for voltage determination by sparking potential measurements is a matter of considerable importance to engineers and has been the subject of much investigation during recent years.[5, 6, 7, 13]

Thus, there is a considerable amount of experimental data with which to compare the calculations and predictions of the present theory. Until recently, the lack of an adequate theory of spark discharge has precluded the theoretical calculation of the voltage required to cause breakdown, though a number of empirical formulae, notably that of Peek,[14] have been developed to enable calculations of breakdown potential to be made. In general, these formulae represent the relation between breakdown potential and gap length over a certain range of values, but they fail when extrapolated outside that range. The tendency is to base such formulae on the supposition that breakdown takes place when the gradient at the sphere surface attains a particular value which is dependent on the radius of the sphere. Thus one frequently sees reference to the supposition that the breakdown strength of air is a function of electrode curvature. The present theory, however, enables the calculation of the breakdown potentials for different sphere diameters and gap lengths without recourse to empiricism. The theory is furthermore found to explain many of the sparking phenomena associated with the sphere gap.

b) *Axial field in a sphere gap.*—The field distribution along the line of centers between two spheres is closely given by the expression[15]

$$X=\frac{2\delta[\delta^2(f+1)+4y^2(f-1)]}{[\delta^2(f+1)-4y^2(f-1)]^2}V. \qquad (33a)$$

where

$$f=\frac{\delta/R+1+\sqrt{(\delta/R+1)^2+8}}{4} \qquad (33b)$$

δ is the gap length in centimeters, y is the distance of the point under consideration from the mid-point joining the line of centers of the spheres in centimeters, R is the sphere radius in centimeters, and V is the potential difference between the spheres.

The gradient at the surface of each sphere is always higher than that in mid-gap. The variation of the gradient across the gap decreases with decreasing gap length, and for short enough gaps the gradient is virtually uniform. However, the variation of the ionization coefficient α across the gap is much more pronounced than the variation of X, for in the region of usual sparking field strength, where $X/p \sim 40$, the value of α/p varies approximately exponentially with X/p.

c) *Calculation for the short gap.*—The breakdown potential of a short gap between spheres is calculated in a manner similar to that for the uniform gap, due regard being paid to the variation of X and α across the gap. In both cases an electron avalanche is originated by an electron leaving the cathode. The avalanche travels across the gap to the anode, where the ion density in the avalanche is such that it gives rise to a positive streamer which develops from anode to cathode to form a conducting filament bridging the gap, and so causes breakdown to occur.

The equation for the calculation of breakdown potential in conformity with Equation 25, page 45, is

$$\int_0^\delta \alpha dx + \log_e \frac{\alpha_A}{p} = 14.46 + \log_e \frac{X_A}{p} + \tfrac{1}{2} \log_e \frac{\delta}{p} \qquad (34)$$

This may be written

$$\int_0^\delta \alpha dx + \log_e \alpha_A = 14.46 + \log_e \frac{X_A}{p} + \tfrac{1}{2} \log_e p\delta \qquad (35)$$

where X_A and α_A are the respective values of field strength and ionization coefficient at the surface of the anode (see page 84). The equation in which the constant term is 12.16 instead of 14.46 may be more correct and the results obtained from both

equations will be compared and discussed later. Meanwhile the calculations will be made on the basis of the foregoing equation with the constant term 14.46.

For a particular gap length between spheres of given radius, the field distribution and the variation of α are plotted for different values of potential difference between the spheres. The value of potential difference which gives such a distribution of X and α in the gap that Equation 35 is satisfied is found by a process of trial and error. This will then be the minimum potential difference to cause breakdown.

Curves giving the variation of X and α across a 2.5-centimeter gap between spheres of 12.5-centimeter radius for a potential difference of 70,000 volts at 760 millimeters pressure are shown in Figure 27 (p. 130). It is found that the values of X and α are such that Equation 35 is nearly satisfied. The exact solution occurs for $V = 70{,}300$ volts, which is in fair agreement with the observed value of about 71,000–73,000 volts. It is slightly lower as it represents a threshold value, while reported values are average values.

It should be pointed out that, while the method of solution is to some extent graphical, there is no need to plot curves for X and α. Their values may be determined at different points in the gap and the evaluation of $\int_0^\delta \alpha dx$ may be performed by Simpson's rule. The number of points necessary is governed by the rapidity of variation of α. For longer gaps, where the field distortion is large, a greater number of points will have to be taken than for the short gap where the field is nearly uniform.

In the case of the 2.5-centimeter gap under consideration, it is sufficient to consider the values of X and α at eight different points in the gap. The method of solution is as follows:

1. Determine the ratio X/V at different points in the gap from Equations 33 for the particular gap conditions.

2. Take a voltage V and determine X, X/p and thus α at the different points.

3. Calculate the average value of α across the gap by Simpson's rule and hence the value of $\int_0^\delta \alpha dx$.

4. Insert the values for $\int_0^\delta \alpha dx$, X_A, α_A, in Equation 35. If the equation is satisfied, the value of V is that to give breakdown. If not, other values of V will have to be chosen until the final solution is obtained by a process of trial and error.

Sample calculations for the 2.5-centimeter gap will now be given:

TABLE VI

Quantity in cm	Value for Different Values of X								
x	0	0.3125	0.625	0.9375	1.25	1.5625	1.875	2.1875	2.5
X/V	0.428	0.408	0.396	0.389	0.386	0.389	0.396	0.408	0.428
X/p $V = 70{,}000$	39.5	37.4	36.5	35.8	35.5	35.8	36.5	37.4	39.5
α	11.8	8.4	7.0	5.9	5.4	5.9	7.0	8.4	11.8

The average value of α is 7.475.

We then have for the left-hand side and right-hand side of Equation 35

Left-hand Side	Right-hand Side
$\bar{\alpha}\delta = 7.475 \times 2.5 = 18.69$	Constant 14.46
$\log_e \alpha_A = \log_e 11.8 = 2.46$	$\log_e X_A = \log_e 39.5 = 3.67$
	$\frac{1}{2} \log_e p\delta = \frac{1}{2} \log_e 1900 = 3.77$
Total = 21.15	Total = 21.90

The agreement is seen to be inexact and warrants a slight increase in voltage. If we take $V = 70{,}500$, the values of X/p and α across the gap are as follows:

TABLE VII

Quantity	X in centimeters								
X/p $V = 70{,}500$	39.8	37.7	36.75	36.05	35.75	36.05	36.75	37.7	39.8
α	12.4	8.9	7.5	6.4	5.8	6.4	7.5	8.9	12.4

The average value of α is 7.975.

Substitution in Equation 35 now gives

Left-hand Side		Right-hand Side	
$\bar{\alpha}\delta = 7.975 \times 2.5 =$	19.94	Constant	14.46
$\log_e \alpha_A = \log_e 12.4 =$	2.52	$\log_e X_A = \log_e 39.8 =$	3.68
		$\frac{1}{2} \log_e p\delta = \frac{1}{2} \log_e 1900 =$	3.77
Total =	22.46	Total =	21.91

It is seen that the increase in V has been too great. In other words, the correct value of V lies between 70,000 and 70,500 volts, and is found to be 70,300 volts.

The calculations above show the solution of the breakdown equation to be a simple matter and that the value of V can quickly be gauged to a close degree of accuracy. While the foregoing gap has been divided into equal sections, this need not necessarily be done but rests with the discretion of the calculator. The greatest number of divisions should be made where the field X and the coefficient α vary most rapidly, i.e., near the sphere surfaces. In the mid-gap region sufficient accuracy is obtained for less frequent divisions, for not only does α vary less rapidly in this region, but also its value is less, and thus the relative contribution to the value of $\int_0^\delta \alpha dx$ is less than near the sphere surfaces.

d) *Calculations for long gaps.*—The mechanism of breakdown for longer gaps differs somewhat from that described above. As the gap length is increased, the voltage gradient between the spheres becomes such that the value of α is virtually zero over most of the mid-gap region. Electron avalanches originating at the cathode will not traverse the gap in a compact filamentary manner, but will diffuse in the mid-gap region of low field strength. Thus such avalanches will not give rise to positive streamers at the anode. The positive streamers will now be initiated by avalanches which have their origin in the gap near

the anode surface, and thus more in the manner of the corona discharge. The formation of a positive streamer at the anode will cause breakdown of the gap provided that the voltage is sufficient to produce the streamer and to permit it to propagate across the gap. (See pages 84 and 89.) If the gap length is sufficiently increased, a gap length will be reached at which the voltage is insufficient to cause such breakdown, i.e., streamers will form but will be unable to cross the gap. This accounts for the experimentally observed fact that a corona onset with streamers is observed to precede breakdown when the gap length is larger than about $8R$, where R is the sphere radius.[16] For such long gaps, the breakdown voltage curve is found to follow that for the positive point to negative sphere. The present calculations are, however, concerned with gap lengths only up to $2R$, where corona is not observed to precede breakdown. Further, up to a gap length of $2R$ reasonably symmetrical conditions can be obtained and the influence of sphere supports and external objects on the field will be slight.

The breakdown of a 20-centimeter gap between spheres of 12.5-centimeter radius will now be considered. The distribution of X and α across the gap for a potential difference of 407,000 volts at 760 millimeters is shown in Figure 28 (p. 130). It is seen that the value of α is of importance only near the sphere surfaces and, as already stated, electron avalanches originating at the cathode will diffuse considerably in the mid-gap region. We have now to consider the electron avalanches which are originated in the mid-gap region close to the anode. Such an avalanche will maintain its compact filamentary form and may give rise to a positive streamer at the anode. The value of $\int \alpha dx$ for such an avalanche is shown by the shaded area of Figure 28. The calculation of the conditions for onset of such a positive streamer, and consequent breakdown of the gap, is given by the equation

$$\int_R^{R+a} \alpha dx + \log_e \frac{a_A}{p} = 14.46 + \log_e \frac{X_A}{p} + \tfrac{1}{2} \log_e \frac{a}{p} \quad (36)$$

This may be written

$$\int_R^{R+a} \alpha dx + \log_e \alpha_A = 14.46 + \log_e \frac{X_A}{p} + \tfrac{1}{2} \log_e pa \qquad (37)$$

where R is the radius of the sphere in centimeters and a is the distance of the point of origin of the electron avalanche from the sphere surface in centimeters. For the purpose of calculation, this point may be taken as that where the value of α is unity, though as will be seen later this criterion has considerable flexibility. It will be noted that the value of $\int_R^{R+a} \alpha dx$, as indicated by the shaded area of Figure 28, is the same as $\frac{1}{2}\int_0^{\delta} \alpha dx$, where δ is the gap length. Thus it is clear that the calculated potential on the new mechanism will be higher than that calculated on the basis that the electron avalanche *traverses the whole gap* to initiate a streamer.

The calculation of the breakdown potential for such gap lengths is again performed graphically. However, curves need not be plotted but the values of X and α can be determined at a sufficient number of points in the gap to enable the calculation of $\int \alpha dx$, by Simpson's rule. The method of solution of the equation will now be illustrated for the case of the 20-centimeter gap between spheres of 12.5-centimeters radius. The value of X/V at different points in the gap is determined from Equation 33. The values of X/p in Table VIII are those for a potential $V = 408{,}000$ volts between the spheres.

TABLE VIII

Quantity	Value of a in Centimeters					
a in cm.....	0	0.5	1.0	1.5	2.0	2.5
X/V	0.0805	0.0746	0.0694	0.0650	0.0611	0.0576
X/p	43.2	40.1	37.5	34.9	32.5	30.9
α	20.4	13.1	8.5	4.5	1.9	1.0

Here $\alpha = 1$ at $a = 2.5$.

The left-hand and right-hand sides of Equation 37 are respectively

Left-hand Side		Right-hand Side	
$\int_R^{R+a} \alpha dx = 7.74 \times 2.5 =$	19.35	Constant	14.46
$\log_e \alpha_A = \log_e 20.4 =$	3.01	$\log_e \frac{X_A}{p} = \log_e 43.2 =$	3.76
		$\frac{1}{2} \log_e pa = \frac{1}{2} \log_e 1900 =$	3.77
Total =	22.36	Total =	21.99

The value chosen for V is seen to be slightly too high to satisfy the equation exactly, and accordingly the solution is again attempted, this time with $V = 406{,}000$ volts.

TABLE IX

Quantity	Value of a in Centimeters					
a in cm.....	0	0.5	1.0	1.5	2.0	2.5
X/p	43.0	39.9	37.3	34.7	32.3	30.7
α	19.9	12.6	8.2	4.2	1.75	0.9

In this case $\alpha = 1$ at $a = 2.4$.

Left-hand Side		Right-hand Side	
$\int_R^{R+a} \alpha dx = 7.34 \times 2.5 =$	18.57	Constant =	14.46
$\log_e \alpha_A = \log_e 19.9 =$	2.97	$\log_e \frac{X_A}{p} = \log_e 43.0 =$	3.76
		$\frac{1}{2} \log_e pa = \frac{1}{2} \log_e 1820 =$	3.75
Total =	21.54	Total =	21.97

Comparison of the two solutions for $V = 408{,}000$ volts and $V = 406{,}000$ volts shows that the correct solution is closely given by $V = 407{,}000$ volts.

e) *Choice of the lower limit of integration for long gaps.*— At this point it might be well to consider the seemingly arbitrary assumption that the point of origin of the electron avalanche is the point where $\alpha = 1$. Clearly some such assumption is necessary in order to specify the value of the term $\frac{1}{2} \log_e pa$. However, this term is little altered by variation of the value

of a. For instance, if we choose $a = 10.0$ cm, $\frac{1}{2}\log_e pa = \frac{1}{2}\log_e 7{,}600 = 4.46$, as compared to 3.75 in the calculation for $a = 2.4$. Thus the change has little effect on the right-hand side of the equation for breakdown. The important feature is that a be sufficiently large that the value of $\int a dx$ has virtually reached a maximum. Reference to Figure 28 indicates that there is little contribution to the term $\int a dx$, as given by the shaded area, beyond the distance 3 centimeters from the sphere surface. Such rapid decay in the value of a with distance from the sphere means that little difference is incurred in the left-hand side of the breakdown equation by taking the origin of the avalanche as the point where $a = 1.0$ or 0.1, for the corresponding change in $\int a dx$ is slight. However, the nature of the breakdown equation is such that even if we take the point where $a = 1.0$ or $a = 0.1$ as the origin of the avalanche, the resultant effect on the final calculated voltage is trivial.

For example, we may consider the present 20-centimeter gap and suppose that the electron avalanche which initiates the positive streamer has its origin in the center of the gap, so that $a = 10.0$ cm. At this point calculations show that $X/p = 20.6$, $a = 0.03$, for the applied potential of 406,000 volts, in line with Table IX. The increment in $\int a dx$ between $a = 2.5$ and $a = 10.0$ is found to be 1.24. The value of $\frac{1}{2}\log_e pa$ is now $\frac{1}{2}\log_e 7{,}600 = 4.46$. Then, for the applied potential $V =$ 406,000 volts, the new values of the left- and right-hand sides of the breakdown equation are

$$LHS = 22.78 \qquad RHS = 22.68$$

as compared with the values

$$LHS = 21.54 \qquad RHS = 21.97$$

as given above for the $a = 1$ origin.

The differences are seen to be slight, and the calculated potential is altered by no more than 1,000 volts, i.e., by about 0.25

per cent only. However, it should be noted that some discretion has to be exercised, particularly in the case of the more uniform field, where α varies slowly and the region of low α may make a real contribution to the value of $\int \alpha dx$. It is possible that one should take the center of the gap as the origin of the avalanche. However, for long gaps it is unlikely that a successful avalanche will form there owing to the low values of X and α, and it is thought to be more probable that the avalanche which leads to breakdown will be originated in the region where α is beginning to be appreciable, i.e., $\alpha > 1$. Thus, although there is virtually no difference in the final calculated voltage on either basis, as seen above, the origin of the avalanche will, in general, be taken as the point where $\alpha \sim 1$. Similar considerations will be found to obtain for the corona discharge. The only exception lies in the transition region between the two types of mechanism for the long and short gaps which will be the subject of further discussion.

f) Comparison between theory and observation.—The ways in which the breakdown of a sphere gap takes place are seen to be dependent on the spacing between the spheres and can be grouped as follows:

I. The electron avalanche proceeds all the way across the gap from cathode to anode and there forms a positive streamer which leads to breakdown. The circumstances leading to breakdown are then similar to those for the uniform gap and occur only for spacings in which the variation of field is slight, as illustrated in Figure 27. The breakdown voltage is determined by Equation 35.

II. The electron avalanche which initiates a positive streamer at the anode, and so causes breakdown, has its origin in the gap near the anode. Such a case is illustrated in Figure 28 and occurs when the voltage gradient varies so much across the gap that the value of α is virtually zero over most of the mid-gap region. The breakdown voltage is determined by Equation 37.

III. Similar to II, except that the voltage required to pro-

duce a positive streamer is less than that required to propagate it across the gap. Such a condition obtains for gap lengths

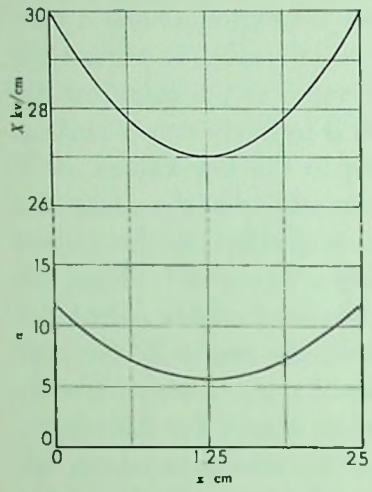

FIG. 27.—Sphere gap $\alpha - x$ short gap

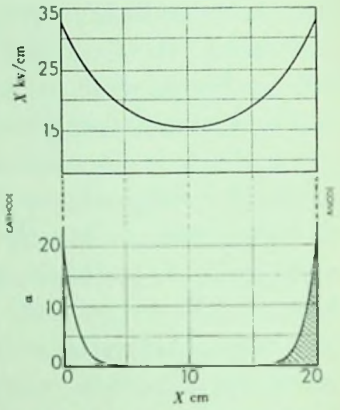

FIG. 28.—Sphere gap $\alpha - x$ longer gap

greater than about $8R$, when corona is observed to appear[16] and the voltage has to be further raised to cause breakdown.

Between types I and II there is a transition region which is of much interest and will be discussed later. The region III is not considered, as it occurs for gap lengths much in excess of those used for calibration purposes and is, of course, much influenced by space charges and the effect of external objects on the sphere-gap field.

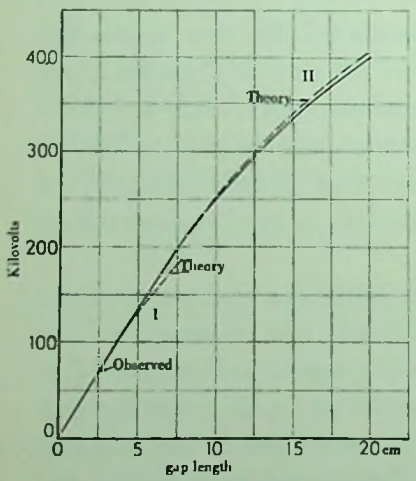

FIG. 29.—Sphere gap spark potential $V_s - x$

Curves to show the calculated and measured potentials for breakdown between spheres of 12.5-centimeters radius are given in Figure 29. The experimental curve is that given by

Hueter[13] for a symmetrical sphere gap, i.e., with voltages $+V/2$ and $-V/2$ on the two spheres. In region I, for the shorter gap lengths, the calculated voltages are in close agreement with experiment up to a gap length of about 4 centimeters, when they fall noticeably below the observed values. At a gap length of 7.5 centimeters such calculations give a voltage of 183,000 volts as compared with the measured 200,000 volts. However, the value of α is very low in the mid-gap region and is less than unity for the central 3 centimeters of the gap. One would then expect that breakdown here occurs on the basis of region II, and actually calculations on this basis give 197,000 volts as that required for breakdown. For yet longer gaps, where the value of α is still further decreased in the mid-gap region, the breakdown mechanism goes over definitely into the region II and the calculated curve is seen to agree closely with that measured.

The calculated curve above is based on Equations 35 and 37, for which the constant term is 14.46. A comparison of the calculated breakdown potentials resulting from these equations and the equations when the constant term is 12.16 is given in Table X. Again the spheres are of 12.5-centimeter radius.

TABLE X

δ cm	Calculation		Measurement	
	$V_{14.46}$	$V_{12.16}$	V_H	V_{ES}
2.5	70,300	69,400	71,000	73,000
5.0	130,000 (I) 139,500 (II)	128,000 (I) 137,500 (II)	137,000	137,000
7.5	183,000 (I) 197,000 (II)	181,000 (I) 195,000 (II)	198,000	197,000
10.0	252,000	248,000	250,000	243,000
12.5	300,000	295,000	295,000	284,000
16.0	354,000	348,000	350,000	328,000
20.0	408,000	402,000	402,000	364,000

The measured values included in Table X are V_H, as observed by Hueter[13] for the symmetrical sphere gap, and V_{ES}, as ob-

served by Edwards and Smee.[5] The latter observations were for the nonsymmetrical gap, i.e., with one sphere earthed, and thus it is found that the values V_{ES} fall below those given by V_H at the longer gaps. Since calculations are made on the basis of a field distribution given by Equation 33, which refers only to the symmetrical field, the calculated results must be compared with the experimental values V_H obtained when the gap is more nearly symmetrical and less likely to be influenced by external objects.

In Table X it will be noted that two values of calculated sparking potential are included for the gaps 5.0 and 7.5 cm, respectively, i.e., in the transition region between I and II. These potentials are calculated on the basis that breakdown occurs wholly by either mechanism I or II, and the respective potentials are so denoted in the table. While there can be no question about the method of calculation for mechanism I, where the electron avalanche travels the whole gap from cathode to anode, some elaboration is needed of the way in which the potential for mechanism II is calculated.

Curves to show the variation of X and α across a 7.5-cm gap between 12.5-cm radius spheres are given in Figure 30. The potential difference between the spheres is 183,000 volts. It is seen that, while the value of α is low in the center of the gap, it does not decline so rapidly as in the case of the 20-cm gap discussed on page 125, and there is no clearly defined termination to the value of $\int_R^{a+R} \alpha dx$ necessary to the calculation of breakdown potential in mechanism II. Avalanches may be originated in the gap near the cathode, may cross the mid-gap region of low field strength, and yet may sufficiently retain their compact filamentary form to initiate a streamer when they reach the anode. For the purposes of calculation, in the transition region the voltage V_2 (on the basis of mechanism II) is calculated on the assumption that the avalanche has its origin at the center of the gap, so that $\int_R^{a+R} \alpha dx$ is given by the shaded area of Figure 30. A similar criterion was given for the longer gap of

20 cm, though there it was shown that there was virtually no difference in the calculated breakdown voltage, if one considered the avalanche to start anywhere between the center of the gap or the point near the anode where $\alpha \sim 1$. Further, in the case of the 20-cm gap, there is no likelihood that an electron avalanche can traverse the full gap in a filamentary form, as is possible for the 7.5-cm gap.

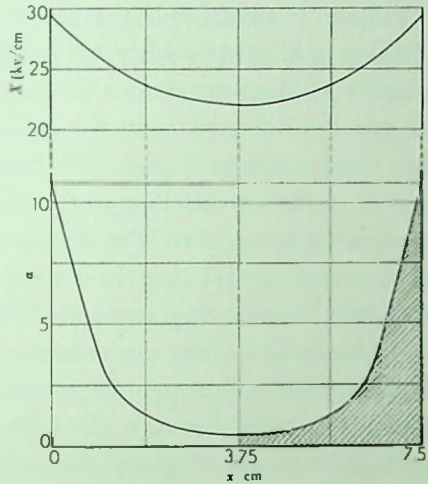

FIG. 30.—Sphere gap $\alpha - x$ large gap

The method of measurement of the breakdown potentials is to raise the potential gradually until breakdown occurs. The mean of the observed values is then taken as the breakdown potential. However, it is clear that the absolute minimum sparking potential is the lowest value observed, provided such a value is not absurdly low and due to extraneous influences. Thus it is probable that the true minimum sparking potential is lower than that usually given by the investigator. In Table X it will be observed that, while $V_{14.46}$ is, in general, slightly higher than the measured V_H, yet $V_{12.16}$ is slightly lower. It would then appear that the more correct value of breakdown potential is

determined from the equation with the constant term 12.16. However, the difference between $V_{14.4G}$, $V_{12.1G}$, and V_{II} is well within the bounds of variation of experimental results, particularly at the longer gap lengths.

The theoretically predicted transition region between I and II is confirmed by observation. Hueter[13] found the scattering of his voltage measurements to increase to a peak at about 8.0-cm spacing. Further, Dattan,[13] again in measurements of the breakdown voltage between spheres of 12.5-cm radius, observed a considerable scattering of his measurements in that region. The peak value of the scattering was as much as 6 per cent, and was greater than 2 per cent for spacings between 5.25 and 7.75 cm. Reference to Figure 29 shows that this is just the region in which such scattering is to be expected on the basis of the present theory. For the value of α becomes so low in the mid-gap region that the chance of a breakdown occurring by mechanism I is extremely remote. Many electrons will have to leave the cathode before a particular electron avalanche crosses the gap under such a propitious chain of circumstances that it succeeds in giving rise to a streamer at the anode. However, if the voltage is raised slightly above that calculated by mechanism I, not only is there an increased chance of a breakdown due to an electron avalanche which leaves the cathode but also breakdown can occur as a result of avalanches originated by electrons in the gap itself. Thus the chance of breakdown is materially increased, and while an occasional breakdown may occur at the voltage calculated on mechanism I the usually measured voltage will have a slightly higher value. Then in the transition region the measured voltage will be intermediate between that calculated on mechanisms I and II, the actual value of the voltage being subject to statistical variations. At the lower end of the transition region mechanism I will predominate, and as the gap length is increased the method of breakdown gradually changes over in a statistical manner to mechanism II. It is this statistical fluctuation which leads to

the large scattering of voltage measurements observed in this region.

Calculations of the breakdown potential curves for spheres of different diameters have been made and give agreement within 2 or 3 per cent of those experimentally observed. Since the experimental values given by many authorities do not themselves agree to much better than 2 per cent it is considered that the theoretically determined values are as satisfactory as the present circumstances warrant.

g) *The effect of air density.*—The variation of sparking potential with pressure for the uniform gap has been discussed in previous sections, where it is shown that Equation 24 gives breakdown potentials in fair agreement with experiment for decreasing pressure down to a value of pressure times gap length of about 200 millimeters of mercury times centimeters. Calculations have now been made for the sphere gap, and the resultant curves for two gap lengths between 12.5-centimeter radius spheres for a pressure variation from 760 to 380 millimeters of mercury are given in Figure 31. Reference to Figure 29 shows that the chosen gap lengths of 4 cm and 12.5 cm fall into the regions I and II respectively.

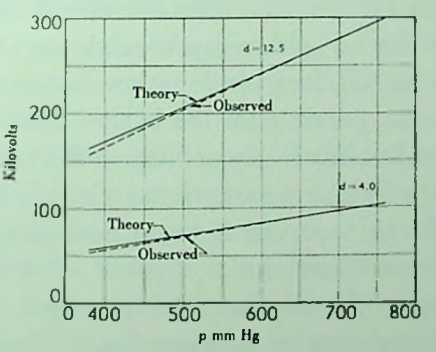

FIG. 31.—Sphere gap $V_s - p$

A comparison with experiment is conveniently obtained by use of an empirical formula given by Peek,[17] which is known

to give an accurate representation of the experimental results over the range of pressure considered. This formula reads $V_p = V_{760}\sqrt{\rho}\left[\frac{\sqrt{\rho R}+0.54}{\sqrt{R}+0.54}\right]$, where V_p and V_{760} are the respective sparking potentials at pressures p and 760 mm Hg. The density ρ is the air density at p relative to that of 760 mm Hg, and R is the sphere radius in centimeters. If one takes the breakdown potential at 760 mm Hg as that calculated, which is known to be closely correct (as seen from the curves in Figure 29), the experimentally observed variation of the sparking potential for the two gaps is given by the dashed curves in Figure 31. There is seen to be close agreement between the degree of variation observed and that determined on the basis of the new theory, the difference being of the same order of magnitude as that to be expected between successive experimental observations.

h) *The Toepler discontinuity.*—At certain low gap settings between spheres a slightly higher potential is required to cause breakdown between spheres of small diameter than for larger spheres at the same gap setting. This phenomenon, now generally known as the Toepler discontinuity,[18] is frequently referred to in articles on sphere-gap breakdown, though there has as yet been no satisfactory explanation forthcoming. Such an explanation is now possible on the basis of the present theory, and will be found to be closely related to the transition between regions I and II to which reference has already been made.

The effect can be observed in the experimentally determined sparking potentials listed by a number of different workers. However, owing to the smallness of the effect, it is frequently masked by inaccuracies in measurement. The lack of agreement between the measurements of different observers is of the same order of magnitude as the effect itself. In the calibration charts published by Edwards and Smee[5] the effect is noticed for a 7.5-centimeter gap, when the breakdown voltages

measured are given as 175, 194, 203, 200 kilovolts for spheres of radii 6.25, 12.5, 25, and 100 cm, respectively. The effect is more pronounced in the results given by Meador[13] for the breakdown voltage V_M of a 5.0-centimeter gap between spheres of different radii, as given in Table XI, where it will be seen that the breakdown voltage for the 12.5-centimeter radius sphere gap is quoted as some 4.6 per cent higher than that for the 25-centimeter radius sphere gap.

TABLE XI

R	V_M	V_I	α_I	V_{II}	α_{II}
25.....	130,000	130,500	2.5	.....	...
12.5.....	136,000	130,000	1.5	139,000	3.6
7.5.....	.....	126,000	0.6	137,000	1.8
6.25.....	128,000	124,600	0.4	136,000	1.1
5.0.....	.....	122,000	0.25	134,000	0.6
2.5.....	.....	.....	...	116,000	0.1

The corresponding calculated breakdown potentials are also given in Table XI. V_I is the voltage determined on the assumption that breakdown takes place according to region I, while V_{II} is that determined on the assumption of a breakdown in region II. α_I and α_{II} are the respective values of α in the center of the gap that correspond to V_I and V_{II}. In the case of the spheres of 25-cm radius the measured breakdown voltage is found to correspond to V_I, which is to be expected since the field distribution in the gap is fairly uniform. For the 12.5-cm and 6.25-cm radius spheres the measured voltage falls between V_I and V_{II}. This is the transition region, where the lack of uniformity of the field in the gap is such that the value of α in the center of the gap is very small, as seen by the values of α_I and α_{II} given in the table. For spheres of still smaller radius the breakdown procedure goes definitely over to the region II. However, it should be recalled that the calculation of V_{II} is based on a symmetrical field distribution, which is not generally obtained in practice for spheres at spacings much larger than their

radius. In general such voltage measurements are made with one sphere at high potential V, while the second sphere is earthed. Such an arrangement leads to lower sparking potentials than those calculated where the voltages on the spheres are considered as $+\frac{V}{2}$ and $-\frac{V}{2}$ and the effect of objects external to the gap is neglected.

The Toepler discontinuity has further been studied in some detail by Claussnitzer,[18] who observed the effect for spheres of radii from 1 cm to 50 cm. He gives values of the gap length at which the effect is observable, though the voltages are not quoted. These gap lengths δ_K cm are given in Table XII.

TABLE XII

R	δ_K	V_M	V_{II}	V_I	α_I
5.0	3.65	101,000	101,000	95,000	0.8
12.5	7.15	190,000	191,000	177,000	0.6
25.0	11.0	285,000	280,000	261,000	0.4
50.0	17.0	430,000	420,000	398,000	0.5

At gap lengths of about $0.5\delta_K$ he finds that the breakdown potential corresponds closely to that for the uniform gap. The breakdown voltage between $0.5\delta_K$ and δ_K is higher than that for the same gap length between spheres of much larger diameter, the deviation being a maximum at about $0.8\delta_K$. For gap lengths greater than δ_K the breakdown voltage is found to be less than for a more uniform field.

The interpretation of these observations is that region I obtains for gap lengths up to about $0.5\delta_K$, and that the transition to region II takes place between $0.5\delta_K$ and δ_K. Thus at δ_K the breakdown mechanism should take place according to region II. That this is the case is borne out to some extent by comparison between the measured and calculated voltages for breakdown, as given in Table XII. The measured values V_M are those given by Hueter.[13] It is seen that V_M is in close agreement with V_{II} and is much higher than V_I. The values of α_I are also included

in Table XII, for interest, and show that this is the region of low mid-gap α when breakdown by mechanism II may be expected.

4. Coaxial Cylinders

The breakdown between coaxial cylinders has been observed by a number of different workers and a fair amount of experimental data has been published.[19] It is thus possible again to compare experiment with theory for a nonuniform field in which the field distribution is known. As in the case of the sphere gap, the breakdown potential is here calculated in the case where steady corona is not observed to precede sparkover. Such corona discharge leads to considerable field distortion by space charges in the gap and complicates the calculations. Thus only those gaps are considered in which corona is not observed and the voltage is sufficient to enable the streamer to propagate across the gap immediately when it has formed and so to cause breakdown. The cases where corona is observed will be discussed in a later section.

The voltage gradient between two coaxial cylinders at a distance x centimeters from the axis is given by

$$X = \frac{V}{x \log_e R/r} \text{ volts/cm} \tag{38}$$

where V is the potential difference in volts between the cylinders, r is the radius of the inner cylinder in centimeters, and R is the radius of the outer cylinder in centimeters.

Calculation of the onset of a streamer and the consequent breakdown of the gap proceeds much in the manner described for the sphere gap under mechanism II, when the central cylinder of radius r is at positive potential. Further considerations are necessary for the case when the central cylinder is negative with relation to the outer cylinder. The case where the inner cylinder is positive will be considered first.

The condition to be satisfied is that an electron avalanche which arrives at the positive inner cylinder should give rise to a streamer. Such a criterion is set by Equation 37, with the constant term 12.16 corresponding to $K = 0.1$.

$$\int_r^{a+r} \alpha dx + \log_e a_A = 12.16 + \log_e \frac{X_A}{p} + \tfrac{1}{2} \log_e pa \qquad (39)$$

This equation, with the constant term 12.16, will be used throughout this section. The variation of X and α in the gap for different values of applied potential V are then determined, and the particular values which satisfy the equation above establish the minimum sparking potential.

Curves which show the variation of X and α for an applied potential difference of 56,400 volts at 760 mm pressure, between cylinders $R = 3.81$ cm, $r = 1.11$ cm, are given in Figure 32. The value of α is seen to decrease rapidly with distance from the surface of the inner cylinder, and the origin of the electron avalanche which initiates the streamer may again

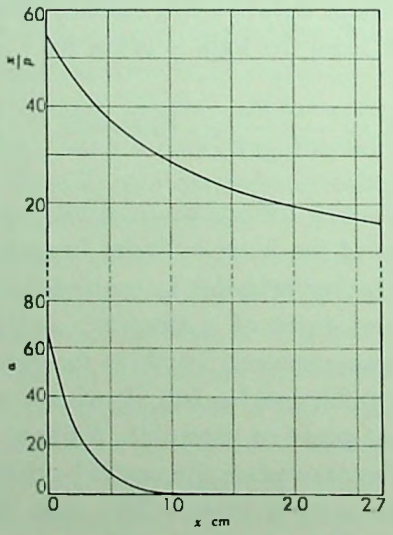

FIG. 32.—Cylinders $a - x$

be taken as the point where α is unity. Beyond this distance there is seen to be virtually no increase in the value of $\int_r^{r+a} \alpha dx$. The particular voltage of 56,400 volts chosen in Figure 32 is that which leads to the solution of Equation 39 and is thus the minimum voltage for breakdown for a positive inner cylinder. The observed breakdown voltage for the same gap conditions is given by Peek[20] as 54,500 volts.

The mechanism of breakdown is different when the inner cylinder is at a negative potential with respect to the outer cylinder. In this case the observed breakdown potential is slightly higher than that for the positive inner cylinder. It is by no means high enough to cause streamer formation at the anode, but it is that which causes the onset of an electron avalanche which proceeds outward from the inner cylinder and gives rise to a retrograde positive streamer, as discussed on page 82. When such an avalanche-retrograde streamer occurs, the field distortion is so great that the negative streamer propagates outward in its stepped manner (see page 85) and may or may not be met by a positive streamer which eventually develops at the anode owing to the induced high field there (see page 92).

It is now necessary to calculate the onset of such a mechanism. The variation of X and α across the gap is again determined for various applied potential differences between the cylinders. The equation now to be satisfied is that in which the radial field equals the external field at some distance a from the inner cylinder. Owing to the rate of decline of α with distance from the electrode surface, the value of a may be taken as that point where $\alpha \sim 1$. For in the calculations it is again found that the term $\int_r^{r+a} \alpha dx$ is the important factor, and that the value of a has little effect on the final solution provided it is large enough so that the full value of $\int_r^{r+a} \alpha dx$ is obtained. The equation for breakdown is then

$$\int_r^{r+a} \alpha dx + \log_e a_0 = 12.16 + \log_e \frac{X_0}{p} + \tfrac{1}{2} \log_e pa \qquad (40)$$

If we take $a_0 = 1$, for which $X_0/p = 31$ at $p = 760$, the equation reads

$$\int_r^{r+a} a dx = 18.9 + \tfrac{1}{2} \log_e (a) \qquad (41)$$

Solution of this equation for the gap considered above where $r = 1.11$ cm, $R = 3.81$ cm, occurs for $V = 58{,}500$ volts. This is 2,100 volts *higher than the value calculated to cause breakdown when the inner cylinder is positive.** The breakdown potential observed by Peek[20] is 55,500 volts, which is 1,000 volts higher than that measured for the positive inner cylinder.

A further comparison between theory and experiment is shown in Figure 33. The measured potentials are again due to

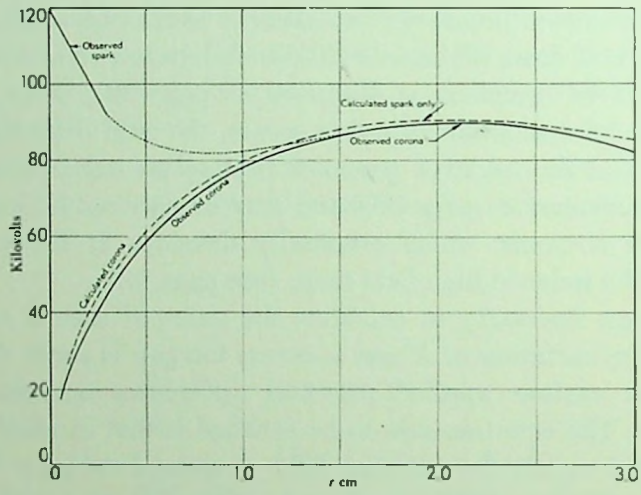

FIG. 33.—Cylinders $V_s - r$

Peek,[21] and are made for the same outer cylinder, $R = 6.67$, but with inner cylinders of differing radii, r. For r less than about 1 cm corona is observed to precede the spark. When $r \sim 1.5$ cm, breakdown is found to occur without any corona,

* The difference for positive and negative wires arises from the fact that the important parameter is $\alpha_x e^{\int_0^x \alpha dx}$. For the positive wire α_x is in a high field and is high. For the negative wire α_x is in a low field and is $\backsim 1$.

and so calculation and experiment may here be compared. Since the experiments were made with A.C. and breakdown occurs at a lower potential when the inner cylinder is positive rather than negative, it is considered that breakdown occurs for a positive inner cylinder and the calculations have been made accordingly. For $r = 2.0$ cm, the calculated breakdown potential is 90,000 volts as compared to 89,500 volts. The agreement is not so good for $r = 3.0$ cm, where the calculated and measured potentials are 85,000 and 82,000 volts respectively.

The foregoing brief comparison between theory and experiment shows that there is fair agreement in some cases, though the discrepancy may be as great as some 5 per cent in others. The agreement is thus not so precise as that obtained for the sphere gap, and in the cases considered it is seen that the calculated potentials are higher than those measured. Several factors tend to contribute to this effect. The air space between coaxial cylinders is relatively confined and in the experiments there may not have been adequate circulation of air. Thus in the gap there may have been a certain amount of nitric oxide, etc., which would lead to a lowering of sparking potential, as discussed on page 54. Further, the field in the gap may be somewhat distorted by space charge and end effects. This is, of course, true in the cases of small r where corona is observed before a spark occurs, and may also be present to some extent for larger r owing to the weak fields at the outer cylinder and some ionization by collision before breakdown. Such effects are not so important in the case of the sphere gap, where the spacing between the electrodes is much more exposed and subject to greater circulation of air.

5. The Variation of Sparking Potential with Initial Photoelectric Current

a) *Introduction.*—The static sparking potential of a uniform-field discharge gap has been observed to be independent of the

intensity of ultraviolet illumination over a considerable range of values. Relatively recently it was found to be lowered appreciably when the cathode of the spark is subjected to the intense radiations produced by a condensed spark. The lowering observed by White[22] for a 5-millimeter gap at atmospheric pressure was as much as 10 per cent. Subsequent experiments by other workers[23] have confirmed White's original measurements and a curve showing the lowering of sparking potential observed by Brinkman[23] for a gap which required 10 kilovolts for breakdown at normal temperature and pressure is given in Figure 34.

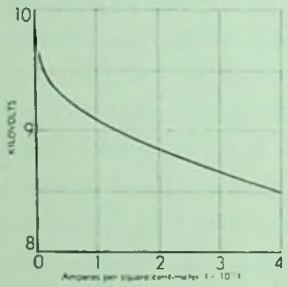

FIG. 34.—$V_s - i$ (photocurrent)

In all the experiments the source of illumination was an auxiliary spark gap, while the variation of intensity was obtained by a change in distance between the source and the gap under observation or by the use of absorbing screens. The equivalent value of the photoelectric current, i_0, was obtained by measurements of the number of photoelectrons released at the cathode, and by assuming the duration of the spark to be $\sim 10^{-4}$ sec. Clearly such an estimate of i_0 is inaccurate and can give only the order of magnitude. For i_0 varies with time in the passage of a single spark and several flashes may occur in a condensed discharge when the circuit is not critically damped. No measurements appear to have been made with steady sources of illumination (e.g., the quartz-mercury arc) giving values of i_0 much higher than about 10^{-13} ampere per square centimeter of cathode.

On the basis of the Townsend theory, Rogowski, Fuchs and Wallraff[24] have shown that the lowering of the sparking potential with increasing i_0 may be accounted for by the presence of a space-charge field produced by positive ions in the gap as a result of the large difference in mobility between the electrons and positive ions. Calculations gave a semi-empirical relation

which, by adjustment of constants and an assumed variation of ion mobility, could be made to approximate the observed experimental data. However, since the Townsend theory is not applicable except at low pressures and short gap lengths, the variation of sparking potential with i_0 for higher values of $p\delta$ remains to be explained. A satisfactory explanation was given by Meek[25] on the basis of the new theory and will now be described. As in the case of Rogowski and Wallraff's work the primary cause of the lowering of sparking potential is ascribed to the effect of the antecedent positive-ion space charge and the consequent variation of field in the gap.

b) *The theoretical calculation of space-charge distortion.*— The effect of the initial photoelectric current and its influence on statistical time lags have been discussed on page 62. The values of i_0 there considered are only such as to produce minor statistically conditioned alterations of the sparking potential and are not sufficient to produce appreciable space-charge distortion in the gap. However, when one considers a spark gap in which there is a large initial photoelectric current, it is possible that a positive ion space-charge distortion may build up owing to the relative mobilities of electrons and positive ions before a spark occurs. The existence of such space-charge distortions was early indicated by Loeb[26] and Rogowski[27] independently as a means by which the second Townsend coefficient would be altered in such a way as to increase the ionization and thus to further enhance the field distortion. Analyses along similar lines were later made by other workers[28] in order to account for the sparking potentials observed, assuming the Townsend mechanism of ionization by positive ions. That such space-charge distortions actually occur in the Townsend gaps and influence the value of the primary coefficient α in the gap was first shown by Posin.[29] The rigorous theory for the evaluation of the steady-state field distortion under the ordinary experimental conditions was set up and solved by Varney and coworkers.[30] It was shown that these distortions would lead to

a spark for adequate gap length. Before such gap lengths are reached, however, spark breakdown occurs by what we now know to be streamer formation.

The theoretically calculated potential for breakdown of a 1-centimeter gap at normal temperature and pressure without space-charge distortion is 32,200 volts, as calculated from Equation 24. For this field strength $\alpha\delta = 18.6$, which is then the condition for a streamer to form in the uniform gap. If the field varies across the gap then $\alpha\delta$ must be replaced by $\int_0^\delta \alpha dx$. Thus, in order to evaluate the effect of j_0 on sparking potential, we must solve the problem of evaluating the space-charge field so that the $\int \alpha dx$ may be calculated. Since the space-charge field requires time to build up, the minimum value of the external applied field occurs when the space-charge field is a maximum, i.e., after a *theoretically* infinite time, so that steady-state conditions virtually apply. We shall then consider the treatment of the space-charge field, as given by Varney,[30] in conjunction with the streamer theory of spark discharge.

Consider two parallel plate electrodes separated by a distance δ and with the cathode illuminated by ultraviolet light, which liberates photoelectrically a current density of electrons, j_0. At any plane in the gas a distance x from the cathode the electron current is given by $j = j_0 e^{\alpha x}$. The current reaching the anode is $j = j_0 e^{\alpha\delta}$. Since the total current crossing any plane parallel to the electrodes must be constant under steady state conditions, the positive-ion current is given by

$$j_+ + j - j_- = j_0(e^{\alpha\delta} - e^{\alpha x})$$

The variation of field in the gap is given by Poisson's equation

$$\frac{\partial X}{\partial x} = -4\pi(\rho_+ - \rho_-)$$

where ρ_+ and ρ_- are the densities of positive ions and electrons respectively. Since $j = \rho v = \rho k X$, where v is the velocity and

k is the mobility ($k = 1.6$ cm/sec/volt/cm for the positive ions at normal temperature and pressure), we obtain

$$\frac{\partial X}{\partial x} = -\frac{4\pi}{X}\left(\frac{j_+}{k_+} - \frac{j_-}{k_-}\right)$$

$$= -\frac{4\pi j_0}{X}\left(\frac{e^{a\delta} - e^{ax}}{k_+} - \frac{e^{ax}}{k_-}\right)$$

Since k_- is about 300 times k_+, $1/k_-$ may be neglected with respect to $1/k_+$, so that

$$X\frac{\partial X}{\partial x} = -\frac{4\pi j_0}{k_+}(e^{a\delta} - e^{ax})$$

Now, a/p is a function of X/p, and since X is not uniform across the gap when the field is distorted by space charge, we should therefore write $e^{\left(\int_0^x a dx\right)}$ for e^{ax} and $e^{\left(\int_0^\delta a dx\right)}$ for $e^{a\delta}$. Denote $\int_0^x a dx$ by u, and $\int_0^\delta a dx$ by u_δ. Then $\partial u/\partial x = a$, and $aX\,\partial X/\partial u = -\frac{4\pi j_0}{k_+}(e^{u_\delta} - e^u)$.

$$\int_{X_0}^{X} aX dX = -\frac{4\pi j_0}{k_+}\int_0^u (e^{u_\delta} - e^u)du$$

$$\phi_X - \phi_{X_0} = \frac{4\pi j_0}{k_+}(ue^{u_\delta} - e^u + 1) \qquad (42)$$

where $\phi_X = \int_0^X aX\,dX$.

This equation was solved by Varney[30] for another purpose by the use of a convenient approximation for a/p as a function of X/p. A more accurate solution may be made graphically for actual values of a and X and will be used later.

c) The calculation of the sparking potential as influenced by equilibrium space-charge distortion.—Having outlined the nature of the effect of intense initial photoelectric current densi-

ties j_0 on sparking potential and having indicated the equations giving space-charge distortion, one must now consider the method of calculation of the lowering.

It was indicated above that, as in the case of geometrically produced nonuniform fields, the sparking potential could be calculated from the condition that the streamer tip field X_1 equal K times the existing space-charge-distorted field X_{x_s} at some point x_s such that streamer formation will lead to breakdown. In equation form this is

$$X_1 = KX_{x_s} = 5.27 \times 10^{-7} \frac{a_{x_s} e^{\int_0^{x_s} a dx}}{(x_s/p)^{1/2}} \text{ volts/cm} \qquad (25)$$

The problem is, however, very much more complicated than for the case of geometrical distortion where one can at once calculate the field, X_x as a function of x, given the applied potential difference, V. In the case of the space-charge-distorted gap, given an initial current density, j_0, the space-charge-distorted field changes for each value of the applied potential, V. In ideal outline, the problem of the effect of j_0 on V_s consists of choosing the desired value of j_0 and choosing what might be an appropriate value of the potential, V, say V_1. From this, then, one should be able to calculate X_{x_1} and X_{A_1}, the fields at any point x and at the anode with the applied potential, V_1. From this, one could calculate the value of $a_A e^{\int_0^{\delta} a dx}$ and thus determine the tip field at the anode, X_{11} for the avalanche. If this is then equal to KX_{A_1}, a streamer could form and a spark will follow. Obviously one will not be lucky enough to find for the first value of $V = V_1$ chosen that $X_{11} = KX_{A_1}$. The value will be either high or low. Then another value of $V = V_2$ is chosen and the process is repeated. From the trend of the computed values of X_1, i.e., X_{11}, X_{12}, etc., relative to KX_{A_1}, KX_{A_2} at the anode a value of $V = V_s$ can finally be chosen that will solve the equation.

Unfortunately, the situation is considerably more involved than even this straightforward procedure would warrant. The solution of Varney's space-charge equation does *not explicitly involve the applied potentials*, V_1, V_2, etc., across the gap, as seen on page 147.

The solution of the equation is expressed in terms of j_0/k_+ and four integrals,

$$\phi_X = \int_0^X \alpha X dX,\ \phi_{X_0} = \int_0^{X_0} \alpha X dX,\ u = \int_0^x \alpha dx,\ \text{and}\ u_\delta = \int_0^\delta \alpha dx.$$

The most convenient way to handle such equations and to associate the solutions with V is as follows. Assume the desired value of j_0/k_+ and a sensible *numerical value* for $u_\delta = \int_0^\delta \alpha dx$. Then by putting in values of u for various values of x across the gap, one may solve the equation for ϕ_{X_0} and for ϕ_X as a function of x. This, then, gives the values of the integral $\int \alpha X dX$ across the gap as a function of x.

Now from the known variation of $\alpha = pf(X/p)$ at the p in question, α can be determined as a $f(X)$ and a curve between X and the value of $\int_0^X \alpha X dX$ can be plotted. From this curve and the preceding solution of $\int_0^X \alpha X dX$ as a function of x, the value of X corresponding to any value of x can at once be read off. The relation between X and α then allows α to be evaluated as a function of x. The value of $\int_0^X X dx$ then gives the desired potential distribution in the gap and $\int_0^\delta X dx = V$ the applied potential. Hence one can correlate the value of V_1, X and α with u_δ for any value of j_0/k_+.

In order to apply the theory for the spark, the equation must be solved by calculating

$$X_{1_x} = 5.27 \times 10^{-7} \frac{\alpha_x e^{\int_0^x \alpha dx}}{(x/p)^{1/2}}$$

for various values of x across the gap to see whether $X_{1_x} = KX_{x_1}$.

After considering the conditions for undistorted plane-parallel gaps, one would be inclined to look for values of u_δ and hence V_1 and X_{A_1} at which

$$5.27 \times 10^{-7} \frac{a_\delta e^{\int_0^\delta a dx}}{(\delta/p)^{\frac{1}{2}}} \text{ gave } X_{1_E} = KX_{A_1}.$$

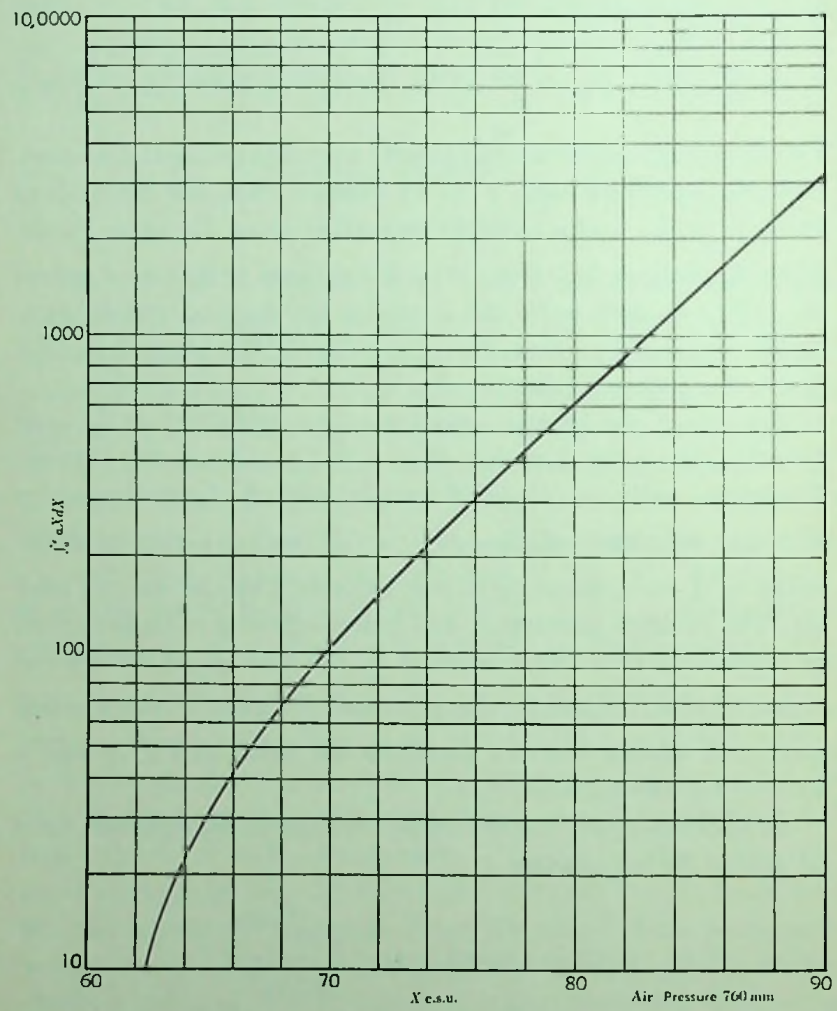

FIG. 35.—$\int_0^x aXdX - X$

Again, however, the situation is not as simple as this procedure indicates. For it happens that the effect of the change in distribution on α is very drastic and that accordingly the value of $\alpha_r e^{\int_0^x \alpha dx}$ varies in a complex fashion across the gap. That this must be so is readily seen by reference to the Figures 35*a*, 36, 37, 38, 39, 40, and 41. Figures 35*a* and 35*b* give the values of $\int_0^x \alpha X dX$ in air at 760 mm for fields ranging

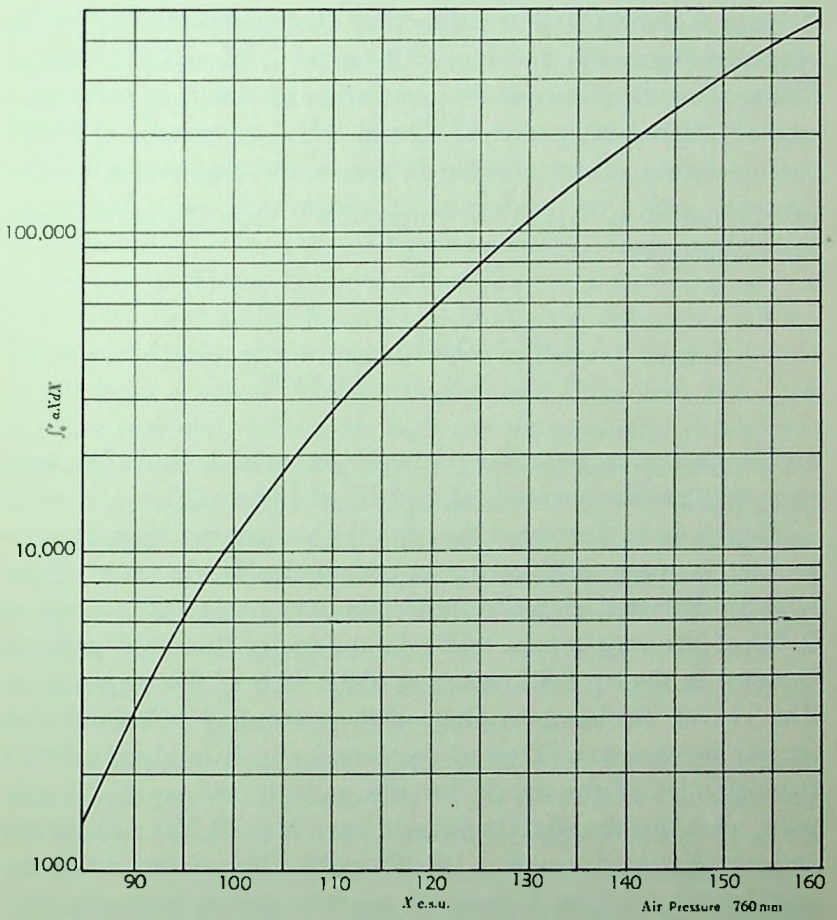

FIG. 36.—$\int_0^x \alpha X dX - X$

from 60 to 160 e.s.u. per centimeter, used in calculation. In Figure 37, curves I, II, and III show the potential distribution as a function of x in the gap for the same $j_0 = 7.5 \times 10^{-13}$ ampere per square centimeter but three different values of V (31,600, 30,700, 29,800 volts, at 760 mm pressure, respectively) giving three different densities of space charge. Curve I is for the undistorted gap, curve II is for the slightly distorted gap, and curve III is for the badly distorted gap. In Figure 38, curves I, II, and III, respectively, show the values of the field strength X_x in the gap as a function of x corresponding to the curves in Figure 37. In Figure 39, curves I, II, and III, respectively, show the corresponding variation of α with x across the gap. In Figure 40, curves I, II, and III, respectively, show the corresponding values of $\int_0^x \alpha\, dx$ across the gap, while in Figure 41, curves I, II, and III, respectively, show the corresponding variation of

$$5.27 \times 10^{-7}\, \alpha_x \frac{e^{\int_0^x \alpha dx}}{X_x (x/p)^{1/2}}$$

across the gap, or better the computed value of $K = X_1/X_x$, corresponding to the curves I, II, and III of Figure 37.

Now it is at once seen that for the undistorted gap the important increase in K occurs at the anode. In the case of the slightly distorted gap the important increase of K occurs at 0.60 of the way across, while in the badly distorted gap the increase in the tip field occurs at about 0.3 of the way across. The curves furthermore show rather peculiar relations that appear inconsistent. Thus at constant j_0/k_+ it is observed that the potential of the anode for the undistorted gap is 31,600 volts, while for the slightly distorted gap it is 30,700 and for the strongly distorted one it is 29,800 volts. This arises from the fact that we solve for V from the space-charge equation for certain values of $u_\delta = \int_0^\delta \alpha dx$. The value of u_δ for the curves

labeled I is 16.4, for those labeled II is 18.5, and for those labeled III is 19.6. Now all that these curves represent are solutions of the equation relating u_δ, j_0, and V at equilibrium. They indicate that for a given j_0 a large u_δ corresponds to a space-charge-distorted gap and is thus associated with a lower V. It does not *predict that physically a larger V will produce a smaller space-charge distortion.* It gives merely the value of V associated with a given u_δ and j_0 at equilibrium. Of this more will be said later.

One must now regard the result of this calculation as it affects the value of V_s. In the undistorted gap the avalanche must cross the gap and start an anode streamer so that $X_1 = KX_A$ fixes the condition for a spark. In the space-charge-distorted gap it is seen that *the achievement of the sparking criterion may occur before the avalanche has crossed the gap.* Thus referring to Figure 41 it is seen that if the space charge conformed to that in the curves labeled II the condition $K = 0.1$ would be reached at $x = 6.0$ mm and if it conformed to that in the curves labeled III it would occur at $x = 3$ mm. Now, in general, when $K \sim 0.1$ it has been assumed that a streamer will form and start back for the cathode. Hence, in both the distributions above mid-gap streamers could progress. Such streamers produce axial field distortions as do mid-gap streamers in overvolted gaps. Obviously these wipe out the existing distortions creating their own. If the new field distributions are adequate to propagate streamers, the gap will break down. It is probable that in both gaps the space charges indicated will propagate streamers and so distort the gap that a spark could follow. At potentials below 29,800 volts this may no longer be true.

The question then arises which value of V for these or other distortions one should choose as V_s. It is obvious that there are still lower values of V corresponding to higher values of u_δ for which streamers may also form. How far down increases in u_δ will cause a lowering of V cannot be determined since the methods of calculation cease to be accurate much above $u_\delta = 22$.

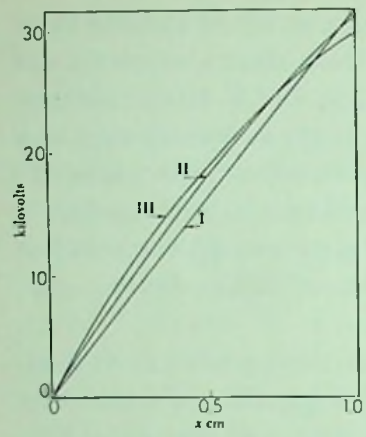

FIG. 37.—$V - x$

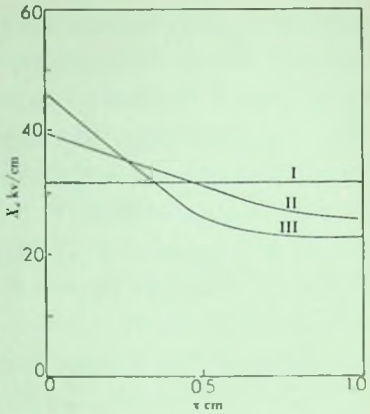

FIG. 38.—$X_x - x$

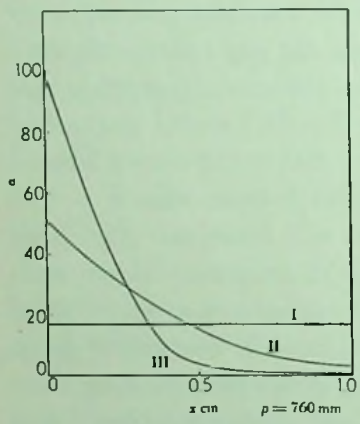

FIG. 39.—$\alpha - x$

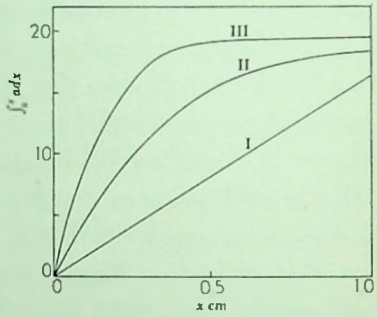

FIG. 40.— $\int_0^x \alpha dx - x$

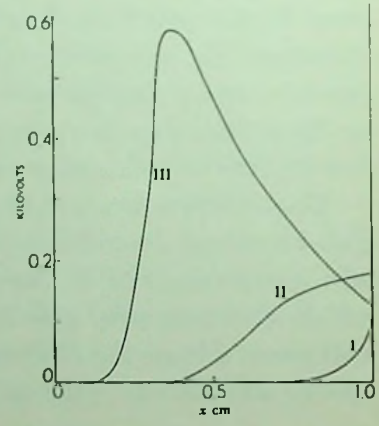

FIG. 41.—$K - x$

Whether the theory has any lower limit to values of V is thus not known. There will be, however, limits to the character of the field distortions which can permit streamers to cross the gap and give sparks. Were these known, the value of V corresponding could be used to calculate V_s and this value could be used as a sparking threshold. Since there is no known lower limit this criterion is useless.

The question of the evaluation of breakdown voltages for the equilibrium field is, however, even more futile than indicated above. All these values of V are *calculated for processes which are highly ideal with no loss of charges from the gap.* They also envisage an indefinitely long time to achieve. Thus, for example, whether at the lowest potential 29,800 volts, the space charge could be built up at all with $j_0 = 7.5 \times 10^{-13}$ ampere per square centimeter may well be raised. The high densities of charge create lateral fields in the gap so that dissipative and diffusive losses become large. Factors such as recombination also cannot be ignored with an infinitely slow growth to the equilibrium condition. Take, for example, the increase of space charge above for the first crossing of positive ions. The first positive-ion group from this initial burst of electrons corresponding to j_0 will in 10^{-5} second raise the field at the cathode by 0.03 per cent. Later bursts increase the field even more slowly. It is thus doubtful whether the spark will be observed at this value of $V = 29{,}800$ volts. It is clear that at the higher value of $V = 30{,}700$ volts the accumulation of space charge might conceivably be fast enough to give a spark under these conditions within a reasonable time despite losses. Unless the losses are known this is only conjecture. Thus it is impossible to fix the lowered value of V_s from any theoretical computations except in order of magnitude.

Experimental studies have not to date been carried out on the lowering of V_s through j_0 *under equilibrium conditions.* The photoelectric intensities for ordinary surfaces with steady sources of ultraviolet light are incapable of giving adequate

values of j_0. It is possible that by the use of specially sensitive alkali metal surfaces one could achieve adequate values of j_0 with steady light sources. Unfortunately these alkali surfaces tend to contaminate the gases with easily ionizable impurities which alter α materially. Thus the chance for a rigorous solution of the effect of j_0 on V_s by means of the equilibrium space-charge distortion either from theory or experiment appears hopeless.

Theory does, however, indicate that, at values of j_0 in the neighborhood of 10^{-12} ampere per square centimeter in air at 760 mm pressure, space-charge distortion may begin to lower V_s by measurable amounts. It indicates that *this lowering will rapidly become larger the higher* j_0 and that the lowering of V_s actually observed will vary with the gap geometry and the time taken for the space charge to accumulate and the spark to appear.

If the potential is gradually raised from very low values, then sparks will appear below the normal threshold at lower values the greater j_0. The lowering will, however, not be very great near the limiting practical current density with usual losses of ions at $j_0 \sim 10^{-12}$ ampere per square centimeter. If a potential V less than V_s but not lower than the minimum V_M for accumulating space charge with losses be suddenly applied, a spark will break as soon as the distortion has reached the appropriate value for a streamer. This may occur somewhat before the equilibrium distortion is achieved.

d) The time of development of a space-charge conditioned spark and values of V_s in short time intervals.—It is now fitting that one consider how fast such a space charge can accumulate in the field, given a potential V_T below V_s but above V_M. It will be seen that by using an appropriate method applicable to the study of the distortions produced by successive waves of positive ions in transit the lowering of V for various values of j_0 can be estimated for time intervals comparable with those studied by White[22] and Rogowski and Wallraff.[23]

The principle of the calculation is simple. One can calculate the number of electrons released by j_0 in t_i, the time of crossing of the positive ions from anode to cathode. This gives the current density of positive ions produced by cumulative ionization. The field distortion produced by this wave of positive ions in transit can be assumed linear to a fair approximation. This then produces an altered field in which the second avalanche of electrons from a burst of ionization j_0 for a second period t_i is moving. Obviously this will alter α over the gap and increase the number of positive ions in a second wave of ionization. Hence a new calculation of the field distortion can be made. In this way the distortion can be computed for successive waves of electrons and ions in successive intervals of time t_i. Now assuming the field linear for these few waves, one can readily calculate the new value of $\int_0^\delta \alpha dx$ and of

$$X_1 = 5.27 \times 10^{-7} a_x \frac{e^{\int_0^x \alpha dx}}{(x/p)^{1/2}}.$$

If after 1, 2, 3, or n waves of ions this integral is such that the field $X_1 = KX_x$ in the gap, we can determine the value of X_A, V_s, and time of breakdown $t = nt_i$. In this general way a study can be made of V_s as a function of j_0 keeping t of the order of the value $t \sim 10^{-5}$ second used by White[22] and Rogowski and Wallraff.[23] The method has the advantage that one sees the space charge build up and can determine at what point the breakdown condition is met. The method is inapplicable to any very large distortions and is at best only approximate.

It has already been pointed out in connection with Figure 38 that the field strength across the gap varies linearly with distance from the cathode except for a small region close to the anode. It will here be assumed that the variation is a completely linear one from cathode to anode. Then the externally applied field strength X_A will be increased by an amount ΔX at the cathode owing to the positive space charge in the gap and will be de-

creased by the same amount ΔX at the anode, as indicated in Figure 42. A further approximation is that the positive ions are all considered to occur at the anode and to travel the full gap. This is of course not true but causes little error, for, owing to the exponential character of electron ionization by collision, the bulk of the positive ions are produced in a small region close to the anode. Further, it will be assumed that the density of positive ions in transit in the gap is uniform. This is again an approximation, for the ions which are about to reach the cathode will have been formed a time, t_i seconds before those which are just leaving the anode, where t_i is the time of transit of positive ions across the gap, while the field will have changed during that time. Thus the density of positive ions near the anode will be slightly greater than that near the cathode on account of the fact that the field in the gap, and therefore $\int_0^\delta \alpha dx$, has meanwhile been augmented.

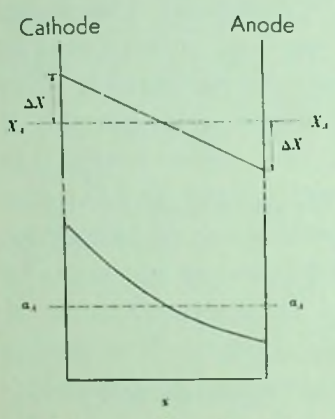

FIG. 42.—$\Delta_x - \alpha_A - x$

The calculation of ΔX due to space charge may be made by means of Poisson's equation. The number of positive ions leaving one square centimeter of the anode per second is $j_0 e^{u_1} \times 3 \times 10^9/\epsilon$ where j_0 is the photoelectric current at the cathode in amperes per square centimeter, $u_1 = \int_0^\delta \alpha dx$, and ϵ is the electronic charge in e.s.u. The time of transit of positive ions across the gap is $t_i = \delta/v = \dfrac{\delta}{k_+ X}$, where $v = k_+ X$ is the mean velocity of the ions. In these calculations it will be considered that the value of X used to determine v will be the mean value of X for the gap, i.e., $X = X_A = V_A/\delta$. Then the density of positive ions in the gap at any instant is

$$N = \frac{j_0 e^{u_1} \times 3 \times 10^9}{\epsilon} \frac{\delta}{k_+ X_A} \frac{1}{\delta}$$

The value of ΔX is then given by

$$2\Delta X = \int_0^\delta 4\pi\rho dx = 4\pi N\epsilon\delta = 4\pi \frac{j_0 e^{u_1} \times 3 \times 10^9 \delta}{k_+ X_A} \text{ e.s.u.}$$

$$\Delta X = 18\pi \times 10^{11} \frac{j_0 e^{u_1}\delta}{k_+ X_A} \text{ volts/cm} \tag{43}$$

Since $k_+ = 1.6$ cm per sec/volt per cm, then for a gap length of one centimeter

$$\Delta X = 3.54 \times 10^{12} \frac{j_0 e^{u_1}}{X_A} \tag{44}$$

The determination of the time lag to breakdown can now be made for any particular values of j_0 and V_A, the applied potential. The value of V_A fixes the field strength X_A of the original undistorted field. The original value of u_1 is ad, where a corresponds to the field strength, X_A. On this basis the value of ΔX due to the first "wave" of positive ions which fills the gap can be determined. The distorted field gives rise to a variation of a across the gap as indicated in Figure 42. From such a curve for a, the value of $\int_0^\delta a dx$ can be calculated. This will give a value, u_2, greater than the u_1 above, owing to the fact that X varies linearly across the gap and a increases with X in such a manner that $\partial^2 a/\partial X^2$ is positive.

If u_2 is still smaller than u_δ, the value of $\int_0^\delta a dx$ required for streamer formation, the quantity u_2 is substituted for u_1 in the expression for ΔX to give a new value of ΔX. The variation of a across the gap is then again obtained, and the new value of $\int_0^\delta a dx = u_3$ is determined. If u_3 is still less than u_δ, the process is repeated until equality is reached. The time lag to breakdown can then be estimated roughly by the number of successive steps required. For the time required by a single positive ion to cross the 1-centimeter gap is approximately $1/k_+X \sim 2 \times 10^{-5}$ sec, where $k_+ = 1.6$ and $X = 31{,}600$ volts/cm. Then if S is the

number of steps in the calculation, the time lag to breakdown is approximately $2 \times 10^{-5}\ S$ sec.

A number of calculations have been made to determine the voltage which will cause breakdown in a time of the order of 2×10^{-5} sec for various values of j_0.

The calculation was made using the value of $K = 0.1$ for a single wave of positive ions crossing the gap. For a given j_0 various values of V were applied and the field distortion was computed starting with $X_A = V/\delta$ in each case. For these distorted fields the quantity X_1 was determined for several points across the gap. It was found that $j_0 = 10^{-11}$ ampere per square centimeter for a certain value of V the space-charge distortion for one avalanche nearly gave $X_1 = KX_A$ with $K = 0.1$ *at the anode.* For a value of V about 0.2 per cent *greater* the value of $K = 0.1$ was reached 7 millimeters from the cathode. Thus a single wave of positive ions in about 10^{-5} sec produced a field distortion so that the avalanche crossing the gap was just able to form an anode streamer and give a spark. A very slightly higher voltage would have caused a mid-gap streamer and breakdown.

When $j_0 = 10^{-8}$ ampere per square centimeter the distortion caused at a value of V very near but below breakdown is already so great that K shows very little increase and even a decrease near the anode and is just short of 0.1. As soon as a value of V is applied which in one wave of positive ions can give $K = 0.1$ anywhere in the gap this value of K will be achieved in mid-gap. Hence, for such high values of j_0 breakdown when it takes place even in the shortest time intervals does so via a mid-gap streamer.

It is seen that this treatment of the problem leads to breakdown at any potential above a very sharply defined threshold. This differs markedly from the case with the equilibrium field. In the case where breakdown is created by a field distortion produced in one to a few waves of positive ions the value of the *initial* field is important not only in determining the time element but also in establishing a spark. In the case of the equi-

librium field the final potential causing breakdown at infinite time is associated with a j_0 and breakdown space-charge distortions are *independent of the initially applied potential.* The latter determines only how fast the field builds up. In the more practical case the potential applied determines whether or not breakdown can take place within a short specified time interval. Thus in this rather crude procedure for calculating the breakdown we find that breakdown achieved with heavy photocurrent densities within $\sim 10^{-5}$ second can have sharply defined lowered values of the sparking potential.

A series of values of V_s computed for a one-centimeter gap in air with various values of j_0 are given in Table XIII.

TABLE XIII

Quantity	Values of Current Density in Amperes per Square Centimeter				
j_0	10^{-14}	10^{-13}	10^{-11}	10^{-10}	10^{-8}
V_s	31,600	31,600	31,350	30,650	28,850

It is seen that a lowered spark breakdown begins well above $j_0 = 10^{-12}$ ampere per square centimeter, and the lowering even at 10^{-11} ampere per square centimeter is not more than 1 per cent. One may compare these calculations with Brinkman's observed results shown in Figure 34. It is seen that the observed lowering of the breakdown potential occurs at somewhat smaller current densities than those computed above. Since the time duration of the intense illumination in Brinkman's spark is uncertain by nearly an order of magnitude, his estimated value of j_0 can be considered uncertain in an equal measure. It is to be noted also that the observed lowering of V_s is somewhat greater than that calculated above. This need not surprise one since in actual periods where j_0 can run for 10^{-5} to 10^{-4} second there can be several waves of positive ions so that the spark can occur for somewhat lower values of the applied potential. Attempts

to calculate the lowering on successive waves of positive ions show that the effectiveness of successive waves in altering the space charge and lowering V_s rapidly decreases after the first few waves of positive ions. Hence the effective lowering of V_s, and thus of the observed sparking potential, occurs in the first few avalanches within short time intervals.

One thing is clear, however, and that is that even on the crude calculations above the predicted lowering of the sparking potential with the streamer theory and the observed lowering are not seriously different. It is probably futile, in view of what has been said both as to the uncertainty in experiments and the difficulties in the application of the theory, to strive for much better agreement at this time. One may, however, leave the subject with the feeling that the effect of dense photoelectric currents from the cathode in lowering the sparking potential is qualitatively in agreement with the streamer mechanism and certainly offers no obstacle to its acceptance.

6. Corona Discharge and Streamer Formation

a) *Introduction.* — Although corona discharge has been known from earliest times (as witness Pigafetta's description of St. Elmo's fire on Magellan's voyage around the world), it has been little understood until relatively recently.[31] It has been studied primarily by engineers in connection with practical problems, so that, while some of its aspects were known, even the very different corona types were not clearly recognized and differentiated. Probably the greatest drawback to an adequate development lay in the inadequate D.C. power sources. Thus much of the corona study has had to do with alternating current. Another difficulty has lain in the lack of proper oscillographs for its study. Thus more recently with adequate aids much progress has been made in the study of the mechanisms at work. These have been found to be remarkably diverse.

Properly speaking the corona *is not a spark discharge* and

should not be discussed in this text. In most aspects the corona discharge is a more or less reversible breakdown caused by intense localization of fields in the neighborhood of conductors of relatively small radius of curvature at high potentials. It appears as a multiplication of ions in the high field regions by the various mechanisms possible, until with adequate densities of these multiplicative processes which are achieved as the fields increase they remain self-sustaining. There is no irreversible aspect to these phenomena at some particular threshold as in a spark. It is then not surprising that in the main the whole behavior of the corona is governed by the space-charge-distorted fields resulting from gap geometry.

On the basis of fundamental mechanisms one must differentiate the positive- and negative-point coronas. Not only that, but one must recognize that these will vary with the point size. For example, the phenomena about points of less than 0.1 mm in size for both signs will suffer restrictions as to possible occurrences not exhibited by larger points, owing to the restricted volume of high field regions. Thus neither positive streamers nor the avalanche-retrograde streamers can occur from such points.

For somewhat larger points both the so-called burst pulses in positive corona (lateral spread of the discharge over the point), and streamers are possible. The streamers occur at the same potentials as the burst pulse spread but in contrast are immediately choked off by space charges that accumulate farther out in the low field regions of the gap. Hence the *real self-sustaining corona onset* occurs as the steady burst pulse glow over the point and streamers disappear. Only at higher fields do streamers succeed in again forming. They then cross the gap and cause breakdown. For such points the negative corona has a totally different form. If conditions are right it forms an active spot on the cathode, the secondary emission by positive-ion bombardment and photoelectric emission giving a finite γ are adequate, and one has a Townsend-like breakdown. The discharge actually

resembles a glow discharge on a small scale. If negative ions form out in the gas the Townsend-like discharge may become quite rhythmic, giving the periodic Trichel pulses. The frequency of these depends on the time of clearing of the negative and positive-ion space-charge fields. When active spots do not form, the corona is composed of very irregular bursts of Townsend discharge that are frequently interrupted. The Trichel pulses require triggering electrons at the cathode and the formation of *negative ions* in low field regions of the gap. The frequency of these depends on the time of clearing the negative- and positive-ion space-charge fields.

As the electrodes become still larger *the field gradients are such as to favor streamer mechanisms from both electrodes.* The positive streamers emerge but cannot at first cross the gap. The negative points have multiple active spots with incipient electron avalanche-retrograde streamer processes. These have been observed to develop in points of intermediate size. At sufficiently high fields both of these streamers tend to propagate across the gap to give spark breakdown as shown on page 89. This process is enhanced by high pressures for reasons given. Here again the space-charge fields in the gap play important roles. Except as geometrical form alters space-charge accumulations it appears that corona discharges are much the same whether they be from points or coaxial cylinders. For calculations with no space-charge distortion cylinders are simpler systems. For experimental study the multiplicity of active spots on cylinders complicates observation and points are preferable.

From the antecedent case of the effect of a space-charge-distorted gap on streamer formation and sparking potential one can see the difficulties inherent in the study of many of the corona problems. Since these problems do not involve the spark discharge proper and are largely insoluble with present-day information they will not be discussed.

There is one set of observations on corona, however, that are of prime interest in spark discharge. *The streamer process un-*

derlying the spark-discharge theory presented in this book appears in controllable form in the positive point-to-plane corona of proper type. In fact it was the observation of these corona streamers that led the senior author directly to the streamer theory of spark discharge.[31] Since the corona streamer can directly be observed, isolated, and studied, the onset of corona streamers has great interest for the student of spark discharge.

Before Meek[32] had evolved his condition for streamer propagation, the senior author recognized the importance of the streamer for spark discharge. He gave to K. S. Fitzsimmons[1] the task of evaluating the anode and gap fields at streamer onset quantitatively with confocal paraboloid electrodes in air. This was in the hope of getting a clue to the criterion of streamer formation. Some difficulties were encountered initially due to changes in the humidity of the air and worse ones with accumulations of nitric oxides in the more confined gaps. Proper ventilation of the gap with dry air gave consistent results. The fields for the onset of streamers in the gaps as a function of distance from the point were measured and computed for four different gaps. The curves fell on each other within the limits of error, thus showing that the streamers indeed depend on the field distribution in the gap for their formation.

These results, owing to the experimental difficulties encountered, were delayed well past the time of development of the quantitative theory for streamer growth and spark discharge by Meek and Loeb.[32] Thus as soon as the fields were calculated by Fitzsimmons[1] from his data there were available reliable figures for a crucial test of the streamer theory. In what follows this test will be applied.

In nearly all previous computations the value $K = 1$ has been used, although it was earlier recognized that a value $K = 0.1$ was probably more accurate as indicated on page 118. Thus, in the comparison of theory and experiment to follow, the streamer theory for spark discharge will be applied to the streamer appearance in corona breakdown for the confocal paraboloid gap

using as a criterion the equation involving the constant setting $K = 0.1$.

b) *Positive corona.*—Streamers are formed at a positive electrode when the field distribution is such that an electron avalanche reaching the electrode produces a radial field of the order of the external applied field at the surface of the electrode. The criterion for streamer formation, as given on page 45, is that

$$\int_0^a \alpha dx + \log_e a_A = 12.16 + \log_e \frac{X_A}{p} + \tfrac{1}{2} \log_e pa \qquad (45)$$

Here a is the distance of the point of origin of the avalanche from the electrode surface in centimeters, X_A is the voltage gradient at the electrode surface, a_A is the value of a which corresponds to X_A. The value of the constant term, 12.16, is that of the "corrected" breakdown equation (see page 119), and is used throughout this calculation.

Since corona discharge occurs only in nonuniform fields, calculations are limited to those fields in which the potential gradient is capable of evaluation. This is possible in the case of electrodes shaped in the form of confocal paraboloids. The potential gradient along the line of foci is given by

$$X = \frac{V}{Z \log b/a} \text{ volts/cm} \qquad (46)$$

where V is the potential difference in volts between the electrodes, a and b are the respective focal lengths of the two paraboloids in centimeters ($b > a$), Z is the distance of the point under consideration from the focus of the inner paraboloid where $b > Z > a$.

The measurements of the onset potential for streamers in the case of confocal paraboloids in dry air at 760 mm pressure made by Fitzsimmons[1] yield the following data. The potential

gradient in the gap for paraboloids with $a = 0.009$ cm, $b = 5.0$ cm at the streamer-onset potential, is shown in Figure 43 as observed by Fitzsimmons. The corresponding curve for α is also given. It is seen that here the origin of the avalanche may be taken as the point where $\alpha \sim 1$, as indicated on page 127, for again the rate of decay of α is so rapid that there is virtually no contribution to $\int \alpha dx$ beyond this point.

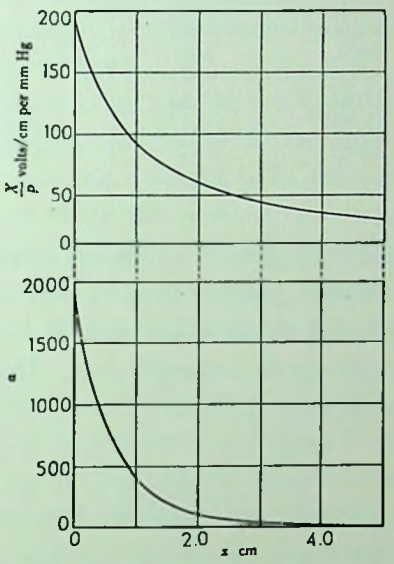

FIG. 43.—Positive corona paraboloids

Such experiments thus give actual data with regard to the values of X_A, α_A and $\int_0^a \alpha dx$ for the onset of streamers. Substitution of these data in Equation 45 then forms a check on the theory. The results of such substitution are shown in Table XIV, by a comparison of the respective values of the left-hand and right-hand side of the equation for various values of b used by Fitzsimmons.[1]

It is seen that Equation 45 is closely satisfied by the experimentally observed values. The actual voltage V_0 which would have been computed from the equation is also compared with

the measured value V_M in Table XIV, and the maximum deviation is seen to be some 3 per cent. Since the agreement is within the experimental uncertainty and within the limits of uncertainty in the constant of the equation, the experiments appear to justify the use of Equation 45.

TABLE XIV

b cm	Left-Hand Side	Right-Hand Side	Difference	$\frac{V_c - V_M}{V_M}$ per cent
2.0.....	18.19	19.13	−0.94	+2.9
3.0.....	18.80	19.17	−0.37	+0.5
5.0.....	19.83	19.23	+0.60	−1.8

c) *Corona onset in concentric cylinders undistorted by space-charge accumulations.*—Another type of nonuniform gap which has been the subject of much experimental investigation is the coaxial cylinder electrode arrangement. Here the potential gradient, as given on page 139, is

$$X = \frac{V}{x \log_e R/r} \tag{38}$$

For such a gap it has already been shown that complete breakdown occurs before corona is observed if the radius r of the inner cylinder is large enough in comparison with R. When r is small, however, a glow round the inner cylinder is seen to occur before the breakdown potential is reached. In most of the experiments with coaxial cylinders the onset potential for this glow discharge is quoted, and the onset potential for streamers is not given. The glow probably corresponds to the steady self-sustaining burst corona observed by Trichel and Kip[31] rather than to the intermittent burst-corona or pre-onset streamers. In this case also the gap is already somewhat fouled by space charge. One may then expect the *measured voltage* to be

slightly higher than that required for pre-onset streamers. Actually it is found that the *calculated onset potential*, which is that for streamer formation, *is slightly higher than that given by the experimental data.*

The observed onset for corona has most certainly been lowered by the presence of nitric oxides, a fact hitherto ignored and whose importance has only recently been emphasized by Haseltine[1] on plane gaps and Fitzsimmons[1] in corona. The discrepancy observed is of proper magnitude and sign to be accounted for in this fashion.

Calculations are carried out on the basis of Equation 39 in the manner indicated on page 139 for the complete spark breakdown between concentric cylinders. In this case, however, the voltage required to cause the onset of a streamer is insufficient to propagate it across the gap to cause breakdown. Again, owing to the rapid rate of decay of α with distance from the inner cylinder, the origin of the avalanche may be taken as that point at which $\alpha \sim 1$.

The results of calculations for $R = 6.67$ cm and various values of r are given in the curve of Figure 33. Corona precedes breakdown for r up to ~ 1 cm and thus it is only this region in which we are interested. It is seen that the calculated values are some 5 per cent higher than those measured, but the general trend of the two curves is the same. Again this may in part be ascribed to oxides of nitrogen. The percentage deviations become the greater as the radius r is decreased. This cannot be due to nitric oxide accumulation. The effect of space charges is, however, completely ignored in these calculations, and since these are seriously affected by changes in geometry the whole difference could be due to this circumstance.

d) Negative corona.—Calculations for the negative corona discharge are made on the assumption that an electron avalanche starting from the cathode should produce a radial field of the order of the external field at some distance a from the cathode. A retrograde positive streamer will then be formed and will

traverse the distance back to the cathode. Such retrograde positive streamers have been observed by Kip. The equation for such a process is

$$\int_0^a \alpha dx + \log_e \alpha_0 = 12.16 + \log_e \frac{X_0}{p} + \tfrac{1}{2} \log_e pa \qquad (47)$$

where X_0 and α_0 are the value of X and α at the point distance a centimeters from the surface of the electrode. As in the case of complete spark breakdown (see page 141), the value of a can be taken as that where $\alpha \sim 1$, for the rate of decline of α is rapid and the value of $\int_0^a \alpha dx$ has virtually reached its final value in the distance where $\alpha \sim 1$. The value of $X/p = 31.0$ gives $\alpha = 1.0$ at $p = 760$ mm Hg. Substitution of such values in Equation 47 makes

$$\int_0^a \alpha dx = 18.9 + \tfrac{1}{2} \log_e (pa) \qquad (48)$$

This is the same equation as that derived on page 141 for breakdown between coaxial cylinders. In the present section, however, we are considering the case where the curvature of the electrode is sufficiently small so that corona discharge is observed to precede breakdown. Calculations show that the potential for the onset of the negative corona is some few per cent higher than that for positive corona on the same electrode, in accordance with observation.

Unfortunately there is little experimental data for the negative corona except in cases where the field distribution is not known too accurately. A certain amount of information has been published for the coaxial cylinder arrangement. However, in general, this information concerns the onset of corona for inner cylinders of very small radius, ~ 0.1 cm or less, where other considerations have to be taken into account. If we consider $r = 0.13$ cm, $R = 3.81$ cm, the onset potential for corona discharge is given by Peek[20] as 25,200 volts. This corresponds to an X/p of 76 at the surface of the inner cylinder. For smaller

values of r the value of X/p at the surface will be still higher. Now experiments by Bowls[4] have shown that the secondary ionization coefficient γ becomes measurable for $X/p > 60$. Thus the negative corona discharge under such conditions is governed by the Townsend mechanism. Positive ions around the cathode will be accelerated in the high fields and will liberate secondary electrons from the electrode surface. Such a mechanism obtains in the case of fine points and wires of small diameter. It leads to a corona-onset potential lower than that calculated by Meek's equation. In fact it lowers the negative corona potential below that for the positive corona when very fine points are used.

Curves to show the onset potential of corona for an outer cylinder of 3.81-cm radius and inner cylinder of different radii r are given in Figure 44. The experimental curve I is that observed by Peek[20] for the steady-glow corona. Curve II gives the calculated onset potential for streamers to form and is seen to lie above I. Curve III is obtained from the Townsend criterion $\gamma e^{\int_0^a \alpha dx} = 1$. Since γ is not measurable for $X/p < 59$, it is considered that for larger values of r the potential of the conductor has to be raised until a value of $X/p = 59$ is reached at the surface. It will be observed that curve III lies below the measured curve for small r but rises to cross it at $r \sim 0.5$ cm, and thereafter the potential increases above that measured. It crosses the calculated streamer-onset-potential curve at $r \sim 0.8$ cm. One may then *consider the Townsend mechanism to obtain in the case of negative corona discharge for conductors of small radius of curvature where corona does not occur until the field at the surface is given by $X/p = 60$ or more.* For electrodes of larger radius of curvature the streamer mechanism becomes the more important.

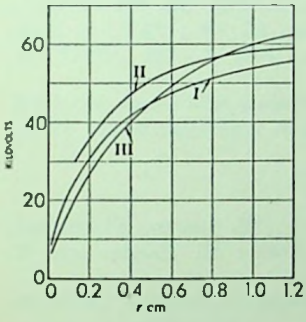

FIG. 44.—Peek's curve

The lack of experimental data for the negative corona discharge precludes a complete quantitative comparison with theory. However, there is seen to be a general qualitative agreement, viz., the corona-onset potential for larger electrodes is higher for a negative potential than for a positive potential. Also, for electrodes of small curvature, the field strength at the surface is so high that the second coefficient γ is important and the Townsend mechanism probably predominates.

REFERENCES TO CHAPTER III

[1] K. S. Fitzsimmons, *Phys. Rev.*, **58**, 187 (1940); W. R. Haseltine, *ibid.*, 188, (1940).

[2] F. H. Sanders, *Phys. Rev.*, **44**, 1020 (1933).

[3] K. Masch, *Archiv f. Elektrotech.*, **26**, 589 (1932).

[4] W. E. Bowls, *Phys. Rev.*, **33**, 293 (1938).

[5] F. S. Edwards and J. F. Smee, *Jour. A.I.E.E.*, **82**, 655 (1938).

[6] R. Davis and G. W. Bowdler, *ibid.*, **82**, 645 (1938).

[7] "Revised Sphere-Gap Sparkover Voltages," *Trans. A.I.E.E.*, **55**, 783 (1936).

[8] C. E. Guye and P. Mercier, *Archives des Sciences*, **52**, 99 (1920); G. Hammerschaimb and P. Mercier, *ibid.*, **3**, 356 (1921); *ibid.*, **3**, 488 (1921); F. Hayashi, *Ann. d. Physik*, **45**, 431 (1914).

[9] L. B. Loeb, *Fundamental Processes of Electrical Discharge in Gases*, pp. 472 ff.

[10] W. O. Schumann, *Durchbruchfeldstärke von Gasen* (Springer, Berlin, 1923), chapter iii, pp. 171 ff.

[11] W. Spath, *Archiv f. Elektrotech.*, **12**, 331 (1923).

[12] K. S. Fitzsimmons, *Phys. Rev.*, **58**, 187 (1940).

[13] J. R. Meador, *Trans. A.I.E.E.*, **53**, 942 (1934); W. Dattan, *Elektrotech. Zeits.*, **57**, 377 (1936); E. Hueter, *ibid.*, **57**, 621 (1936); W. Weicker and W. Hörcher, *ibid.*, **59**, 1029 (1938); **59**, 1064 (1938).

[14] F. W. Peek, *Dielectric Phenomena in High-Voltage Engineering* (McGraw-Hill, 1929), p. 73.

[15] F. W. Peek, *Dielectric Phenomena in High-Voltage Engineering*, p. 69.

[16] F. W. Peek, *Dielectric Phenomena in High-Voltage Engineering*, p. 68.

[17] F. W. Peek, *Dielectric Phenomena in High-Voltage Engineering*, p. 125.

[18] M. Toepler, *Elektrotech. Zeits.*, **53**, 1219 (1932); W. Dattan, *ibid.*, **57**, 377 (1936); J. Claussnitzer, *ibid.*, **57**, 177 (1936).

[19] F. W. Peek, *Dielectric Phenomena in High-Voltage Engineering*, chapters iv and v.

[20] F. W. Peek, *ibid.*, p. 377.

[21] F. W. Peek, *ibid.*, p. 115.

[22] H. J. White, *Phys. Rev.*, **48**, 113 (1935).

[23] W. Rogowski and A. Wallraff, *Zeits. f. Physik*, **97**, 758 (1935); W. Fuchs and W. Seitz, *ibid.*, **103**, 1 (1936); C. Brinkman, *ibid.*, **111**, 737 (1939).

[24] W. Rogowski and W. Fuchs, *Archiv f. Elektrotech.*, **29**, 362 (1935); W. Fuchs, *Zeits. f. Physik*, **98**, 66 (1936); W. Rogowski and A. Wallraff, *ibid.*, **102**, 183 (1936); **108**, 1 (1938); W. Rogowski, *ibid.*, **114**, 1 (1940).

[25] J. M. Meek, *Proc. Phys. Soc.*, **52**, 547, 822 (1940).

[26] L. B. Loeb, *Jour. Franklin Inst.*, **205**, 305 (1928).

[27] W. Rogowski, *Archiv f. Elektrotech.*, **20**, 99 (1928).

[28] J. Franck and A. von Hippel, *Zeits. f. Physik*, **57**, 696 (1929); W. Schumann, *Zeits. f. Technische Physik*, **11**, 131 (1930); J. J. Sämmer, *Zeits. f. Physik*, **81**, 440 (1933); N. Kapzov, *Physik. Zeits. Sowjetunion*, **6**, 82 (1934).

[29] D. Q. Posin, *Phys. Rev.*, **50**, 650 (1936).

[30] R. N. Varney, H. J. White, L. B. Loeb, and D. Q. Posin, *Phys. Rev.*, **48**, 818 (1935).

[31] L. B. Loeb, *Fundamental Processes of Electrical Discharge in Gases*, pp. 514 ff.; A. F. Kip, *Phys. Rev.*, **54**, 139 (1938); **55**, 549 (1939); G. W. Trichel, *ibid.*, **54**, 1078 (1938); **55**, 382 (1939); L. B. Loeb and A. F. Kip, *Jour. Applied Phys.*, **10**, 142 (1939).

[32] J. M. Meek, *Phys. Rev.*, **57**, 722 (1940); L. B. Loeb and J. M. Meek, *Jour. Applied Phys.*, **11**, 438, 459 (1940).

Indexes

AUTHOR INDEX

SUBJECT INDEX

Page numbers in italics refer to places where topic is extensively discussed.

T

Date Due

Jan 19 '48	NOV 16 '60		
Oct 19 '48			
Dec 15 '48	FEB 12 '63		
Dec 14, '49			
Jan 21 '50	OCT 3 '62		
Oct 23 '50			
Nov 6 '50	JAN 17 '64		
Nov 6 '50			
Feb 22 '52	APR 24 '67		
Oct 15 '52			
MAR 13 1953			
SEP 20 1955			
OCT 31 1956			
JAN 22 '59			
JAN 20 '60			

HH 202

537.53 I82m

Carnegie Institute of Technology
Library
PITTSBURGH, PA

Rules for Lending Books:

1. Reserved books may be used only in the library until 8 P. M. After that hour they may be requested for outside use, due the following morning at 9:30. Ask at the desk about week-end borrowing privileges.
2. Books not of strictly reference nature, and not on reserve may be borrowed for longer periods, on request. Date due is stamped on date slip in book.
3. A fine of five cents an hour is charged on overdue reserve book. Two cents a day fine is charged on overdue unreserved books.

11-46